KfK 4658
EUR 11396 EN
November 1989

Evaluation of Forced Reflooding Experiments using the FLUT-FDWR-MM (Modified Version of FLUT-FDWR with Moving Mesh in Heat Conductor Model)

T. Mori, M. Cigarini, M. Dalle Donne
Institut für Neutronenphysik und Reaktortechnik
Projektgruppe LWR-Sicherheit

Kernforschungszentrum Karlsruhe

KERNFORSCHUNGSZENTRUM KARLSRUHE
Institut für Neutronenphysik und Reaktortechnik
Projektgruppe LWR-Sicherheit

KfK 4658
EUR 11396 EN

Evaluation of Forced Reflooding Experiments using the FLUT-FDWR-MM (Modified Version of FLUT-FDWR with Moving Mesh in Heat Conductor Model)

T. Mori[1)]

M. Cigarini[2)]

M. Dalle Donne[3)]

1) Visiting researcher from Japan Atomic Energy Research Institute, Tokai-mura, Naka-gun, Ibaraki-ken, 319-11, Japan
2) Present address: c/o Mercedes Benz, Untertürkheim, Stuttgart
3) Delegated from Euratom to Kernforschungszentrum Karlsruhe, Institut für Neutronenphysik und Reaktortechnik

Kernforschungszentrum Karlsruhe GmbH, Karlsruhe

Kernforschungszentrum Karlsruhe GmbH
Postfach 3640, 7500 Karlsruhe 1

ISSN 0303-4003

Abstract

MORI, Takamasa, CIGARINI, Marco and DALLE DONNE, Mario :
Evaluation of Forced Reflooding Experiments using the FLUT-FDWR-MM (Modified Version of FLUT-FDWR with Moving Mesh in Heat Conductor Model)

A new version of the FLUT-FDWR code, named FLUT-FDWR-MM, has been developed in KfK in order to reduce an oscillation trend observed in the predictions by the original code. In the new version, a finer mesh moving with the quench-front propagation is introduced into the heat conductor model. This version has been tested by means of post test calculations of various reflooding experiments in both PWR (FEBA/SEFLEX, NEPTUN I and II) and APWR (NEPTUN III) geometries. The parameters R_v and R_I of Oseen's relation for interfacial drag between liquid and vapour phases are reoptimised for the new version.

Zusammenfassung

MORI, Takamasa, CIGARINI, Marco und DALLE DONNE, Mario :
Auswertung von Zwangsflutungsexperimenten durch das Rechenprogramm FLUT-FDWR-MM (Modifizierte Version von FLUT-FDWR mit einem beweglichen Maschennetz in dem Wärmeleitungssegmentmodell)

Eine neue Version des FLUT-FDWR Rechenprogramms, genannt FLUT-FDWR-MM, wurde entwickelt, um die numerischen Oszillationen in den Ergebnissen mit der Originalversion von FLUT-FDWR zu reduzieren. In der neuen Version wurde eine feinere Mascheneinteilung in das Wärmeleitungssegmentmodell eingeführt. Diese feine Brennstabsegmentdiskretisierung bewegt sich mit der Benetzungsfront. Die neue Version wurde mit nach-Test-Berechnungen von verschiedenen Flutexperimenten für DWR (FEBA/SEFLEX, NEPTUN I und II) und FDWR (NEPTUN III) Geometrien geprüft. Die Parameter R_v und R_I der Beziehung von Oseen für die Zwischenphasenreibung wurden für die neue Version wieder optimiert.

Table of Contents

List of Illustrations

List of Tables

Nomenclature

d	fuel rod outer diameter (m)
d_h	hydraulic diameter (m)
d_1	average diameter of the water droplets in the zone of length L immediately downstream of the quench front (m)
d_2	average diameter of the water droplets in the remaining part, beyond the zone of length L, of the dispersed flow region (m)
L	axial length of the zone of dispersed flow film boiling immediately downstream of the quench front where the average droplet diameter d_1 is used (m)
L_0	length L for the reference experiment FLECHT 32114 (m)
p	pressure (Pa); pitch (m)
Q	volumetric power density in the fluid at reflooding beginning (W/m^3)
Q_0	value of Q for the reference experiment FLECHT 32114 (W/m^3)
Q_{rod}	power per fuel rod (W)
R_l ,R_v	geometrical parameters for the calculation of the interfacial drag coefficient between vapor and liquid water (m)
T_{cl}	maximum cladding temperature at the beginning (°C)
v_{fl}	flooding rate (m/s)
ΔT	subcooling of flooding water (°C)
T_1	flooding water temperature (°C)

Greek

α	void fraction
ΔT	cladding superheat at the beginning of the reflooding phase (°C)
ΔT_0	value of ΔT for the reference experiment FLECHT 32114 (°C)

1. Introduction

In the concept of the Advanced Pressurized Water Reactor (APWR) with improved uranium utilisation, the main new feature is the introduction of a tight lattice core in order to achieve an higher conversion ratio than in the conventional PWR. For the determination of the optimum design in consideration of the safety requirements, it is necessary to establish flexibly-applicable and highly-accurate predictive methods for core thermal-hydraulic behaviour under accident conditions.

For the past few years, much work is being made in this field at the Institut für Neutronenphysik und Reaktortechnik des Kernforschungszentrums Karlsruhe (INR/KfK). The computer codes RELAP5/MOD1-EUR /1/ and FLUT (GRS-Garching) /2/ have been implemented and further improved in this center. New correlations and physical models based on both theoretical and experimental work on thermohydraulic in hexagonal rod bundels with tight lattice have been introduced in the codes and the new developed versions RELAP5-APWR /3/ and FLUT-FDWR[1] /4/ have been used to analyse the behaviour of three main reference designs of APWR during an Anticipated Transient Without Scram (ATWS) and during a Loss of Coolant Accident (LOCA).

The high prediction capability of FLUT-FDWR, used for the analysis of the reflooding phase of the LOCA, has been shown by many post-test calculations of forced flooding experiments in PWR geometry as well as in APWR-geometry /4/ /5//6/. However, there usually appears a low-frequency oscillation trend in the calculation results which has no correspondence in the measurement. This unphysical oscillation, as pointed out in the previous reports /4//6/, is caused by the large heat flow from the heat conductor segment to the fluid within a short time interval just after the conductor segment is quenched. This large heat flow produces a high evapouration rate in the fluid cell connected to the conductor segment and high vapour and liquid mass flow rates. As a result, sharp peaks or dips appear in the other calculated quantities. The frequency and amplitude depend directly on the axial discretisation of the heat conductors. The nodalisation of the heat conductors makes a significant effect in some cases not only on the oscillation but also on the overall behaviour of important quantities such as the amount of water carry over and the quench-front propagation.

---

[1] FDWR = Fortgeschrittener Druckwasserreaktor = Advanced Pressurized Water Reactor.

In the present work, a finer mesh moving with the advancement of the quench-front (moving mesh) has been introduced in the heat conductor model of FLUT-FDWR in order to reduce the oscillation without much increase of computing time. The post-test calculations have been made for several experiments in the PWR geometry (some of FEBA/SEFLEX series /7/ /8/ /9//10/ and NEPTUN-I & II series /11/ /12//13/) and the APWR geometry (NEPTUN-III series /14/ /15//16/) by using the new version of the code called FLUT-FDWR-MM.

This report describes the general features of the physical model of FLUT-FDWR, the newly introduced moving mesh and the results of the post-test calculations.

2. The Computer Code FLUT-FDWR and Its New Version FLUT-FDWR-MM

2.1 FLUT-FDWR

A few years ago the version No. 5 of the computer code FLUT, developed by the GRS-Garching /2/ for the calculation of the reflooding phase after a LOCA in a PWR-plant of German design, was implemented on the IBM 3090/SIEMENS 7890 computer configuration of the Kernforschungszentrum Karlsruhe. The hydrodynamic model in FLUT is a two-fluid model with six conservation equations for mass, momentum and energy. The interaction between the phases is modelled by a very simple set of constitutive equations for mass transfer rate, interfacial drag and interfacial heat transfer, which fulfils basic requirements as symmetry of phases, increase of phase interaction with growing deviation from equilibrium and correct behaviour of the disappearing phase (interaction terms gradually decrease as one phase is disappearing), while the dependence on the flow regime appears only indirectly /17/. This proved to be an advantage for the calculations in APWR-geometry. As a matter of fact, most of the presently used flow maps are based on experimental evidences for pipes or for bundles in normal PWR geometry. Their previsions in case of a different geometry may fail completely. The pretest calculations of the first forced reflooding experiment in a very tight APWR geometry with different codes proved this fact /18/. On the other hand the simpler

formulation of the FLUT code assures a wider generality and can better cope with this new geometrical configurations /19/.

The one dimensional heat conduction model of the code is able to simulate plates and hollow or full cylinders. Each heat conductor can have up to three material zones separated by gaps. Heat generation can be considered in material zones. Suitable heat transfer correlations depending on the flow regime connect the fluid and the heat conductor model. The positions of the lower and upper quench-front for each fuel rod is calculated explicitly by means of analytical correlations for the quench-front velocity /20//21/. This compensates partly the lack of the axial conduction in the one dimensional heat conductor model. For the simulation of a reactor primary system, a network of one dimensional flow elements (pipes) and special plenum cells (lumps) is applied. The reactor core may comprise parallel cells with fuel rods of different power connected to each flow channel. For the primary coolant pumps, a centrifugal pump model is available. The temperatures of the secondary side of the steam generator tubes and the injected mass flow rates of the ECCS must be given as input data.

The modified version FLUT-FDWR contains some new correlations and physical models which improved its prevision capability /4/.

The criterion of Hsu and Young for the onset of the quench-front /22/ was introduced in order to avoid a too early quenching of the rod cladding from above. This criterion allows the beginning of the rewettig process only when the void fraction α is less then 0.95 and the cladding temperature T_{cl} is lower then 540°C and gave satisfactory results when applied in some cases in PWR geometry /23/.

A new droplet model for the zone immediately downstream the lower quench-front improved the calculation of the precooling effect in the cases in which the quenching of the cladding takes place at a high void fraction ($\alpha \geq 0.8$ at the quench-front). Figure 1 on page 32 shows the flow patterns of the two extreme reflooding situations: flow pattern A occurs usually for high flooding rates (more then 4 cm/s) while flow pattern B is typical of low flooding rates /24/. The establishment of one or the other of these flow patterns is also affected by the inlet subcooling of the flooding water and by the volumetric power density in the bundle: lower inlet subcooling and high power density support the pattern B. In an APWR core, where the power density is higher than in a PWR, pattern B may become of major importance.

The original package of heat transfer correlations of the FLUT code is based on a flow pattern of type A and underestimates the precooling of the cladding before

quenching in case of pattern B, where the zone of the dispersed flow film boiling begins directly above the quench-front. A very important parameter in this flow regime is the average droplet diameter used to calculate the heat transfer coefficient and the interfacial area between vapour and water droplets. In the original version of FLUT this parameter was set to a unique constant value. Basing on a study of R. Lee about droplet generation at the quench-front and their subsequent evolution /25/, a simplified model was implemented in FLUT-FDWR. Here the region of dispersed flow is divided into two subregions (see Figure 1 on page 32):

a zone of length L, immediately downstream the quench-front, in which the calculation uses a value $d_1 = 0.127$ mm for the droplet average diameter, accounting for the presence in this subregion of two kinds of droplets generated below (in the zone of transition boiling) by the bursting of bubbles;

the remaining part of the dispersed flow region, in which the value $d_2 = 2$ mm is used as in the original version of the program (in this zone only the bigger droplets survive, as the smaller ones evaporate completely within the first zone of length L).

For the length of the zone in which the diameter d_1 is used a reference value $L_0 = 0.2$ m was determined by means of optimisation calculations of the experiment FLECHT No. 32114. For the other cases L was calculated by means of a simplified energy balance. Supposing that the zone of influence of the small droplets depends linearly on the volumetric power density on the fluid Q and on the initial cladding superheat ΔT, referring to the value L_0 we obtain:

$$L = L_0 (Q_0/Q)(\Delta T_0/\Delta T)$$

where the values with index 0 refer to FLECHT exp. No. 32114 /26/. This simplification gave good results in the calculation of many experiments in PWR and APWR geometry /4/ and was used also in the present work.

For the calculation of the friction factors, new relations for a properly evaluation in APWR core channels were introduced in FLUT-FDWR /4/.

The dependence of the interfacial drag coefficient on the channel geometry can be accounted for in FLUT-FDWR by giving different values of the parameters R_v and R_l of the relation of Oseen /27/ in the different component of a system. According to the results of parametric calculations of many reflooding exper-

iments and to the experiences of other authors, the following reference values have been established /4/:

$R_v = R_l = 0.70$ m for a very tight APWR rod lattice (p/d = 1.06, d_h = 2.6 mm)

$R_v = R_l = 0.25$ m for a PWR geometry (square rod lattice with $d_h \simeq 12.0$ mm)

$R_v = R_l = 0.10$ m for pipes.

2.2 FLUT-FDWR-MM

The moving mesh has been introduced into the heat conductor model of FLUT-FDWR in order to reduce the oscillation trend caused according to the propagation of the quench-front. The conceptual illustration of the moving mesh is given in Figure 2 on page 33. The nodalisation shown on the left of this figure is usually used in the FLUT-FDWR calculation. The axial length of each heat conductor is usually 4 ~ 6 cm. In the new version of the code, several heat conductor cells around the quench-front are divided into finer ones. Six finer cells per eachone of the three conductor cells around the quench-front, which are shown in this figure, are used as a standard nodalisation in the present work. The number of divided cells, their location relative to the quench-front and the number of finer cells can be changed by input. The part of conductors divided into the finer cells is moving with the propagation of the quench-front. When the conductor cell is divided into finer ones, the same temperature distribution as that of the divided cell is assigned to each finer cell. On the other hand, the temperature is assumed to be an arithmetic average of those of the finer cells when the finer cells are combined into one large cell.

The important parameters for the physical model of FLUT-FDWR, L of the droplet model and R_v and R_l of the relation of Oseen for interfacial drag between liquid and vapour phases, were optimised for the coarse mesh used in the FLUT-FDWR calculation /4//5/. However, the nodalisation effect on the calculation result is very large and very important as pointed out in the previous works /4//6/. This means that the values of these parameters should be reoptimised for the new version using the moving mesh. Through the course of post-test calculations for various reflooding experiments in the present work, the optimum values for R_v and R_l were determined as follows:

$R_v = R_l = 0.25$ m for a PWR geometry (square rod lattice with $d_h \simeq 12.0$ mm)

$R_v = R_l = 0.10$ m for a APWR geometry (triangular rod lattice p/d = 1.13 d_h = 4.17 mm)

Note that smaller values of R_v and R_l mean stronger interfacial drag.

As an optimum value of L, we adopted the same value as that established for the coarse mesh mentioned above since the tests in the present work have low sensitivity to this parameter.

3. Comparison with the Experimental Data

To assess the reliability of the new version FLUT-FDWR-MM, we have performed calculations for various reflooding experiments in both PWR and APWR geometries.

3.1 PWR Geometry

Among the many reflooding experiments for PWR geometry available in the literature, we have chosen some representative experiments from the FEBA/SEFLEX series /7/ /8/ /9//10/ and from the NEPTUN I & II series /11/ /12//13/. Tables 1 and 2 show the main data of the test sections and of the tests calculated with FLUT-FDWR-MM, respectively. The FEBA/SEFLEX series were adopted in the assessment work of FLUT-FDWR in the previous work /4/. The NEPTUN series have been first analysed by the present work. Accordingly, the results by FLUT-FDWR-MM are compared below with those by FLUT-FDWR as well as the experimental results.

	FEBA/SEFLEX	NEPTUN I and II
Rod diameter (mm)	10.75	10.72
Rod pitch (mm)	14.3	14.3
Rod heated length (m)	3.90	1.68
Number of rods	25	33
Flow area (cm^2)	38.9	43.0
Hydraulic diameter (mm)	13.47	10.42
Power axial form factor	1.19	1.58
Power radial form factor	1.0	1.0

Table 1. Main Data of Test Sections (PWR Geometry)

Test No.	Q_{rod} (kW)	T_{cl}(°C)	v_{ff}(cm/s)	p (bar)	T_1 (°C)	Gap
SEFLEX-05	8.00	793	3.81	2.11	40	Helium
SEFLEX-07	8.00	780	3.81	2.12	54	Argon
FEBA-216	8.00	802	3.81	4.12	40	No
NEPTUN 5036	2.45	675	1.5	4.1	134	No
NEPTUN 5171	4.54	860	10.4	4.12	135	No

Table 2. Main Data of the Calculated Reflood Tests (PWR Geometry)

Figure 3 on page 34 shows the nodalisation used in the calculation, where the moving mesh is not presented. These nodalisations were used in the FLUT-FDWR calculation. For the NEPTUN series, each of the three conductor cells around the lower quench-front and the upper quench-front respectively is divided into six finer cells (standard case). On the other hand, 12 finer cells are used for the lower quench-front in the case of the FEBA/SEFLEX series, since we used fairly long

conductor cells of 32.5 cm length in the FLUT-FDWR calculation in order to take into account the effect of the housing wall /5/. The modelling of the heater rod for both series are described in References /5/ and /6/, respectively.

All the calculations were performed using the droplet model shortly described in Chapter 2. For the droplet diameters d_1 and d_2, the standard values were adopted in all cases. For the length L, the equation of Chapter 2 gave results greater than the limit value 0.2 m in all the cases except NEPTUN 5171. Then the limit value was used in the calculations. In the case of NEPTUN 5171, a value of 0.1818 m was calculated. As the geometric parameters for the interfacial drag coefficient, a value of 0.25 m for the PWR geometry was used in all calculations, which is the same value as used in FLUT-FDWR calculation.

3.1.1 FEBA/SEFLEX Series

The main results of FLUT-FDWR-MM are shown in Figure 4 on page 35 to Figure 24 on page 45, where the FLUT-FDWR-MM predictions are compared with the measured values. As for the FLUT-FDWR predictions, we should refer to the previous report /5/. On the basis of these figures, the following conclusions can be drawn:

Oscillation trend: Compared with the results by FLUT-FDWR in Reference /5/, a considerable reduction of the oscillation trend by using the moving mesh is clearly seen in almost all figures, especially in the results for the cladding temperature and the pressure difference.

Quench-front curve: As for the quench-front propagation, the measured values are not available. From the comparison with the results by FLUT-FDWR, it can be said that FLUT-FDWR-MM gives generally slightly shorter lower quench times (5 $\sim$ 10 %) than FLUT-FDWR.

Cladding temperature: For the three tests, the predicted cladding temperatures can be compared with the measured ones (see Figure 5 on page 35 to Figure 8 on page 37 for FEBA 216, Figure 12 on page 39 to Figure 15 on page 40 for SEFLEX 5 and Figure 19 on page 42 to Figure 22 on page 44 for SEFLEX 7). Agreement between the calculation and the measurement is generally good for the quench time and the quench temperature (temperature at which the quenching phenomenon begins), though the calculation shows a slightly shorter quench time for FEBA 216 and SEFLEX 5 and a slightly longer one for SEFLEX 7.

The overall trend, however, is quite different between the calculation and the measurement in the case of FEBA 216 and SEFLEX 5. The calculated temperature begins to decrease much earlier and becomes lower than the measured one. A similar trend is observed at the first two levels of SEFLEX 7 (z = 1205 mm and 1750 mm). This trend was also seen in the results by FLUT-FDWR /5/, but it is much stronger in the present results. On the other hand, the overall trend is well predicted at z = 2295 mm and 3385 mm of SEFLEX 7.

Water carry over: For the water carry over, the slopes of the calculated and measured curves are quite similar, though the former is slightly higher in the case of the SEFLEX 5 and SEFLEX 7 experiments (see Figure 9 on page 37 for FEBA 216, Figure 16 on page 41 for SEFLEX 5 and Figure 23 on page 44 for SEFLEX 7).

Pressure difference: The pressure difference between the inlet and the outlet of the test section is well predicted by the FLUT-FDWR-MM calculation (see Figure 10 on page 38 for FEBA 216, Figure 17 on page 41 for SEFLEX 5 and Figure 24 on page 45 for SEFLEX 7).

3.1.2 NEPTUN I and II Series

NEPTUN 5036: The main results for NEPTUN 5036 are shown in Figure 25 on page 45 to Figure 33 on page 49, where the FLUT-FDWR-MM predictions are compared with the experimental results and the FLUT-FDWR predictions. The experimental values are taken from the magnetic tape prepared by J. Dreier of Paul Scherrer Institute, Switzerland (PSI). In the comparison, we exclude the measured values of cladding temperature on some heater rods on which the LOFT type thermocouples were used, since these thermocouples are placed outside the heater rods and the quenching phenomenon occurs much earlier than on the other rods due to a flow disturbance caused by the thermocouples themselves.

The improvement of FLUT-FDWR-MM is obvious. The reduction of oscillation trend is clearly seen in most figures, especially in the vapour temperature (see Figure 30 on page 48) and in the pressure difference predictions (see Figure 32 on page 49 and Figure 33 on page 49). FLUT-FDWR-MM predicts quicker lower quench-front propagation than FLUT-FDWR, and as a result the agreement with the measurement becomes better (see Figure 25 on page 45). As for the cladding temperature (see Figure 27 on page 46 to Figure 29 on page 47), the FLUT-FDWR-MM prediction shows decreasing tendency earlier than the FLUT-FDWR one, which results in better agreement with the measurement. In

these figures, two measured curves which give the shortest and the longest quench times are shown to take account of the spread of the measured temperatures. For an amount of water carry over, FLUT-FDWR-MM gives a sufficiently good prediction, while FLUT-FDWR gives much more carry over than the measurement (see Figure 31 on page 48).

NEPTUN 5171: Similar comparison is made for NEPTUN 5171 in Figure 34 on page 50 to Figure 41 on page 53. In this case characterized by a high flooding rate, the observations are quite different from those for NEPTUN 5036 with a low flooding rate. Use of the moving mesh reduces the oscillation as seen in Figure 35 on page 50, Figure 40 on page 53 and Figure 41 on page 53. However, the overall trend of prediction is quite similar between the two codes. Compared with the measurement, both codes give a slower lower quench-front velocity, a quicker upper quench-front velocity (see Figure 34 on page 50) and higher cladding temperatures (see Figure 36 on page 51 to Figure 38 on page 52). However, the predicted water carry over and pressure difference are in good agreement with the measured ones (see Figure 39 on page 52, Figure 40 on page 53 and Figure 41 on page 53).

3.2 *APWR Geometry*

For the test in APWR geometry, we have chosen the NEPTUN III series of reflooding experiments recently carried out at PSI /14/ /15//16/. Tables 3 and 4 show the main data of the test section and of the tests calculated with FLUT-FDWR-MM, respectively. This series of tests were analysed by FLUT-FDWR and the results are presented elsewhere /6/, from which the results are taken for comparison.

The nodalisation used in the calculation is similar to that used for NEPTUN I and II tests, which is shown in Figure 3 on page 34. For these tests, eachone of the three conductor cells around the lower quench-front and the upper quench-front is divided into six finer cells (standard nodalisation). The modelling of the heater rod is given in Reference /6/.

All the calculations were performed using the droplet model with the standard values for the droplet diameters d_1 and d_2. For the length L, the equation of Chapter 2 gave results greater than the limit value 0.2 m in all the cases with lower power. Then the limit value was used in the calculations. For the two tests

with higher rod power, APWR1 and APWR5 in Table 4 on page 12, L values of 0.1273 m and 0.1723 m were calculated, respectively.

The geometric parameters for the interfacial drag coefficient were determined to be 0.1 from the comparison of calculated and measured water carry over for the APWR8 test. The same value is used in all calculations. This value of $R_v = R_l = 0.1$ is much smaller compared with $R_v = R_l = 0.62$ for the coarse nodalisation used in the FLUT-FDWR calculation.

The measured values of the first 7 tests are taken from Reference /14/. The quench-front progress of all these 7 tests and the cladding temperature of the first one are available. Those of the last one are taken from the magnetic tape prepared by PSI for the benchmark test.

	NEPTUN III
Rod diameter (mm)	10.7
Rod pitch (mm)	12.1
Rod heated length (m)	1.68
Number of rods	37
Flow area (cm^2)	15.59
Hydraulic diameter (mm)	4.17
Power axial form factor	1.58
Power radial form factor	1.0

Table 3. Main Data of Test Section (APWR Geometry)

Test No.	Q_{rod} (kW)	T_{cl}(°C)	v_{fl}(cm/s)	p (bar)	ΔT_{sub}(°C)
APWR1	2.45	757	10	4.1	80
APWR2	1.19	757	4.5	4.1	80
APWR3	1.19	597	4.5	4.1	80
APWR4	1.19	477	4.5	4.1	80
APWR5	2.45	597	4.5	4.1	80
APWR6	1.19	757	10	4.1	80
APWR7	1.19	757	15	4.1	80
APWR8 (NEPTUN-benchmark)	1.19	597	2.5	4.1	80

Table 4. **Main Data of the Calculated Reflood Tests (APWR Geometry):** The data for the first 7 tests are taken from /14/. The data for the 8th test are taken from /16/.

3.2.1 NEPTUN III Series

APWR8 (NEPTUN benchmark): Main results of calculation are shown in Figure 42 on page 54 to Figure 55 on page 60, where the FLUT-FDWR-MM results are compared with both the experimental results and the FLUT-FDWR predictions. To obtain the effect of the moving mesh, the FLUT-FDWR-MM calculation using the same values of $R_v = R_l = 0.62$ as used in the FLUT-FDWR calculation are also shown in these figures.

Figure 42 on page 54 shows the quench-front propagation. From the comparison between the results with and without the moving mesh by using the same R_v and R_l values ($R = 0.62$), it is seen that the calculation with the moving mesh (dashed line) gives a rather quicker propagation of lower quench-front than that without the moving mesh (dotted line). This quicker propagation corresponds to the higher collapsed water level in Figure 43 on page 54 and the smaller amount of water carry over in Figure 44 on page 55. The FLUT-FDWR-MM calculation with $R_v = R_l = 0.62$ gives an amount of water carry over, which is almost zero and much

smaller than the measured one. On the other hand, the calculation with smaller values of $R_v = R_l = 0.1$ shows better agreement with the measurement. This calculation predicts sufficiently well the slope of the curve (water carry over rate). From this fact, we determined the optimum values of $R_v = R_l = 0.1$ for the present APWR geometry. By using this value, the agreement of quench-front propagation is considerably improved as seen in Figure 42 on page 54, though the calculation gives a slightly quicker propagation of the lower quench-front than the measurement. As for the outlet vapour mass flow rate, the improvement is obvious (see Figure 45 on page 55 to Figure 47 on page 56). The moving mesh reduces considerably the oscillation trend. The smaller R value gives better agreement with the measured value. The remaining large dips in the FLUT-FDWR-MM results are due to the fairly rough nodalisation of fluid cells.

The cladding temperatures at three measured levels are compared in Figure 48 on page 57 to Figure 50 on page 58. In these figures, we give the measured values on several rods which give the highest and lowest maximum temperature, and the quickest and slowest quenching phenomenon. The improvement by FLUT-FDWR-MM with $R_v = R_l = 0.1$ is obvious.

Figure 51 on page 58 to Figure 53 on page 59 show the vapour temperature. The pressure difference is compared in Figure 54 on page 60 to Figure 56 on page 61. In these figures, we can see obviously the improvement by the FLUT-FDWR-MM calculation with $R_v = R_l = 0.1$.

APWR1 ~ APWR7: Comparison of the quecnh-front propagation is shown in Figure 57 on page 61 to Figure 63 on page 64. FLUT-FDWR-MM gives a better prediction of the quench-front velocity (slope of the curve) than FLUT-FDWR except for APWR5, though the prediction by FLUT-FDWR-MM shows a slightly longer quench time compared with the measurement. This tendency of longer quench time is opposite to that observed in APWR8 (NEPTUN benchmark). In these cases with a higher flooding rate, the effect of using the moving mesh is small compared with APWR8, as shown in Figure 61 on page 63 and Figure 63 on page 64. This fact might suggest the necessity of a correlation for R_v and R_l depending not only on the geometry but also on the flow regime.

Figure 64 on page 65 to Figure 66 on page 66 show the comparison of cladding temperature of APWR1. The results by FLUT-FDWR-MM show better agreement with the measurement. The graphs of the measured cladding temperatures for the experiments APWR2 to APWR7 are not available to us.

4. Conclusions

A new version of the FLUT-FDWR code, named FLUT-FDWR-MM, has been developed in KfK in order to reduce the oscillations observed in the predictions of the original code. In the new version, a finer mesh moving with the quench-front propagation is introduced into the heat conductor model. This version has been tested by means of post-test calculations of various reflooding experiments in both PWR (FEBA/SEFLEX, NEPTUN I and II) and APWR (NEPTUN III) geometries. The parameters R_v and R_l of Oseen's relation for interfacial drag between liquid and vapour phases are reoptimised for the new version.

The new version of the code (FLUT-FDWR-MM) reduces effectively the oscillation trend observed in the FLUT-FDWR predictions. The results of the FLUT-FDWR-MM calculations with the optimised parameters show generally good agreement with the measured values. However, there are some cases for which the agreement is insufficient (cladding temperature trend in FEBA/SEFLEX, quench-front propagation in NEPTUN 5171 and APWR5 (NEPTUN III)). This fact might suggest the necessity of a correlation for the interfacial drag between liquid and vapour phases which is a function of the flow regime and also reconsideration of the heat transfer correlation for the region downstream the quench-front.

Appendix A. Additional Input for FLUT-FDWR-MM

The input for FLUT-FDWR-MM is a little changed from that for FLUT-FDWR. Users should refer to the input instruction for FLUT-FDWR in Reference /26/. The present modification refers only to Chapter 8 'Heat Conductor Input Data'. The modification is as follows:

1. Meaning of the first input (IHV) on the first line (1/1)

1/1 (I4) IHV ≥0 the same as in the original version.
number of conductors.
<0 the absolute value of IHV means the number of conductors and the moving mesh is used in the calculation. In this case, the following line is required.

2. One additional line is required following the first line when IHV < 0.

1'/1 (I4) NU1 number of heat conductor cells which are divided into finer cells around the lower quench-front. When NU1 = 0, the moving finer mesh is not used for the lower quench-front.

1'/2 (I4) NU2 number of finer cells per each heat conductor cell (lower quench-front).

1'/3 (I4) NU3 this parameter specifies the relative location of divided cells around the lower quench-front. The finer cells are used for heat conductor cells from (IQU + NU3-(NU1-1))th to (IQU + NU3)th, where IQU shows the heat conductor cell in which the lower quench-front exists.

1'/4 (I4) NO1 number of heat conductor cells which are divided into finer cells around the upper quench-front. When NO1 = 0, the moving finer mesh is not used for the upper quench-front.

1'/5 (I4) NO2 number of finer cells per each heat conductor

cell (upper quench-front).

1′/6 (I4) NO3 this parameter specifies the relative location of divided cells around the upper quench-front.
The finer cells are used for heat conductor cells from (IQO + NO3)th to
(IQU + NO3 + (NO1-1)th.
where IQO shows the heat conductor cell in which the lower quench-front exists.
Note that NO3 is usually negative.

Appendix B. Example of Job Control Language and Input Data for FLUT-FDWR-MM

The Job Control Language and input data for NEPTUN benchmark calculation are given below.

```
//PROJECTG JOB (____,___,_____),MORI,TIME=20,
// REGION=3000K,NOTIFY=PROJECT,MSGCLASS=A
//**-----------------------------------------
//*
//*
//*
//*MAIN LINES=20
//**AIN SYSTEM=M7890                                              21.08.89
//*                    PROJECT.NEPTUN3.DATA                         T.MORI
//*****************************************************************************
//*
//*                     JCL TO  START  'PROJECT.FLUTFDWR.LOAD(A5)'
//*                     LOAD MODULE OF FLUT-FDWR-MM
//*
//*      ***********         S T A R T    R U N              ***********
//*
//*****************************************************************************
//*
// EXEC PGM=A5
//STEPLIB DD DSN=PROJECT.FLUTFDWR.LOAD,DISP=SHR
//*
//*********** TEMPORARY DISK TO BUFFER INPUT DATA ********************
//FT01F001 DD UNIT=SYSDA,DCB=DCB.DATA
//*
//************STOFFWERTE*************************************************
//FT03F001 DD DSN=PROJECT.FLUTN5.STOFF,DISP=SHR,LABEL=(,,,IN)
//*
//************ OUTPUT DATA SET ***************************************
//FT06F001 DD SYSOUT=*,DCB=(RECFM=FBA,LRECL=137,BLKSIZE=137,BUFNO=1)
//*
//************ D E B U G ********************************************
//FT07F001 DD SYSOUT=A,DCB=*.FT06F001
//*
//************P L O T -DATASET*****************************************
//**09F001 DD DSN=PROJECT.NEPA8H.F09,DISP=SHR
//FT09F001 DD DSN=PROJECT.NEPA8H.F09,UNIT=DISK,VOL=SER=BAT00C,
//         DISP=(NEW,CATLG),SPACE=(TRK,(2,5),RLSE),
//         DCB=(RECFM=VBS,LRECL=19065,BLKSIZE=19069)
//FT10F001 DD DSN=PROJECT.NEPA8H.F10,UNIT=DISK,VOL=SER=BAT00C,
//         DISP=(NEW,CATLG),SPACE=(CYL,(1,5),RLSE),
//         DCB=(RECFM=VBS,LRECL=19065,BLKSIZE=19069)
//**10F001 DD DSN=PROJECT.NEPA8H.F10,DISP=SHR
//*
//************H E C U - D A T A  FOR SPECIAL INPUT DATA  SET********
//*
//*  NOT USED IN THIS CASE
//*
//FT11F001 DD DUMMY
//*
//*********** R E S T A R T - DATASET  ******************************
//*   WRITTEN IN CASE OF START RUN
//FT12F001 DD DSN=PROJECT.NEPA8H.REST,UNIT=DISK,VOL=SER=BAT00C,
//         DISP=(NEW,CATLG),SPACE=(CYL,(1,2),RLSE),
//         DCB=(RECFM=VBS,LRECL=19065,BLKSIZE=19069)
//**12F001 DD DSN=PROJECT.NEPA8H.REST,DISP=SHR
//*
//************ INPUT DATA ********************************************
```

```
//FT05F001 DD *
=      NEPTUN  (APWR8 BENCHMARK ) DATASET FOR FLUT-FDWR-MM
=*************************************************************************
=
=                       F L U T - F D W R - M M
=
=
=          WITH DROPLET MODEL (INDDQ=1)
=          IWR=5, NR=3
=          RV=RL=0.10
=
=          INLET PRESSURE LOSS COEFFICIENT = 1.2
=
=          8 CELLS: THE FIRST IS CONNECTED WITH AN UNHEATED SEGMENT
=          43 HEAT SLABS
=          HM = 0.1
=          CLIMV(5) = 0.1 , CLIMV(6) = 0.01
=
=          INITIAL CONDITIONS:
=                              FIRST CELL WITH ALPHA=0.21
=                              AND NO HEAT ADDED
=                              ZQU=0.  (SHOULD BE 0.042)
=
=          CALCULATION WITH NEW MATERIAL DATA AND THE ORIGINAL FLUT-FDWR
=                             ================
=*************************************************************************
=    TEIL1:   DIE DIMENSIONIERUNG BESTIMMENDE GROESSEN
=*************************************************************************
= MAXG : ANZAHL DER VARIABLEN              I1D
= M    : MAXIMALE ANZAHL VON BOXEN/ROHR    I=1
= MG   : ANZAHL ALLER BOXEN IM SYSTEM
= I1D  : ANZAHL DER 1D-TEILE
= ILUMP: ANZAHL DER LUMP-TEILE
=
=       MAXG           M        MGES         I1D       ILUMP       NQEXT
           6           8           8           1           2           1
=
=*************************************************************************
=    TEIL 2:  GROESSEN ZUR NETZSTRUKTUR
=*************************************************************************
=
=   LA = BEZEICHNUNG DES 'LINKEN'  (LA) LUMP-TEILS (TOP(1:I1D))
=   LE = BEZEICHNUNG DES 'RECHTEN' (LE) LUMP-TEILS (TOP(I1D+1:2*I1D)
=
=   XL/YL = KOORDINATEN DES LINKEN  LUMP-TEILS (GEO(1:2*I1D))
=   XR/YR = KOORDINATEN DES RECHTEN LUMP-TEILS (GEO(2*I1D+1):4*I1D)
=   NBOX  = ANZAHL DER BOXEN/ROHR
=
=ROHR-NR SYST-NR  LA  LE      XL      YL      XR      YR  NBOX
       1       0   1   2     0.0     0.0     0.0     0.0     8
=                                                              00470000
= LUMP-TYPEN-TABELLE                                           00480000
= ------------------                                           00490000
=  TYP :  STEUERPARAMETER FUER UP FKTLUM UND KNOTEN            00491006
=         (VERSCHIEDENE MOEGLICHKEITEN DER BERECHNUNG         00492006
=         DER LUMP-ZEITABLEITUNGEN, UND VERLAENGERTEN         00493006
=         GESCHWINDIGKEITEN*FL AUF ROHRANFANG(ENDE)           00494006
```

```
 =     TYP GROESSER ALS NULL - ABLEITUNGEN BERECHNET                    00495006
 =     TYP KLEINER,GLEICH NULL - ABLEITUNGEN=0                          00496006
 =     TYP = +-1  UV,UL AUF NULL GESETZT                                00497006
 =     TYP = +-2  UV,UL GLEICH UV,UL AM ROHRRAND                        00498006
 =     TYP = +-3  BEI EINSTROEMUNG UV,UL GLEICH NULL                    00499006
 =              BEI AUSSTROEMUNG UV,UL GLEICH UV,UL AM ROHRRAND         00499106
 =       IQEXT:  STEUERPARAMETER  FUER  BELEGUNG  DER  THERME  FUER  EXTERNE
QUELLEN00499206
 =          ( IQEXT=0: KEINE EXT. QUELLE )                               00499306
 =                                                                       00540000
 =
 =LUMP-NR SYST-NR     TYP    IQEXT
        1        0       1        1
        2        0       0        0
 =
 =*************************************************************************
 =    TEIL 3:   GROESSEN ZUR RESTART- UND AUSGABESTEUERUNG
 =*************************************************************************
 = INTEST : T -> ES ERFOLGT KEINE RECHNUNG, NUR EINGABETEST
 = RESTART: LRSTRT MUSS AUF .TRUE. GESETZT WERDEN;
   INTEST: F
   LRSTRT: F
 = ISTEP: JEDEN ISTEP-TEN ZEITSCHRITT WERDEN DATEN FUER RESTART AUF
 =        PLATTENBEREICH GESCHRIEBEN
 = ISTART: DER RESTART BEINNT MIT DEM ISTART-TEN ZEITSCHRITT DES 1. LAUFS
 =        (ISTART=0: RESTARTBEGINN MIT LETZTEM ZEITSCHRITT DES 1. LAUFS)
 =       ISTEP       ISTART
           100         3350
 =
 = STEUERGROESSEN FUER AUSDRUCK
 =
 = JEDER IWISH1-TE ZEITPUNKT WIRD AUSGEDRUCKT
 =      IWISH1       IWISH2       IWISH3
           400          100           10
 =       NOUTU        NOUTO
         40000        40000
 =
 =
 =  LPEING = T:    AUSDRUCK DER EINGABEDATEN NACH EINGABEVERARBEITUNG
 =  OUTZU2 = T:    AUSDRUCK VON MASSENSTROM-  UND ENERGIEDICHTE
 =  OUTZU3 = T:    AUSDRUCK DER VOLLSTAENDIGEN PLOT-TABELLE
 =  LPTEST = T:    TESTAUSDRUCK IN EINIGEN PROGRAMMEN
 =  LPEING OZU1 OZU2  OZU3  LPTEST
      T     F     T     T     F
 = LPRTA  LGRENZ
      T     T
 =
 =  STEUERGROESSEN FUER AUSDRUCK VON AUSGEWAEHLTEN VARIABLEN
 =  ZU JEDEM ZEITSCHRITT
 =  NSOUT: ANZAHL DER ZU DRUCKENDEN VARIABLEN
 =  IOROHR(I),I=1,...,I1D  : ROHR-NUMMER
 =  IOPKT(I), I=1,...,NSOUT: ORTSPUNKT (1)=IOPKT)=(2*M+3))
 =  IOVAR(I), I=1,...,NSOUT: VARIABLENNUMMER (1: ALPHA, 2: P, 3: HV,
 =                                            4: HL, 5: WV, 6: WL)
 =                                 (DIMENSION. IN BLDATA FUER NSOUT)=20)
 =       NSOUT
             0
```

```
=  IOROHR(I)     IOPKT(I)     IOVAR(I)
=           1            3            1
=
=
=    AUSGABE VON ZUSATZAUSDRUCK
 BOXRANDPUNKTE
 FUER     1 ROHRE (0 ROHRE = KEIN ZUSATZAUSDRUCK)
=
 ROHR NR     1     2 PUNKTE
=BOXNUMMER
     1
     2
=
 BOXMITTELPUNKTE
 FUER     1 ROHRE (0 ROHRE = KEIN ZUSATZAUSDRUCK)
=
 ROHR NR     1     3 PUNKTE
=BOXNUMMER
     1
     2
     3
=
=    STEUERUNG DER PLOTAUSGABE
=    -------------------------
=
=     1  ALPHA                    AV          20  DAMPFTEMPERATUR      TVAX
=     2  DRUCK                     P          21  WASSERTEMPERATUR     TLAX
=     3  ENTHALPIE DAMPF          HV          22  SAETTIGKEITSTEMP.    TSAX
=     4  ENTHALPIE WASSER         HL          23  BRENNST.-TEMP.         TT
=                                             24  WANDTEMP. LINKS       TSL
=                                             25  WANDTEMP. RECHTS      TSR
=     5  GESCHWINDIGKEIT DAMPF   WV          26  WAERMEUEB.-ZAHL      ALFA
=     6  GESCHW. WASSER           WL          27  WU-ZAHL DAMPF       ALFAV
=     7  THERMOGROESSE            VV          28  WS-DI DAMPF LINKS    QHVL
=     8  THERMOGROESSE            VL          29  WS-DI GESAMT LINKS    QHL
=     9  THERMOGROESSE            TV          30  WS-DI DAMPF RECHTS   QHVR
=    10  THERMOGROESSE            TL          31  WS-DI GESAMT RECHTS   QHR
=    11  THERMOGROESSE            TS          32  MASSENSTROM GV         GV
=    12  MASSENBILANZ            BIL          33  MASSENSTROM WASSER     GL
=                                             34  MASSENSTROM GES.        G
=    13  ENERGIEBILANZ          EBIL          35  QUENCHFR. U. LINKS    ZQUL
=    14  IMPULSBILANZ           FBIL          36  QUENCHFR. U. RECHTS   ZQUR
=    15  COLLAPSLEVEL           COLE          37  QUENCHFR. O. LINKS    ZQOL
=    16  DUMMY (RESERVE)      ADUMMY          38  QUENCHFR. O. RECHTS   ZQOR
=    17  OXIDAT.-SCHICHTDICKE  DXOX          39  LEIST.-DI. DAMPF       QFV
=    18  FLUIDTEMP. LINKS        TTL          40  LEIST.-DI. WASSER      QFL
=    19  FLUIDTEMP. RECHTS       TTR          41  ZEITSCHRITT DT
=                                             42  BEN. CPU-ZEIT  TCPU
=                                             43  DP PUMPE
=                                             44  UMDREH. PUMPE
=                                             45  REM
=                                             46  RED
=                                             47  REW
=
=  1  2  3  4  5  6  7  8  9 10 11 12 13 14 15 16 17 18 19 20
   T  T  T  T  T  T  T  T  T  T  T  T  T  T  T  F  F  F  T  F
= 21 22 23 24 25 26 27 28 29 30 31 32 33 34 35 36 37 38 39 40
```

```
    F  F  F  T  T  T  T  F  F  T  T  T  T  T  F  T  F  T  T  T
 = 41 42 43 44 45 46 47
    T  T  F  F  T  T  T
 =
 =
 =*************************************************************************
 =    TEIL 4:   STEUER- UND SKALIERUNGSGROESSEN
 =*************************************************************************
 =
 =           STEUERUNG DES LOESUNGSVERFAHRENS
 = IFTRIX=1  ENRIGHT-VERFAHREN
 = IFTRIX=2  ENRIGHT-VERFAHREN MIT AUSNUTZ. DER BLOCKTRIDIAGONALSTRUKTUR
 = IFTRIX=3  FTRIX - VERFAHREN MIT AUSNUTZ. DER BLOCKTRIDIAGONALSTRUKTUR
 = IFTRIX
     3
 =
 =
 = DEFINITION DES RECHENBEREICHES
 = TO: PROBLEMANFANGSZEIT   TEND:PROBLEMENDZEIT
 =          TO          TEND
   0.00000D00      300.0D0
 = H: ANFANGSZEITSCHRITT    HM: MAXIMALER ZEITSCHRITT
 =           H           HM
   1.00000D-5      1.0D-01
 =
 = STEUERGROESSEN FUER DIE ZEITINTEGRATION:
 =
 = INTEGRATIONSMETHODE: IMEX
 = RECHENGENAUIGKEIT
 =         EPS       ECKSCH       GRESCH        CHMAX
 =     5.0D-03       1.0D-6       1.0D-6      5.0D 00
       1.0D-02       1.0D-6       1.0D-7      5.0D 00
 =
 =     TIP(AV)      TIP( P)      TIP(HV)      TIP(HL)      TIP(WV)      TIP(WL)
             T            T            T            T            T            T
 =
 =     TSE(AV)      TSE( P)      TSE(HV)      TSE(HL)      TSE(WV)      TSE(WL)
             F            F            F            F            F            F
 =
 =   CLIMV(AV)    CLIMV( P)    CLIMV(HV)    CLIMV(HL)    CLIMV(WV)    CLIMV(WL)
       1.0D-04      1.0D-04      1.0D-04      1.0D-04      1.0D-02      1.0D-04
 =     1.0D-04      1.0D-04      1.0D-04      1.0D-04      1.0D-01      1.0D-02
 =
 =
 = BERECHNUNG DER JACOBIMATRIX: RELATIVE STOERUNG
 = EH1JAC(AV)  EH1JAC( P)  EH1JAC(HV)  EH1JAC(HL)  EH1JAC(WV)  EH1JAC(WL)
 =     1.0D-04      1.0D-05      1.0D-05      1.0D-05      1.0D-04      1.0D-04
       1.0D-05      1.0D-04      1.0D-04      1.0D-04      1.0D-03      1.0D-03
 =
 = BERECHNUNG DER JACOBIMATRIX: MAXIMALE STOERUNG
 = HM1JAC(AV)  HM1JAC( P)  HM1JAC(HV)  HM1JAC(HL)  HM1JAC(WV)  HM1JAC(WL)
       1.0D-06      1.0D-02      1.0D-01      1.0D-01      1.0D-05      1.0D-05
 =
 =*************************************************************************
 = TEIL 5: DAS PHYSIKALISCHE MODELL BESCHREIBENDE EINGANGSGROESSEN
 =*************************************************************************
 =
```

```
=
= SKALIERUNGSGROESSEN FUER DIE VERSCHNEIDUNG DER ORTSABLEITUNGEN (QAS)1)
=       QAS1         QAS2         QAS3         QAS4
      0.0D 00      0.0D 00      0.0D 00      0.0D 00
=
=
=  FAKTOR FUER DRUCKKORREKTUR NACH BERNOULLI (ROHRRAND - LUMP)
=       CWFL         CWFR
      0.0D 00      0.0D 00
=
=
=       EPSAV        EPSAL
      1.0D-06      1.0D-08
=
=
=   PARAMETER FUER DIE WANDREIBUNG UND DIE ZWISCHENPHASNREIBUNG
=       ETAV         ETAL           RV           RL
      1.3D-05      2.0D-04      1.0D-01      1.0D-01
=
=   PARAMETER FUER DEN PHASENUEBERGANGS-ENERGIEAUSTAUSCH
=       CVERD        CKOND          CS3          CS4          CS5          CS6
      1.0D 02      1.0D 01      1.0D 03      1.0D 03      1.0D-04      1.0D-01
=
=   ENERGIEZUFUHR VON AUSSEN (QWVL)
= CW01 (VAP)  CW02 (LIQ)
      0.0D 00      0.0D 00
=
=       CAWV1        CAWV2        CAWL1        CAWL2         RWVL         RWLV
      1.0D-03      1.0D-02 1.000  D 00 0.99999D 00      1.0D 00      1.0D 00
=
=         AVT          AVR          ALT          ALR
      1.0D-10      1.0D-10      1.0D-10     1.0 D-10
=
=   ALPHAMAX         PMAX         HVMAX        HLMAX        WVMAX        WLMAX
  1.0001D 00     1.80D 07     6.00D 06     1.74D 06     1.00D 05     1.00D 05
=
=   ALPHAMIN         PMIN         HVMIN        HLMIN        WVMIN        WLMIN
  -1.000D-06     1.00D 04      2.4D 06      1.0D 05    -1.00D 05    -1.00D 05
=
= ***************************************************************************
=  TEIL 6:    ROHRDATEN
= ***************************************************************************
 ROHR NR     1:
 ==========
=      A) GEOMETRISCHE DATEN
=      ====================
= DDX(I): BOXLAENGEN FUER DIE BOXEN I=1,NBOX(1)
=         DDX
   1.150 D-01
   2.000 D-01
   2.400 D-01
   2.400 D-01
   2.400 D-01
   2.400 D-01
   2.400 D-01
   2.400 D-01
   2.400 D-01
```

```
  1.000 D-01
=
= HOEHENUNTERSCHIED ZWISCHEN ROHRANFANG UND ENDE UND LUMPMITTE
=         HRA         HRE         INDDQ
  0.115 D 00   -.100 D 00          1
=
=      DISTAN        DSMA         DLAR          RV         RL
       0.2000      .127D-3     2.00D-3         .10        .10
= CFL (I) QUERSCHNITTSFLAECHE FL
= DHYD(I) HYDR.DURCHMESSER
= CST (I) ROHRNEIGUNG (COS DES ZWISCHENWINKELS ROHR-SENKRECHTE)
=                 AM PUNKT I, I = 1,...,2*(NBOX(J)+3
=
=         CFL          DHYD           CST       ZETAFV       ZETAFR
  1.5590D-03  4.170 D- 3  +1.0 D 00  0.0   D 00  0.00  D 00
  1.5590D-03  4.170 D- 3  +1.0 D 00  1.20  D 00  1.20  D 00
  1.5590D-03  4.170 D- 3  +1.0 D 00  0.885 D 00  0.885 D 00
  1.5590D-03  4.170 D- 3  +1.0 D 00  0.57  D 00  0.57  D 00
  1.5590D-03  4.170 D- 3  +1.0 D 00  0.57  D 00  0.57  D 00
  1.5590D-03  4.170 D- 3  +1.0 D 00  0.57  D 00  0.57  D 00
  1.5590D-03  4.170 D- 3  +1.0 D 00  0.57  D 00  0.57  D 00
  1.5590D-03  4.170 D- 3  +1.0 D 00  0.57  D 00  0.57  D 00
  1.5590D-03  4.170 D- 3  +1.0 D 00  0.57  D 00  0.57  D 00
  1.5590D-03  4.170 D- 3  +1.0 D 00  0.57  D 00  0.57  D 00
  1.5590D-03  4.170 D- 3  +1.0 D 00  0.57  D 00  0.57  D 00
  1.5590D-03  4.170 D- 3  +1.0 D 00  0.57  D 00  0.57  D 00
  1.5590D-03  4.170 D- 3  +1.0 D 00  0.57  D 00  0.57  D 00
  1.5590D-03  4.170 D- 3  +1.0 D 00  0.57  D 00  0.57  D 00
  1.5590D-03  4.170 D- 3  +1.0 D 00  0.57  D 00  0.57  D 00
  1.5590D-03  4.170 D- 3  +1.0 D 00  0.57  D 00  0.57  D 00
  1.5590D-03  4.170 D- 3  +1.0 D 00  0.385 D 00  0.385 D 00
  1.5590D-03  4.170 D- 3  +1.0 D 00  0.2   D 00  0.20  D 00
  1.5590D-03  4.170 D- 3  +1.0 D 00  0.2   D 00  0.20  D 00
=
= PARAMETER FUER WANDREIBUNGSVERLUST
=         IWR        CVISCV       CVISCL
            5   0.0    D 00  0.00  D 00
=          NR         PROD         DROD           HSP
            3   12.12 D-03   10.72 D-03         0.D-0
=
=
=         B) ANFANGSWERTE
=            ==============
=
=
= .  .  .  .  .  .  .  .  .  .  .  .  .  .  .  .  .  .  .
= PUNKTWERTEINGABE (ANFANGS- UND ENDWERT ODER 2*M+3 WERTE)
= (NPKTW = 2      BEI EINGABE DER DATEN AM ROHRANFANG UND ROHRENDE,
=           2*M+3 BEI EINGABE ALLER PUNKTWERTE)
=
=      NPKTW (ANZAHL DER PRO VARIABLE EINZULES. WERTE (2 BZW. 2*M+3))
           19
=
=          AV            P            HV            HL           WV           WL
  0.0    D 00 4.20    D 05 2.740   D 06 2.8575 D 05 2.42    D-02 2.42    D-02
  0.0    D 00 4.19    D 05 2.740   D 06 2.8575 D 05 2.42    D-02 2.42    D-02
  0.79   D 00 4.18    D 05 2.740   D 06 2.8575 D 05 2.42    D-02 2.42    D-02
  1.0    D 00 4.18    D 05 2.740   D 06 4.5000 D 05 2.42    D-02 2.42    D-02
```

```
   1.0   D 00 4.18   D 05 2.740  D 06 6.1300 D 05 2.42   D-02 2.42   D-02
   1.0   D 00 4.18   D 05 2.740  D 06 6.1300 D 05 0.0    D 00 0.0    D 00
   1.0   D 00 4.18   D 05 2.85   D 06 6.1300 D 05 0.0    D 00 0.0    D 00
   1.0   D 00 4.18   D 05 2.90   D 06 6.1300 D 05 0.0    D 00 0.0    D 00
   1.0   D 00 4.18   D 05 2.98   D 06 6.1300 D 05 0.0    D 00 0.0    D 00
   1.0   D 00 4.18   D 05 3.05   D 06 6.1300 D 05 0.0    D 00 0.0    D 00
   1.0   D 00 4.18   D 05 3.12   D 06 6.1300 D 05 0.0    D 00 0.0    D 00
   1.0   D 00 4.18   D 05 3.20   D 06 6.1300 D 05 0.0    D 00 0.0    D 00
   1.0   D 00 4.18   D 05 3.15   D 06 6.1300 D 05 0.0    D 00 0.0    D 00
   1.0   D 00 4.18   D 05 3.10   D 06 6.1300 D 05 0.0    D 00 0.0    D 00
   1.0   D 00 4.18   D 05 3.05   D 06 6.1300 D 05 0.0    D 00 0.0    D 00
   1.0   D 00 4.18   D 05 3.00   D 06 6.1300 D 05 0.0    D 00 0.0    D 00
   1.0   D 00 4.18   D 05 2.95   D 06 6.1300 D 05 0.0    D 00 0.0    D 00
   1.0   D 00 4.18   D 05 2.90   D 06 6.1300 D 05 0.0    D 00 0.0    D 00
   1.0   D 00 4.18   D 05 2.90   D 06 6.1300 D 05 0.0    D 00 0.0    D 00
=
=*************************************************************************
=*************************************************************************
=
=
=*************************************************************************
=     TEIL 7:     LUMP-SPEZIFISCHE ANGABEN:
=*************************************************************************
=
=LUMP-NR          VOL
       1  6.236 D-04
       2  1.000 D 03
=
= VORBELEGUNG FUER LUMP-TEILE
= ANZ. DER VORBEL. LUMP-TEILE:
       0
=
= DRUCK AN DER BRUCHSTELLE
= LUMPNR   NPBRU
       2       0
= PBRU(NPBRU)
= 4.1   D 05 0.00   D 00 4.1    D 05 1.5    D 02
=
= BELEGUNG DER QUELLTHERME
= (FUER JEDEN QUELLENTYP IQTYP, ZUORDNUNG ZUM LUMP DURCH IQEXT)
=  IQTYP          QFL          QAV          QHV          QHL
       1  1.5590D-03   0.0  D 00 2.740  D 06  2.8575D 05
=                 QWV          QWL         QROV         QROL
           2.420 D-02   2.420D-02   2.264D 00  9.7980D 02
=
=
= FLUTRATEN FUER IQTYP=1
= NFLRA1    KALTEINSP.
       0
= FLRA1(NFLRA1) -NUR EINGEBEN, WENN NFLRA1 .GT. 0
=3.65817D-01 0.00   D 00 3.65817D-01 67.00  D 00 4.06789D-01 67.10  D 00
=4.06789D-01 202.   D 00 4.41907D-01 202.1  D 00 4.41907D-01 540.0  D 00
=4.53613D-01 540.1  D 00 4.53613D-01 643.   D 00 4.53613D-01 900.0  D 00
= NFLRA2    HEISSEINSPEIS.
       0
= FLRA2(NFLRA2)  NUR WENN NFLRA2 .GT. 0
= NFLRA3
```

```
        0
= NFLRA4
        0
=
=-------------------------------------------------------------------------
=
= ENDE DATEN EINGABE FLUID-DYNAMIK
=
=-------------------------------------------------------------------------
=*************************************************************************
=    PUMPENDATEN
=IARM2
     0
=
=*************************************************************************
=
=        HECU- EINGABEDATEN FUER FLUT
=
=IHV    NHTE       NM      NER      NAL     NROHR
=   NROD      NQ       NT      NNK     IOPTHC
 -43    1    0    1    3    0    0    0    0    3    1
=NU1 NU2 NU3 NO1 NO2 NO3 ============================>>>>>>> NEW INPUT
   3    6    1    3    6   -1
=NOLAYS
=
   8    8    8    8    8    8    8    8    8    8    8    8    8    8    8    8    8    8
   8    8    8    8    8    8    8    8    8    8    8    8    8    8    8    8    8    8
   8    8    8    8    8    8    8
=
=*************************************************************************
=-------------------------------------------------------------------------
=
=        HECU-FLUT ZUSATZ-INFORMATIONEN
=
= INTOPT=0: NACHGEZOGENER HECU-ZEITSCHRITT
=         1: IMPL. Q-BERECHN. FUER DE- UND SW-HEATSL. MIT TFLUID-AKT.
=         2: IMPL. Q-BERECHN. FUER DE- UND SW-HEATSL. MIT TFLUID-AKT.UND
=                                                       HTC-AKT.
= INTOPT LTTLES
     0      F
=
=
=     _____ BRENNSTAB _______
=
= ID: ROHR- BZW. LUMPKENNZEICHNUNG (R BZW. L)
= ITEIL:ROHR- BZW. LUMPNAME (S. EINGABETEIL NETZSTRUKTUR)
=      ID ITEIL NMTYP NRODK
        R     1    43     1
=
=MHV1 2 NSKL R   HTCL(1)      HTCL(2)      HTCL(3)      HTCL(4)          QAB
  1   1   0  1          0.      25.D+04       3.D+04 2.00    D+02     0.00D+00
  2   2   0  2          0.      25.D+04       3.D+04 3.13    D+02     0.00D+00
  3   3   0  2          0.      25.D+04       3.D+04 3.46    D+02     0.00D+00
  4   4   0  2          0.      25.D+04       3.D+04 3.73    D+02     0.00D+00
  5   5   0  2          0.      25.D+04       3.D+04 3.99    D+02     0.00D+00
  6   6   0  2          0.      25.D+04       3.D+04 4.26    D+02     0.00D+00
  7   7   0  2          0.      25.D+04       3.D+04 4.56    D+02     0.00D+00
```

```
  8   8   0   3          0.      25.D+04      3.D+04 4.86    D+02     0.00D+00
  9   9   0   3          0.      25.D+04      3.D+04 5.07    D+02     0.00D+00
 10  10   0   3          0.      25.D+04      3.D+04 5.25    D+02     0.00D+00
 11  11   0   3          0.      25.D+04      3.D+04 5.46    D+02     0.00D+00
 12  12   0   3          0.      25.D+04      3.D+04 5.67    D+02     0.00D+00
 13  13   0   3          0.      25.D+04      3.D+04 5.79    D+02     0.00D+00
 14  14   0   4          0.      25.D+04      3.D+04 5.91    D+02     0.00D+00
 15  15   0   4          0.      25.D+04      3.D+04 6.00    D+02     0.00D+00
 16  16   0   4          0.      25.D+04      3.D+04 6.09    D+02     0.00D+00
 17  17   0   4          0.      25.D+04      3.D+04 6.11    D+02     0.00D+00
 18  18   0   4          0.      25.D+04      3.D+04 6.18    D+02     0.00D+00
 19  19   0   4          0.      25.D+04      3.D+04 6.15    D+02     0.00D+00
 20  20   0   5          0.      25.D+04      3.D+04 6.09    D+02     0.00D+00
 21  21   0   5          0.      25.D+04      3.D+04 6.03    D+02     0.00D+00
 22  22   0   5          0.      25.D+04      3.D+04 5.94    D+02     0.00D+00
 23  23   0   5          0.      25.D+04      3.D+04 5.85    D+02     0.00D+00
 24  24   0   5          0.      25.D+04      3.D+04 5.64    D+02     0.00D+00
 25  25   0   5          0.      25.D+04      3.D+04 5.46    D+02     0.00D+00
 26  26   0   6          0.      25.D+04      3.D+04 5.31    D+02     0.00D+00
 27  27   0   6          0.      25.D+04      3.D+04 5.10    D+02     0.00D+00
 28  28   0   6          0.      25.D+04      3.D+04 4.86    D+02     0.00D+00
 29  29   0   6          0.      25.D+04      3.D+04 4.65    D+02     0.00D+00
 30  30   0   6          0.      25.D+04      3.D+04 4.41    D+02     0.00D+00
 31  31   0   6          0.      25.D+04      3.D+04 4.11    D+02     0.00D+00
 32  32   0   7          0.      25.D+04      3.D+04 3.87    D+02     0.00D+00
 33  33   0   7          0.      25.D+04      3.D+04 3.55    D+02     0.00D+00
 34  34   0   7          0.      25.D+04      3.D+04 3.25    D+02     0.00D+00
 35  35   0   7          0.      25.D+04      3.D+04 2.95    D+02     0.00D+00
 36  36   0   7          0.      25.D+04      3.D+04 2.59    D+02     0.00D+00
 37  37   0   7          0.      25.D+04      3.D+04 2.32    D+02     0.00D+00
 38  38   0   8          0.      25.D+04      3.D+04 2.17    D+02     0.00D+00
 39  39   0   8          0.      25.D+04      3.D+04 2.17    D+02     0.00D+00
 40  40   0   8          0.      25.D+04      3.D+04 2.17    D+02     0.00D+00
 41  41   0   8          0.      25.D+04      3.D+04 2.17    D+02     0.00D+00
 42  42   0   8          0.      25.D+04      3.D+04 2.17    D+02     0.00D+00
 43  43   0   8          0.      25.D+04      3.D+04 2.17    D+02     0.00D+00
=
=  WAERMEUEBERGANGS- UND QUENCHMODELL FLUT
=  ======================================
=
= ICHF : AUSWAHL DES QUENCH- UND WAERMEUEBERGANGSMODELLS
=         1: QUENCHMODELL FUER BS, HTCSEG (MIT QF)
=         0: KEIN QUENCHMODELL   , HTCSW  (OHNE QF)  WUE FUER SW-SLABS
=        -1: KEIN QUENCHMODELL   , HTCSTG (OHNE QF)  WUE FUER DE-SLABS
= ICHF
      1
=      DTLEID        SIGMA       WUCHFO       WUCHF          WQ
= 1.6000D+02  0.0520D+00  1.0000D+04  5.0000D+04    0.03D+00
  1.6000D+02  0.0520D+00  0.5000D+05  3.0000D+05    0.10D+00
=       DTCHF        ALFSE        AVCRI
 6.00000D+01 4.00000D+02  0.8000D+00
=IFRKOR IQUENU
      0    -2
=
=-------------------------------------------------------------------------
=************************ HEATSLAB DATEN **********************************
=LLENG
```

```
     F
=NGEOR    N2     N3 MATL1 MATL2 MATL3   IALPHA
     2     4      2    -1    -2    -3   0   0   0   1
=PARTIT  (1)          (2)          (3)          (4)          (5)          (6)
          0.     1.725D-3           0.     2.775D-3           0.      8.60D-4
=  HLENGT WIRD IN HCINP BERECHNET (BOXLAENGE/HEATSLABS)
=  AORXL: PLATTE -->AORXL = PLATTENOBERFLAECHE
=         ZYLINDER->AORXL = FAKTOR FUER BERECHNUNG DER OBERFLAECHE
=                           (BS:F=1, DE:F=ANZ. U-ROHRE)
=       AORXL       HLENGT         DHYL         DHYR
     1.000D 0   4.000D-02            0.      4.17D-3
=       WLF(1)      WLF(2)       WLF(3)       CPL(1)       CPL(2)       CPL(3)
          0.0         0.0          0.0       0.0 D0       0.0 D0        0.0D0
=RHOL     (1)         (2)          (3)      ATTL(1)          (2)          (3)
       0.0 D0      0.0 D0       0.0 D0           0.           0.           0.
=
= MATERIALEIGENSCHAFTEN
= ***** CP = F (T) ******     KANTHAL
=     I  NPTS   FNAME
      1     2  CPMAT1
=         TEMP          CP
      0.0 D0     4.20 D  2
   1150.0 D0     7.96 D  2
= ***** CP = F (T) ******     PSEUDOMATERIAL
=     I  NPTS   FNAME
      2    12  CPMAT2
=         TEMP          CP
     20.  D0     4.7379D 2
     50.  D0     4.9518D 2
    100.  D0     5.2195D 2
    200.  D0     5.6351D 2
    300.  D0     5.9704D 2
    400.  D0     6.2534D 2
    500.  D0     6.4948D 2
    600.  D0     6.7385D 2
    700.  D0     6.9946D 2
    800.  D0     7.1759D 2
    900.  D0     7.3019D 2
   1000.  D0     7.4106D 2
= ***** CP = F (T) ******      INCONEL 600
=     I  NPTS   FNAME
      3    10  CPMAT3
=         TEMP          CP
       0. D0     4.35 D  2
      50. D0     4.49 D  2
     100. D0     4.63 D  2
     200. D0     4.87 D  2
     300. D0     5.09 D  2
     400. D0     5.27 D  2
     500. D0     5.42 D  2
     560. D0     5.51 D  2
     740. D0     6.12 D  2
    1150. D0     6.37 D  2
= *****WLF = F (T) ******
=     I  NPTS   FNAME
      1     2 WLFMAT1
=         TEMP         WLF
```

```
    0.00 D0     16.4 D  0
 1150.00 D0     31.8 D  0
= *****WLF = F (T) ******
=     I  NPTS   FNAME
      2    12 WLFMAT2
=        TEMP          WLF
   20.0  D0     16.197 D0
   50.0  D0     16.059 D0
  100.0  D0     15.787 D0
  200.0  D0     15.103 D0
  300.0  D0     14.272 D0
  400.0  D0     13.548 D0
  500.0  D0     12.975 D0
  600.0  D0     12.390 D0
  700.0  D0     11.846 D0
  800.0  D0     11.483 D0
  900.0  D0     11.219 D0
 1000.0  D0     10.997 D0
= *****WLF = F (T) ******
=     I  NPTS   FNAME
      3     2 WLFMAT3
=        TEMP          WLF
    0.0  D0     14.10  D0
 1150.0  D0     33.60  D0
= *****RHO = F (T) ******
=     I  NPTS   FNAME
      1     2 RHOMAT1
=        TEMP          RHO
     0.00D0     7.100D  3
  1200.00D0     7.100D  3
= *****RHO = F (T) ******
=     I  NPTS   FNAME
      2     2 RHOMAT2
=        TEMP          RHO
      0. D0     6.060D  3
   1200. D0     6.060D  3
= *****RHO = F (T) ******
=     I  NPTS   FNAME
      3     2 RHOMAT3
=        TEMP          RHO
      0. D0     8.430D  3
   1200. D0     8.430D  3
=
=
= HEIZLEISTUNGSKONTROLLKURVEN
=    IQ   NPTS
      1     2
=TQ         QNORM
=     ZEIT(I)     DECAY(I)
    0.0      1.0
  500.0      1.0
=
= NSEGS(I)
    43
=
=
= ROHR-NUMMER 1
```

= IROD	IZONE	IQF	RODFAC	QROD	LLAY	IZLAY	LZROX
1	1	1	37.	1.2000D3	F	1	F

= MHV	SPOW1	SPOW2	SPOW3
1	0.00	0.00	0.00
2	0.56	0.56	0.56
3	0.67	0.67	0.67
4	0.76	0.76	0.76
5	0.85	0.85	0.85
6	0.94	0.94	0.94
7	1.04	1.04	1.04
8	1.14	1.14	1.14
9	1.21	1.21	1.21
10	1.27	1.27	1.27
11	1.34	1.34	1.34
12	1.41	1.41	1.41
13	1.45	1.45	1.45
14	1.49	1.49	1.49
15	1.52	1.52	1.52
16	1.55	1.55	1.55
17	1.56	1.56	1.56
18	1.58	1.58	1.58
19	1.57	1.57	1.57
20	1.55	1.55	1.55
21	1.53	1.53	1.53
22	1.50	1.50	1.50
23	1.47	1.47	1.47
24	1.40	1.40	1.40
25	1.34	1.34	1.34
26	1.29	1.29	1.29
27	1.22	1.22	1.22
28	1.14	1.14	1.14
29	1.07	1.07	1.07
30	0.99	0.99	0.99
31	0.89	0.89	0.89
32	0.81	0.81	0.81
33	0.70	0.70	0.70
34	0.60	0.60	0.60
35	0.49	0.49	0.49
36	0.37	0.37	0.38
37	0.29	0.29	0.29
38	0.24	0.24	0.24
39	0.24	0.24	0.24
40	0.24	0.24	0.24
41	0.24	0.24	0.24
42	0.24	0.24	0.24
43	0.24	0.24	0.24

= ENDE DER HECU EINGABE-DATEN FUER FLUT

References

/1/ H.STAEDTKE and W.KOLAR, "Predictions Capabilities of RELAP5/Mod1-EUR; An Improved Version of the LWR Safety Code RELAP5/Mod1," Trans. 4th Int. ENS/ANS Conf. and 9th Foratom Congress (ENC '86) Nuclear Energy of Today and Tomorrow, Geneva, Switzerland, June 1-6, 1986, Vol. 3, p.535.

/2/ V.TESCHENDORFF, "The Two Fluid Code FLUT for LOCA Reflood Analysis," presented at Workshop International Atomic Energy Agency Program in Uses of Computer Codes for Safety Analysis, Varna, Bulgaria, (May 1984).

/3/ M.DALLE DONNE and C.FERRERO, "Loss-of-Coolant-Accident and Anticipated Transient without SCRAM Calculations for Homogeneous and Heterogeneous Advanced Pressurized Water Reactors," Nucl. Technol. **80**, 133 (1988).

/4/ M.CIGARINI and M.DALLE DONNE, "The Reflooding Phase after a Loss -of-Coolant Accident in an Advanced Pressurized Water Reactor," Nucl. Technol. **84**, 33 (1988).

/5/ M.CIGARINI, "Thermohydraulische Untersuchungen zu den Vorgängen wärend der Flutphase nach einem Kühlmittelverlust bei einem fortgeschrittenen Druckwasserreaktor," KfK-4302, Karlsruhe (1987).

/6/ M.CIGARINI, "Evaluation of Forced Reflooding Experiments in APWR-Geometry (NEPTUN-III Facility) using the Advanced Computer Code FLUT-FDWR," KfK 4585, Karlsruhe (1989).

/7/ P.IHLE and K.RUST,"BEBA-Flooding Experiments with Blocked Arrays, Evaluation Report," KfK-3657, Karlsruhe (1984).

/8/ P.IHLE and K.RUST,"BEBA-Flooding Experiments with Blocked Arrays, Data Report 1, Test Series I to IV," KfK-3658, Karlsruhe (1984).

/9/ P.IHLE and K.RUST,"SEFLEX Fuel Rod Simulation Effects in Flooding Experiments-Evaluation Report," KfK-4024, Karlsruhe (1986).

/10/ P.IHLE and K.RUST,"SEFLEX Fuel Rod Simulation Effects in Flooding Experiments-Unblocked Bundle Data," KfK-4025, Karlsruhe (1986).

/11/ H.GRÜTTER, F.STIERLI, S.N.ASKAN and G.VARADI, "NEPTUN Bundle Reflooding Experiments: Test Facility Description," EIR-Bericht Nr. 386, Würenlingen (1980).

/12/ E.FREI and F.STIERLI, "NEPTUN, Information about the Reflood-Experiments 5012-5056," EIR Internal Report TM-32-83-6 (1983).

/13/ F.STIERLI and S.YANAR, "Flutversuche NEPTUN 2: Übersicht, Unterlagen," EIR Internal Report TM-32-85-30 (1985).

/14/ J.DREIER et al., "Experimental Simulation of LOCA Reflooding Conditions for Light Water High Converter Reactors," Proc. 4th European Nuclear Conf. and 9th Foratom Congress (ENC 86) on Nuclear Energy, Geneva, Switzerland, June 1, 1986, Vol. 2, p. 575, European Nuclear Society (1986).

/15/ J.DREIER, G.ANALYTIS and R.CHAWLA, "NEPTUN-III Reflooding and Boiloff Experiments with an LWHCR Fuel Bundle Simulator: Experimental Results and Initial Code Assessment Efforts," Nucl. Technol. **80**, 93 (1988).

/16/ J.DREIER, not published report, Paul Scherrer Institut, Würenlingen, (1988).

/17/ A.HORA,CH.MICHETSCHLÄGER,H.G.SONNENBURG,V.TESCHENDORFF, "Analysis of Reflood Phenomena by the Two Fluid Code FLUT," Proc. of NATO Advanced Research Workshop Spitzingsee/Schliersee, Aug.31-Sept.3, 1982.

/18/ F.J.ERBACHER and K.WIEHR, "Experimental Investigation on Reflooding and Deformation Behaviour of an APWR Tight Lattice Fuel Rod Bundle in a LOCA," Nucl. Technol. **80**, 153 (1988).

/19/ M.CIGARINI, "Vorausberechnung des ersten FDWR-Flutexperimentes mit dem FLUT-Rechenprogramm," PNS-Jahresbericht 1986, pp. 4100-97, KfK 4100, Karlsruhe, (1987).

/20/ R.SEMERIA and B.MARTINET, "Calefaction Spots on a Heating Wall: Temperature Distribution and Resorption," Proc. Inst. Mech. Engr.,180, 192, (1966).

/21/ A.YAMANOUCHI, "Effect of Spray Cooling in Transient State after Loss of Coolant Accident," Journ. of Nucl. Sci. and Tecn., 5(11), 547, (1968).

/22/ Y.Y.HSU and M.W.YOUNG, "A Criterion for the Onset of Quench for Low Flow Reflood," NUREG 0915, (1982).

/23/ M.CIGARINI, "Nachrechnung des FEBA Versuchs Nr. 216 mit dem FLUT Programm," PNS-Jahresbericht 1984, pp. 4100-61, KfK 3550, Karlsruhe, (1985).

/24/ L.E.HOCHREITER and K.RIEDLE, "Reflood Heat Transfer and Hydraulics in Pressurized Water Reactors," Symposium on the Thermal and Hydraulic Aspects of Nuclear Reactor Safety, Vol. 1, ASME, pp. 75-107, (1977).

/25/ R.LEE, "Dispersed Flow Heat Transfer above a Quench Front during Reflood in a Pressurized Water Reactor after a Large Break Loss-of-Coolant Accident," University of Maryland, Ph.D. Thesis, (1982).

/26/ M.CIGARINI, internal KfK-report (1989).

/27/ C.W.OSEEN, "Neuere Methoden und Ergebnisse in der Hydrodynamik," Akademische Verlagsgesellschaft m.b.H. Leipzig, (1927).

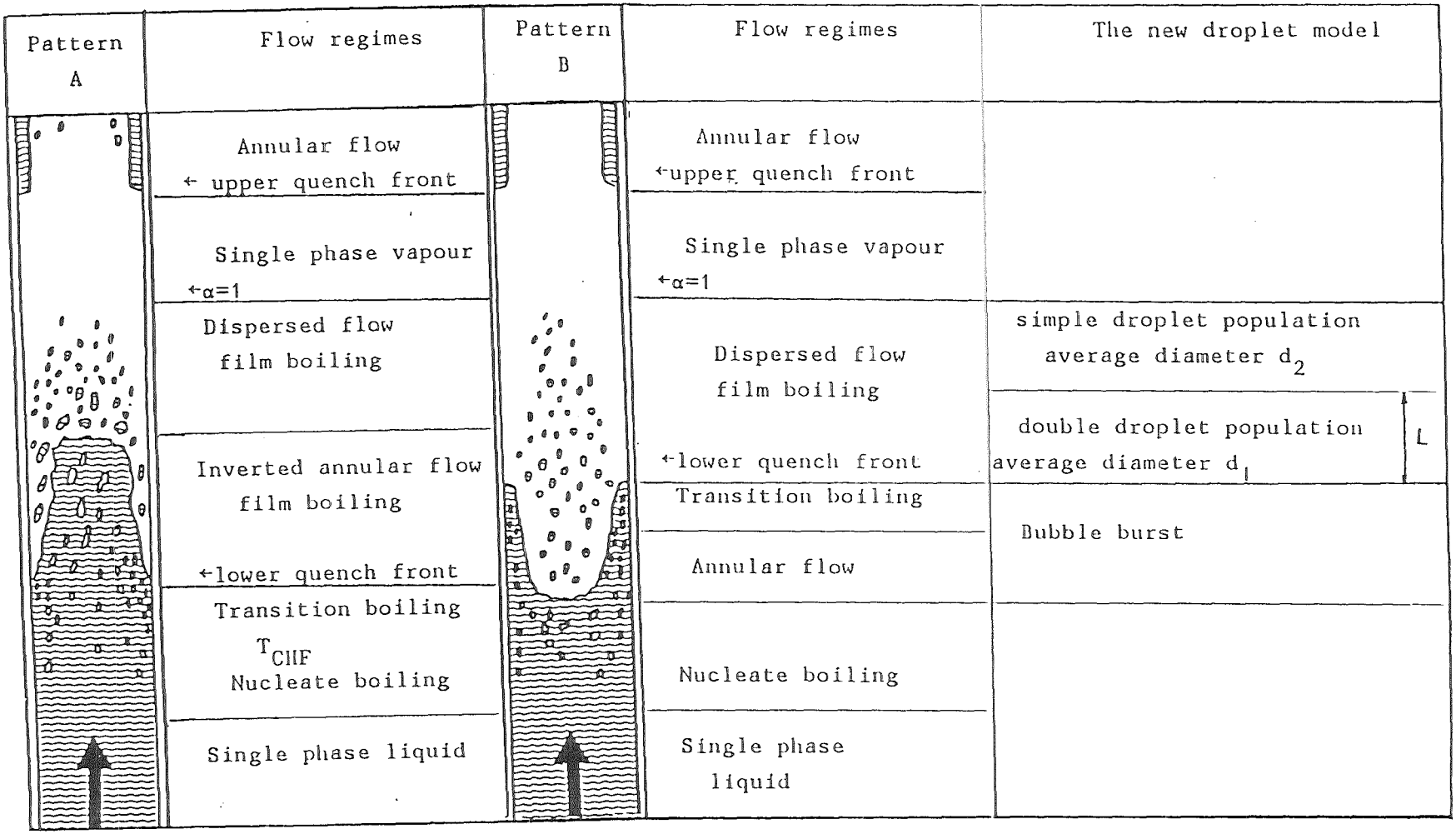

Figure 1. Reflood flow regimes and droplet model.

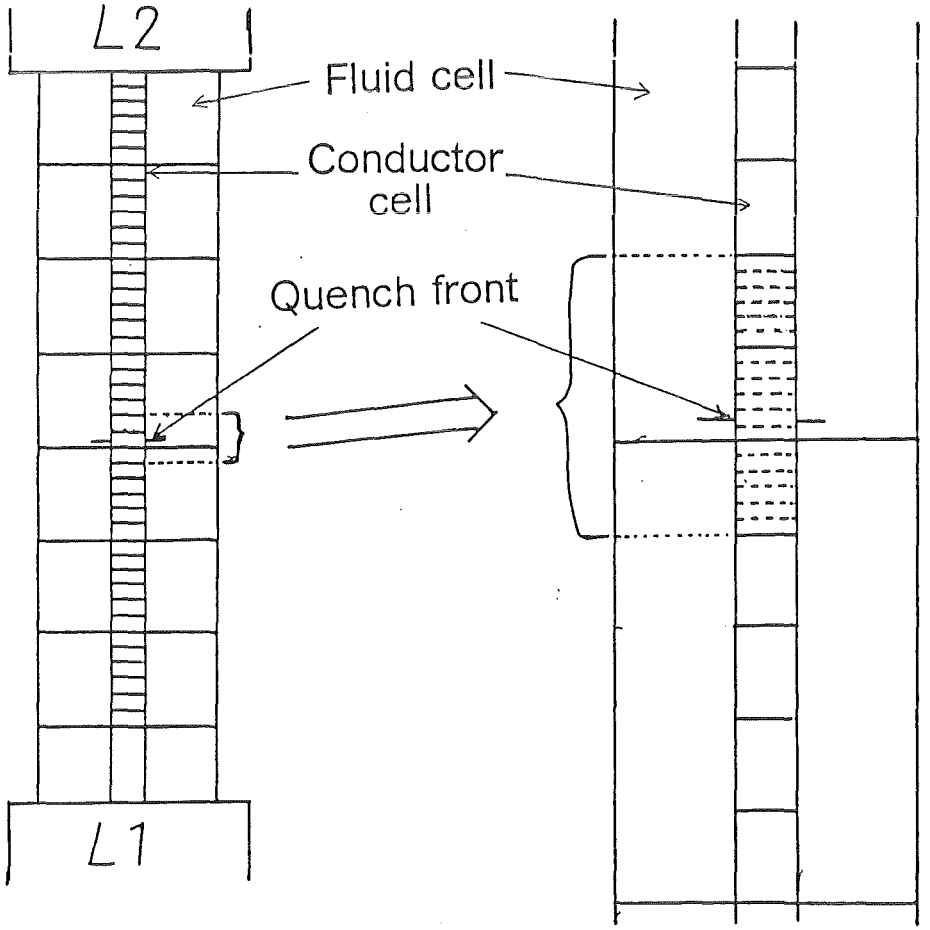

Figure 2. Conceptual illustration of moving mesh.

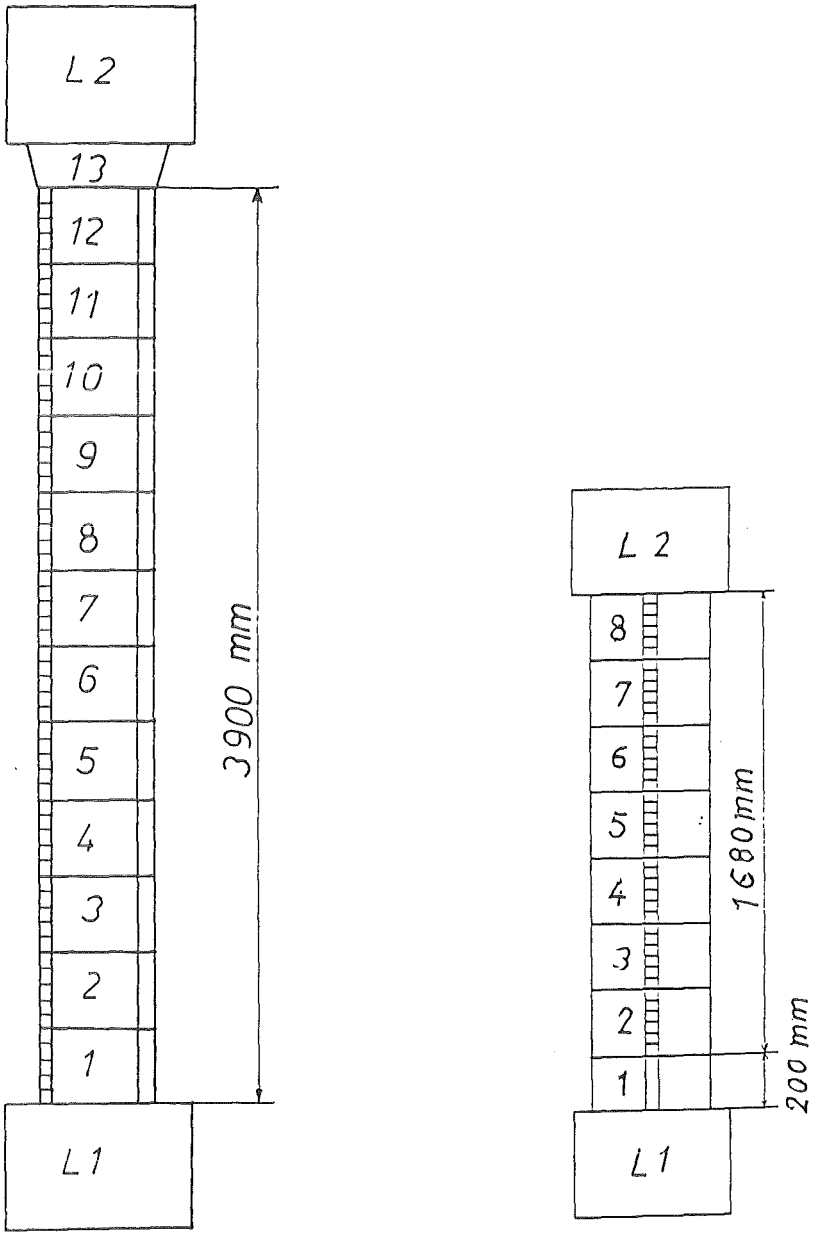

A) FEBA/SEFLEX

1 Pipe (13 Fluid cells)
2 Lumps (L1 and L2)
60 Heat conductor cells

B) NEPTUN

1 Pipe (8 Fluid cells)
2 Lumps (L1 and L2)
43 Heat conductor cells

Figure 3. FLUT-Nodalisation of the FEBA/SEFLEX and NEPTUN test section.

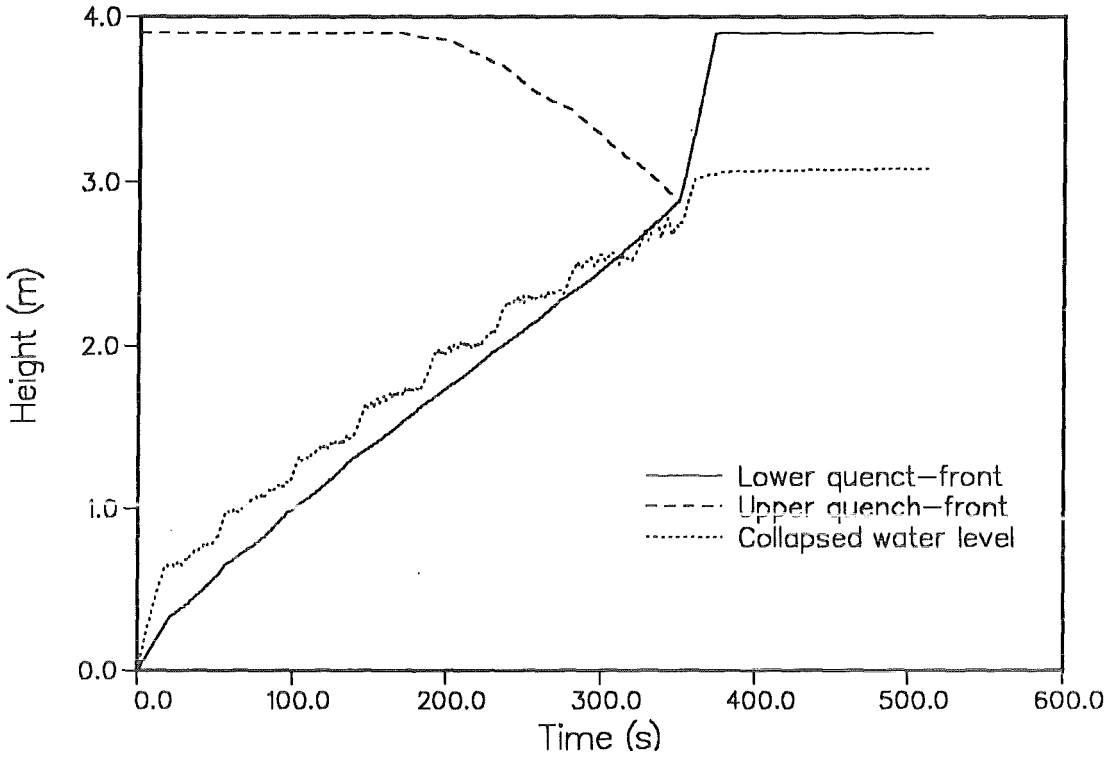

Figure 4. FEBA 216 - Quench-front propagation and collapsed water level.

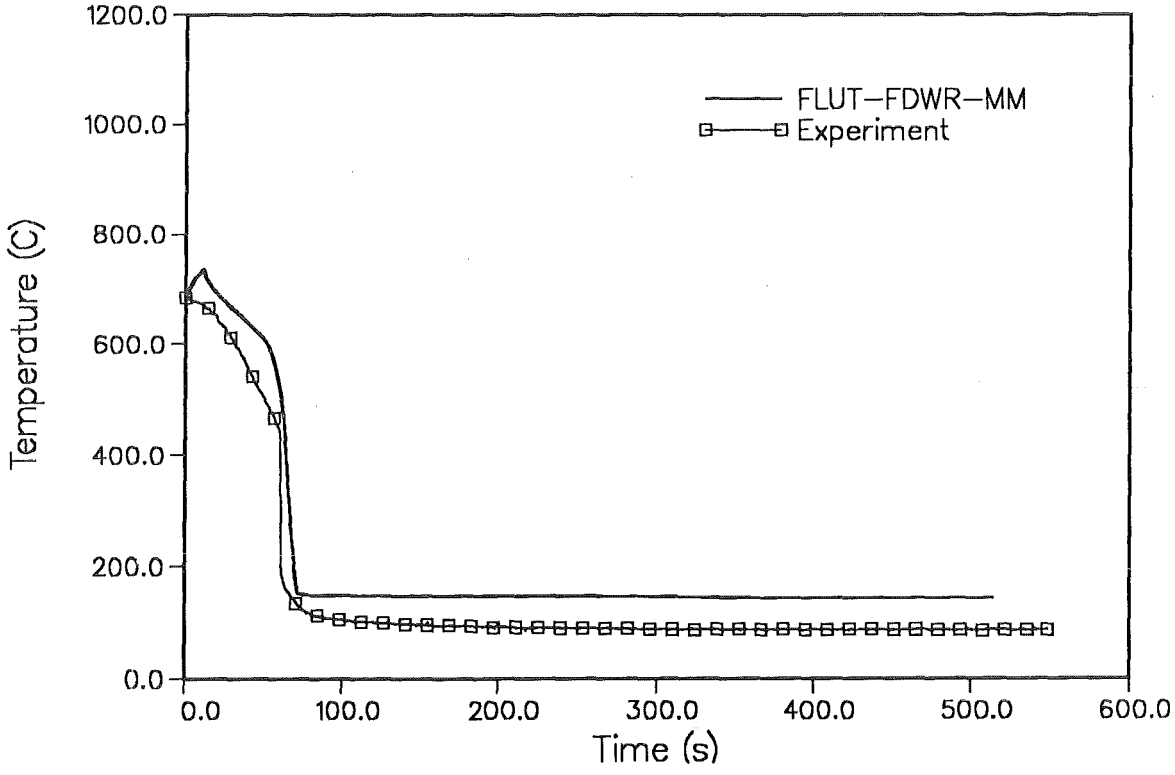

Figure 5. FEBA 216 - Cladding temperature at z = 660 mm.

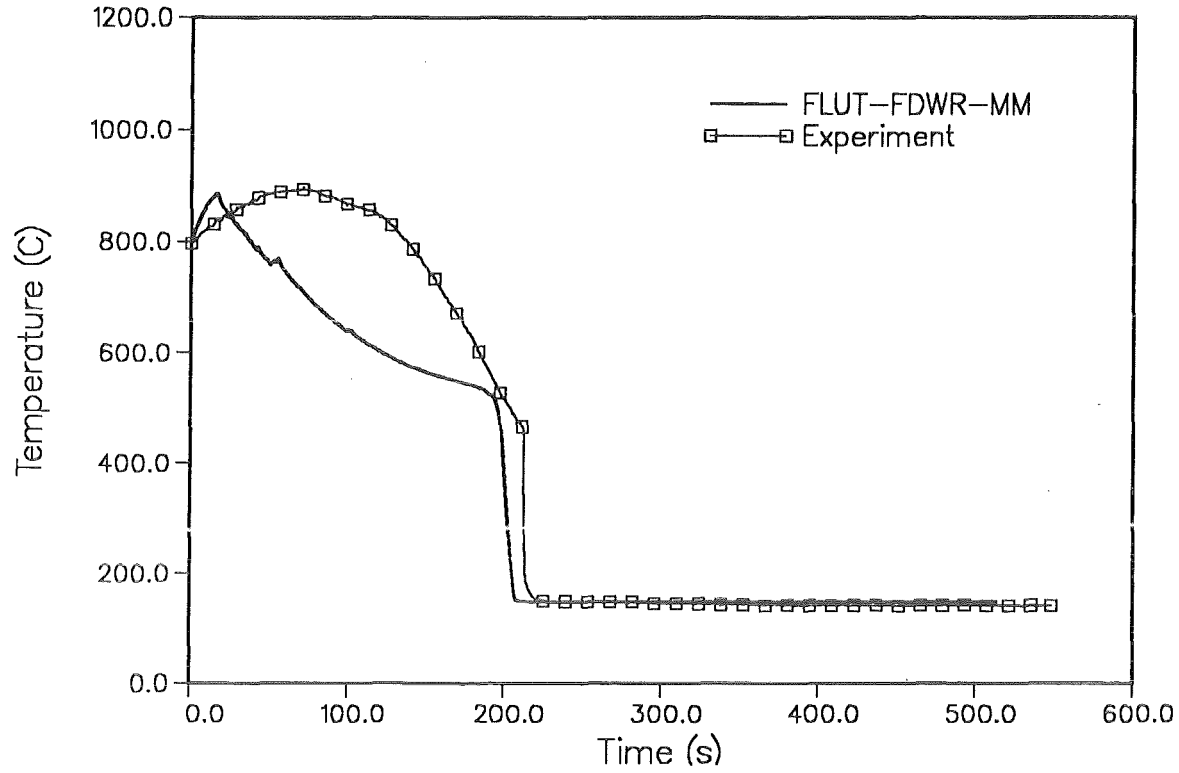

Figure 6. FEBA 216 - Cladding temperature at z = 1750 mm.

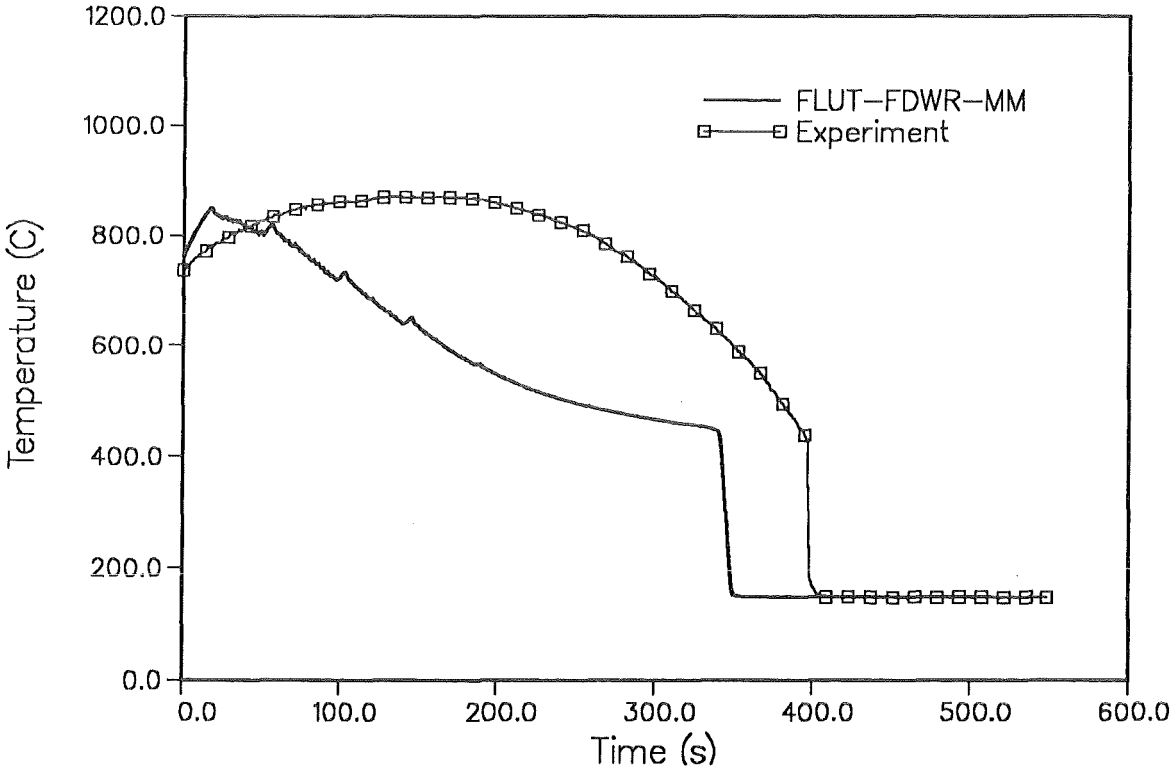

Figure 7. FEBA 216 - Cladding temperature at z = 2840 mm.

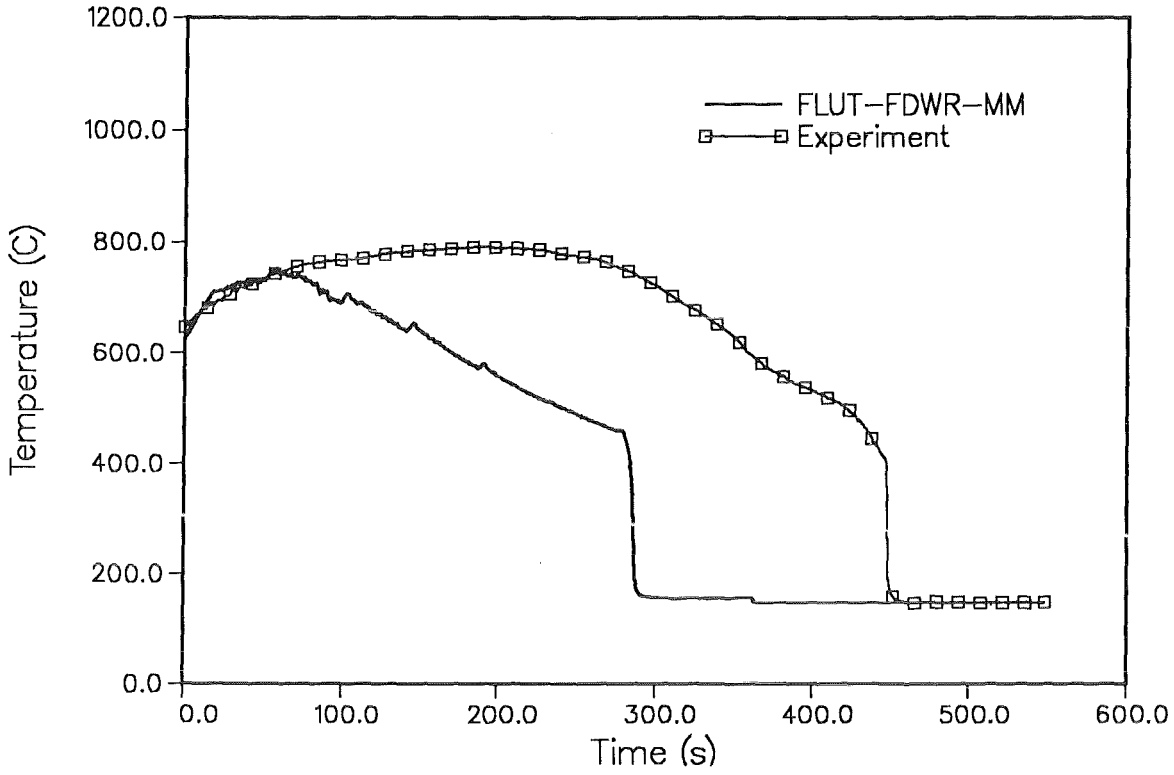

Figure 8. FEBA 216 - Cladding temperature at z = 3385 mm.

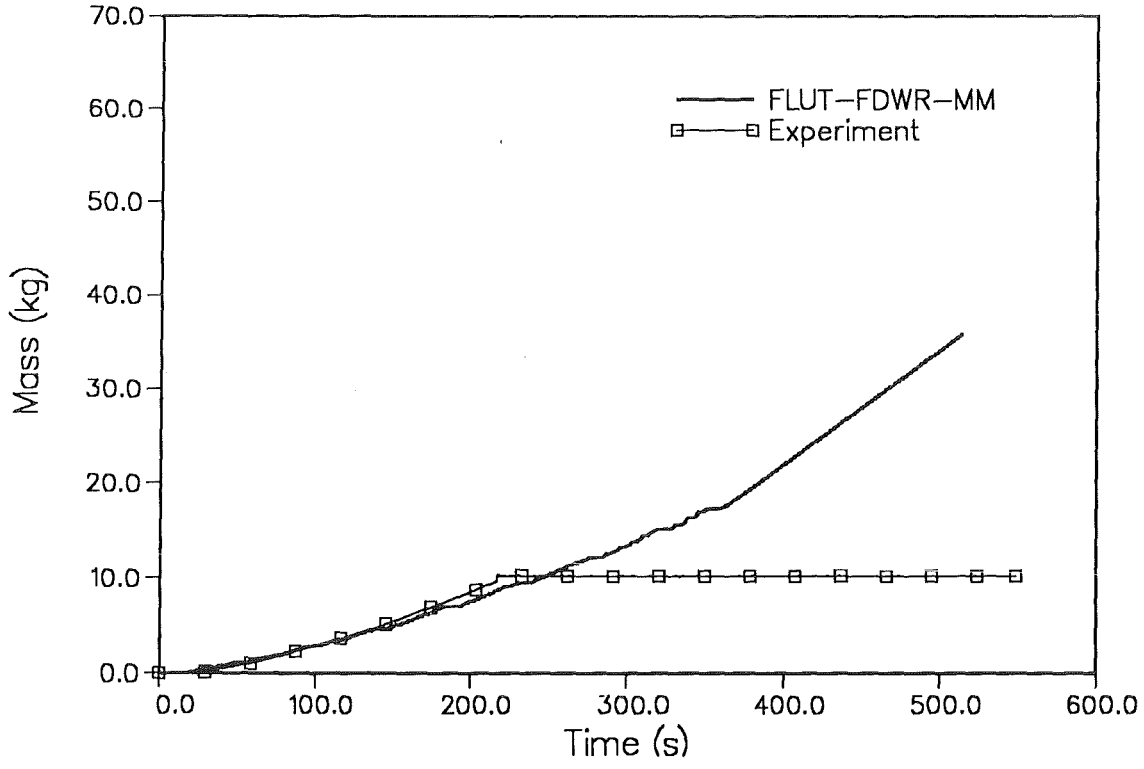

Figure 9. FEBA 216 - Water carry over.

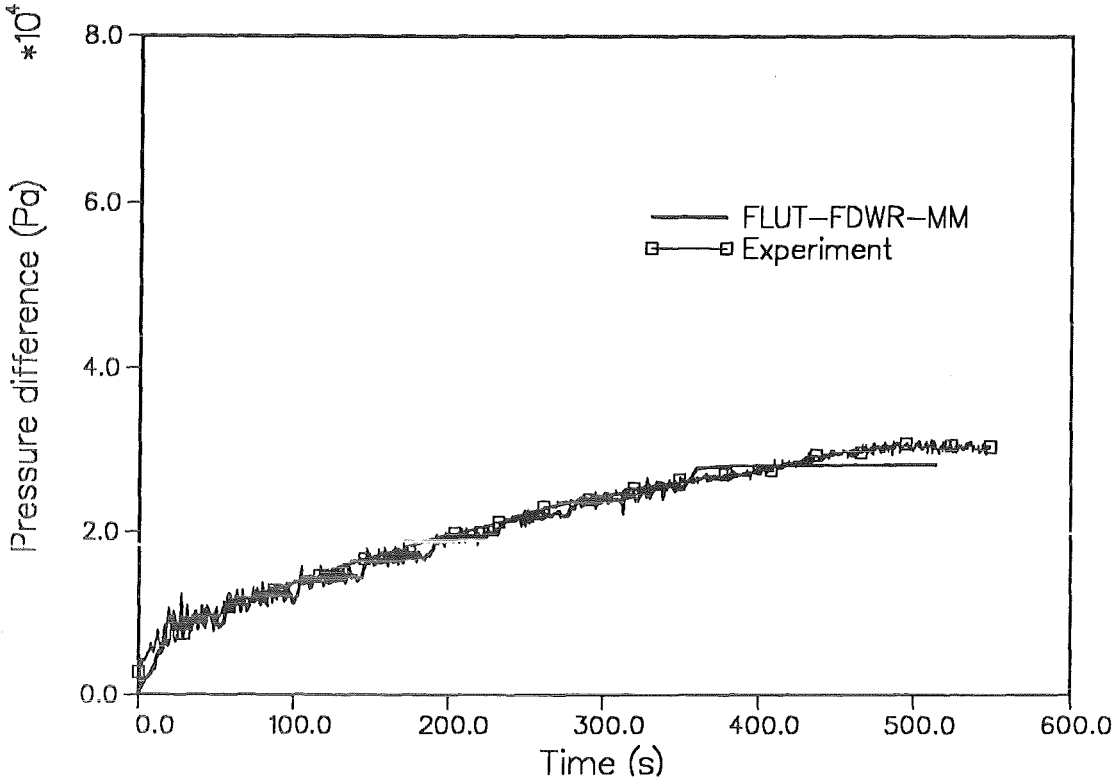

Figure 10. FEBA 216 - Pressure difference.

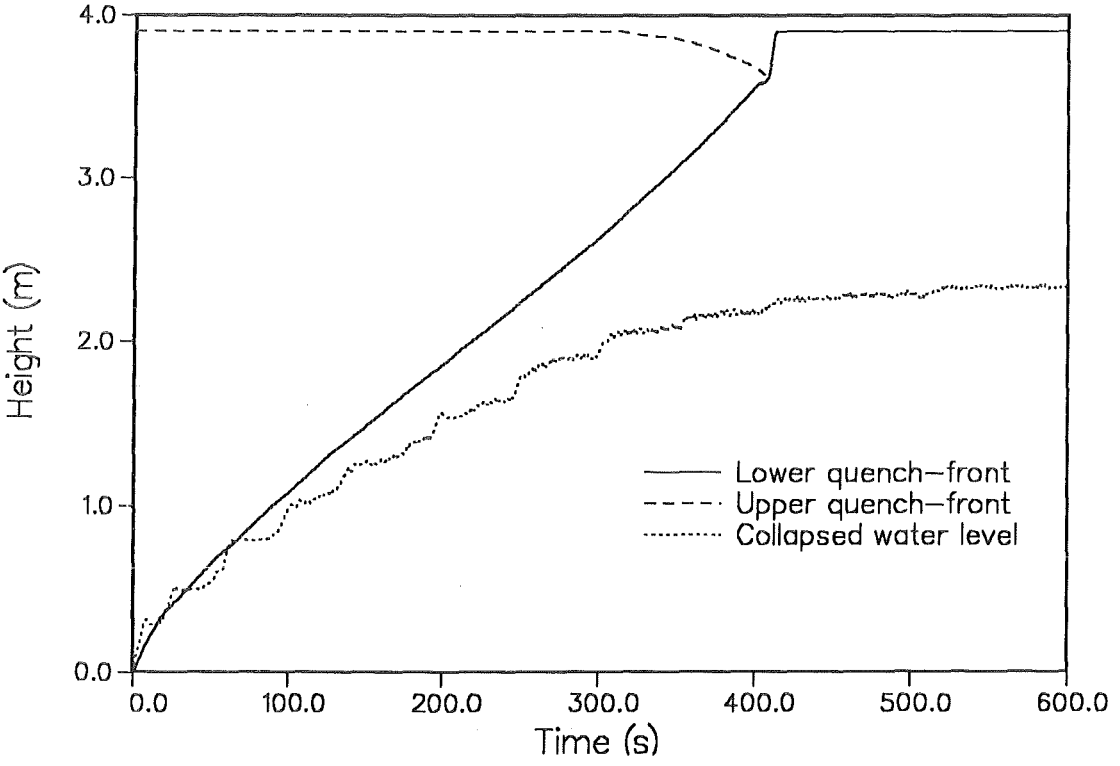

Figure 11. SEFLEX 5 - Quench-front propagation and collapsed water level.

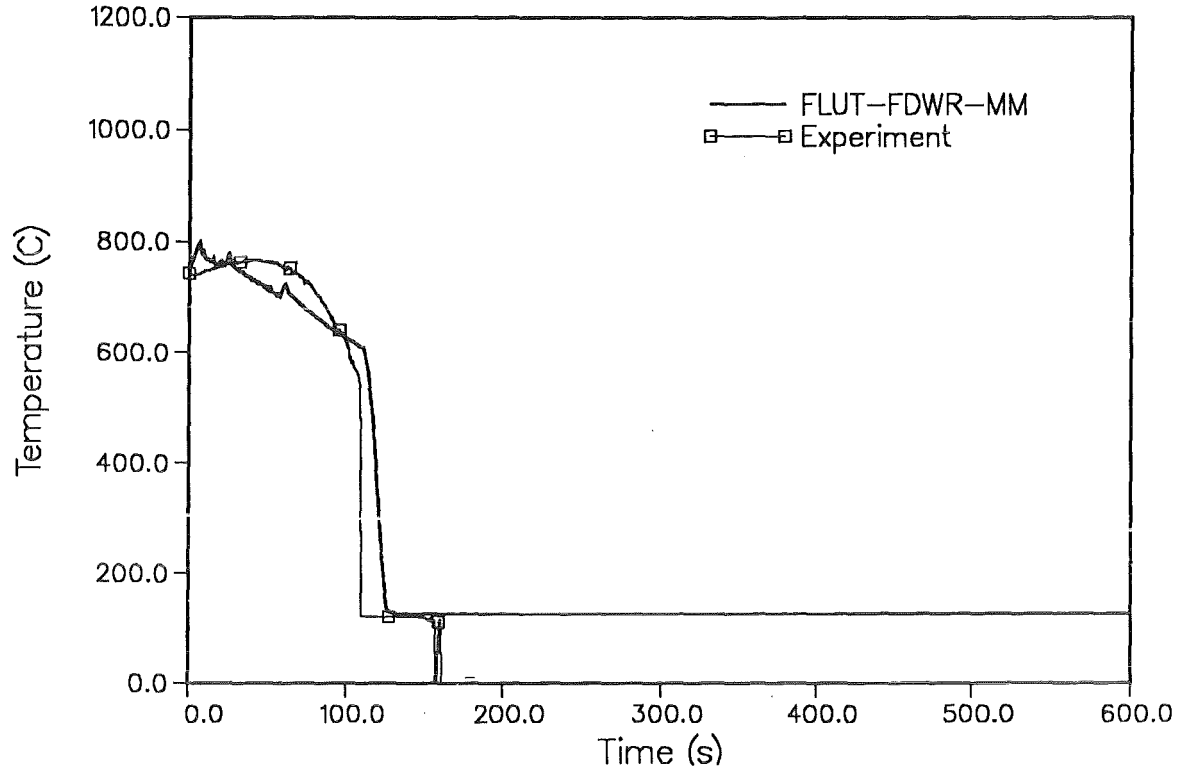

Figure 12. SEFLEX 5 - Cladding temperature at z=1205 mm.

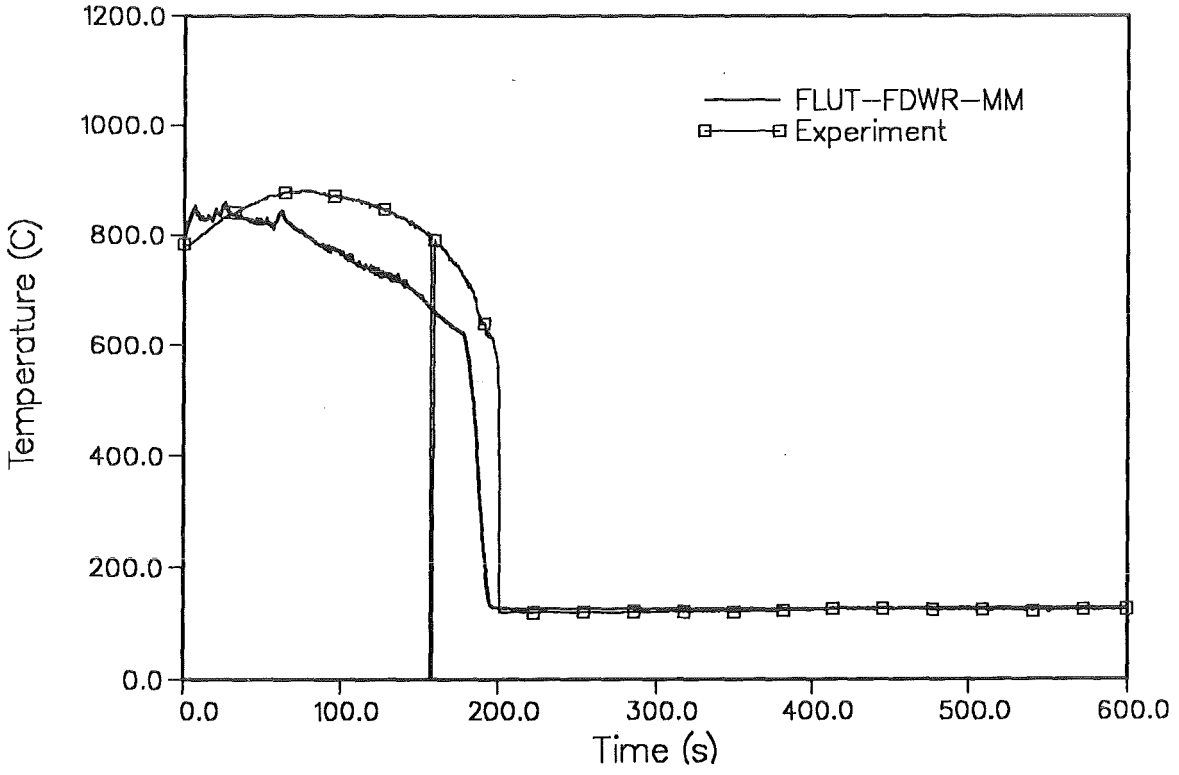

Figure 13. SEFLEX 5 - Cladding temperature at z=1750 mm.

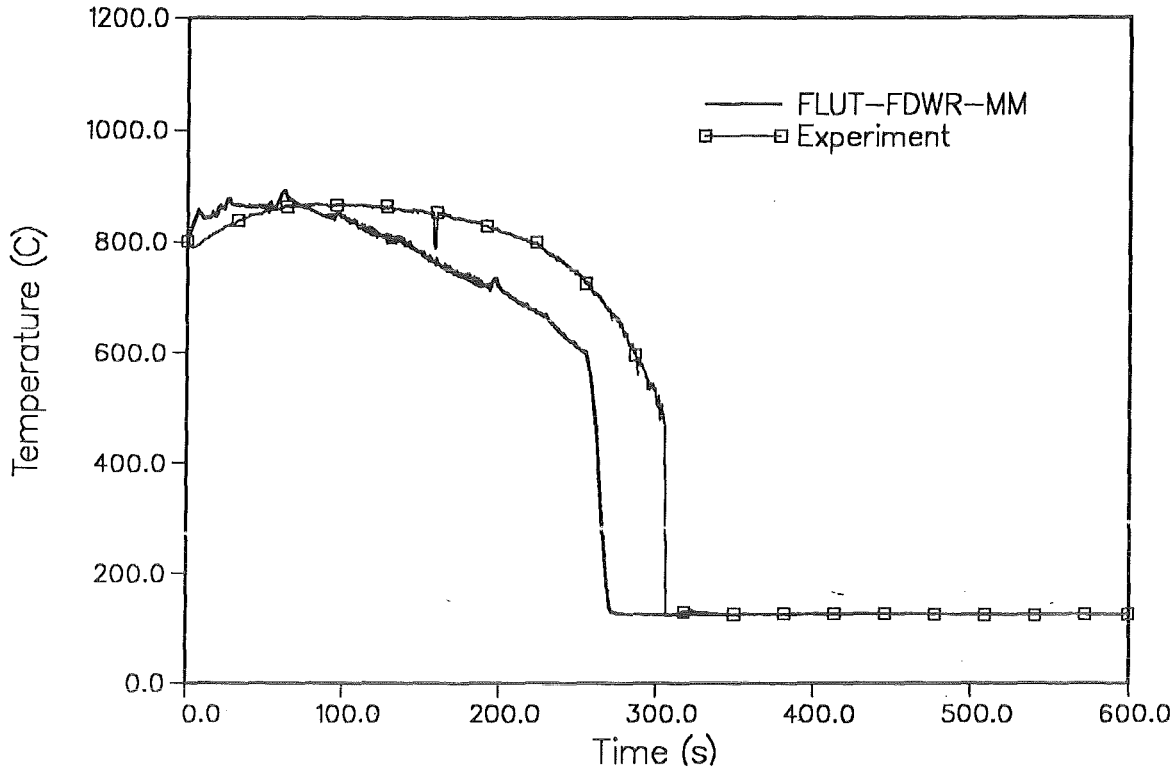

Figure 14. SEFLEX 5 - Cladding temperature at z = 2295 mm.

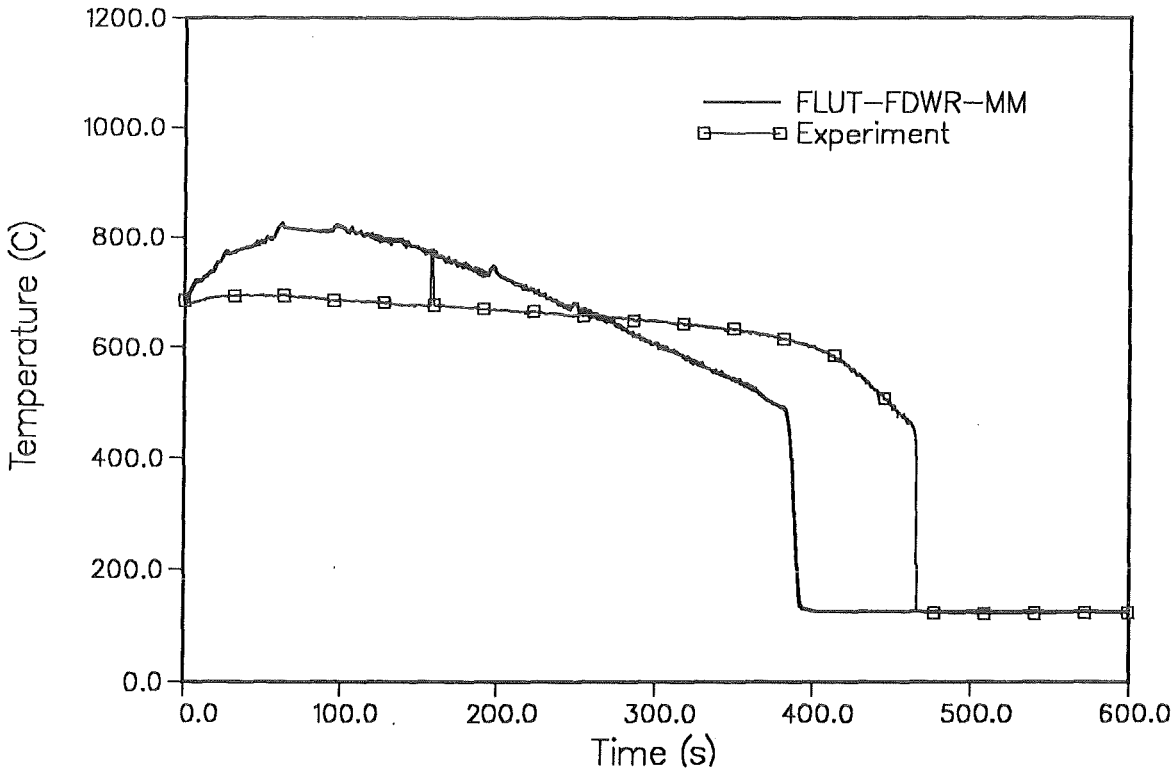

Figure 15. SEFLEX 5 - Cladding temperature at z = 3385 mm.

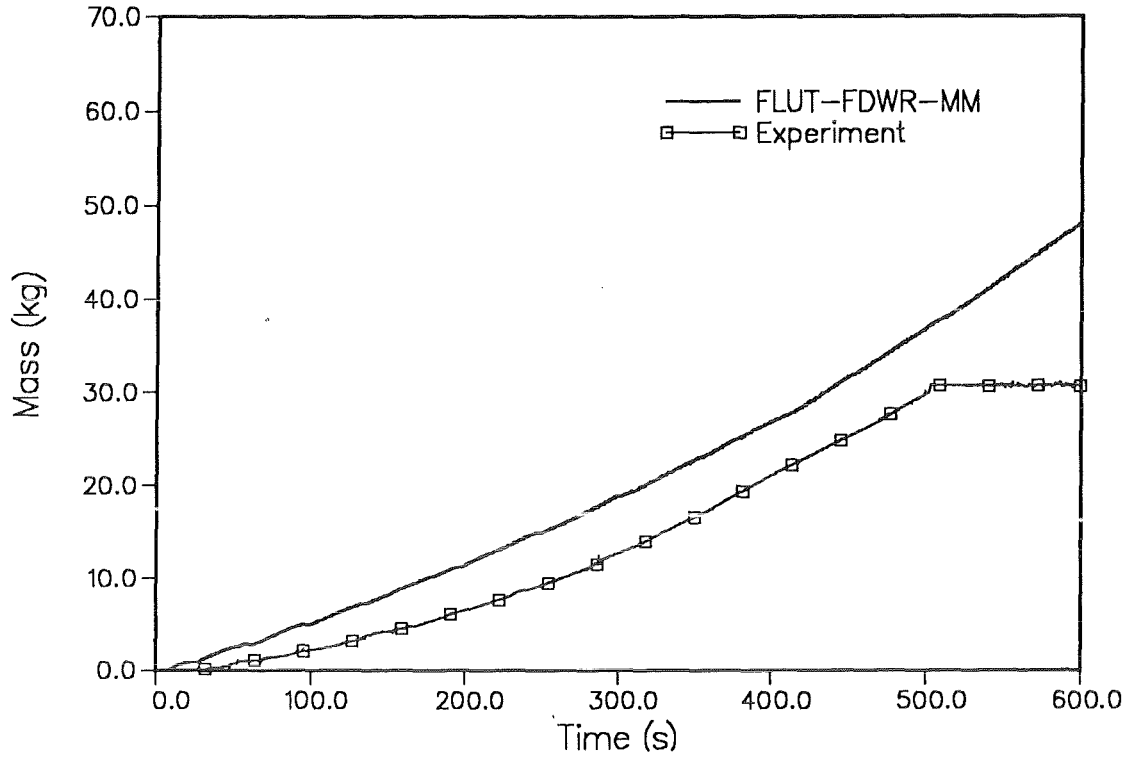

Figure 16. SEFLEX 5 - Water carry over.

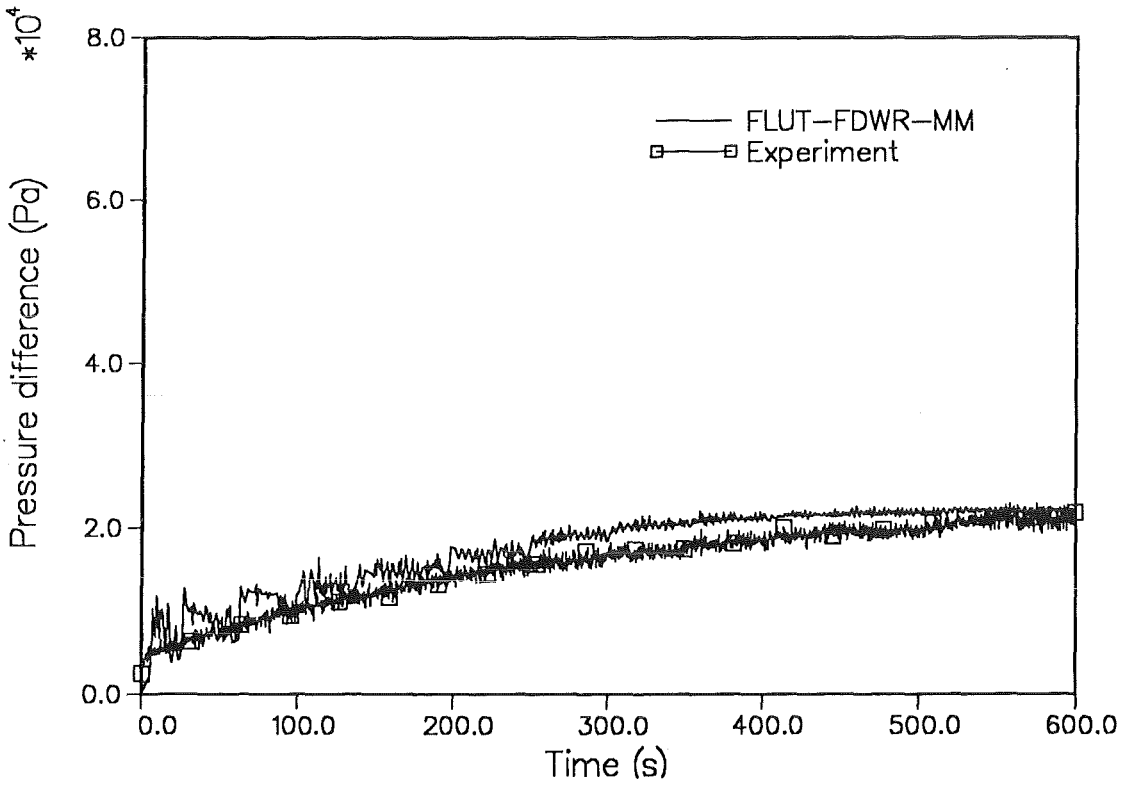

Figure 17. SEFLEX 5 - Pressure difference.

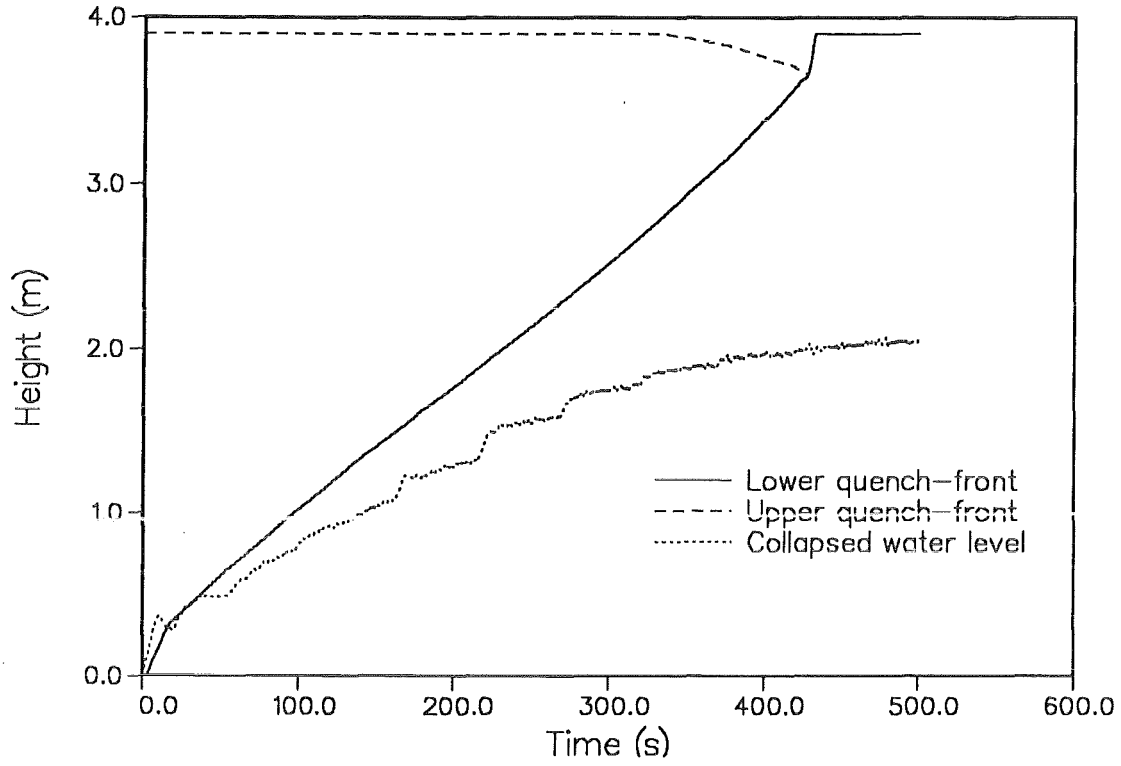

Figure 18. SEFLEX 7 - Quench-front propagation and collapsed water level.

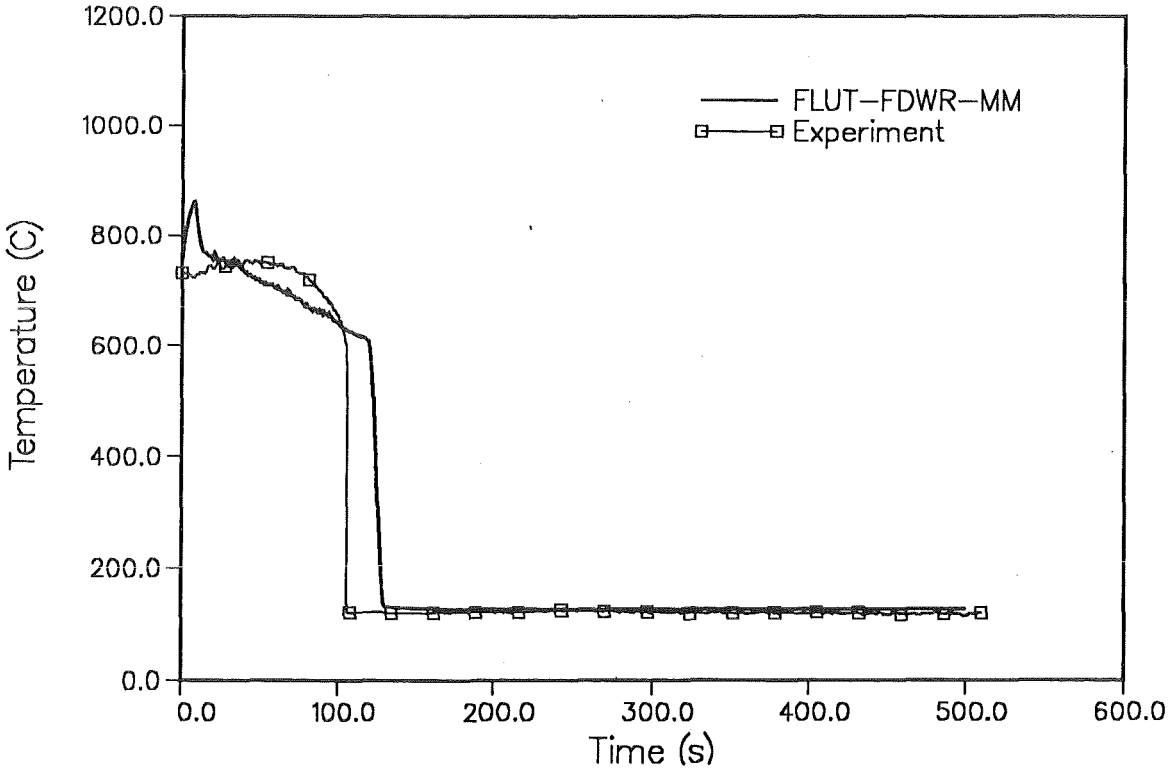

Figure 19. SEFLEX 7 - Cladding temperature at z = 1205 mm.

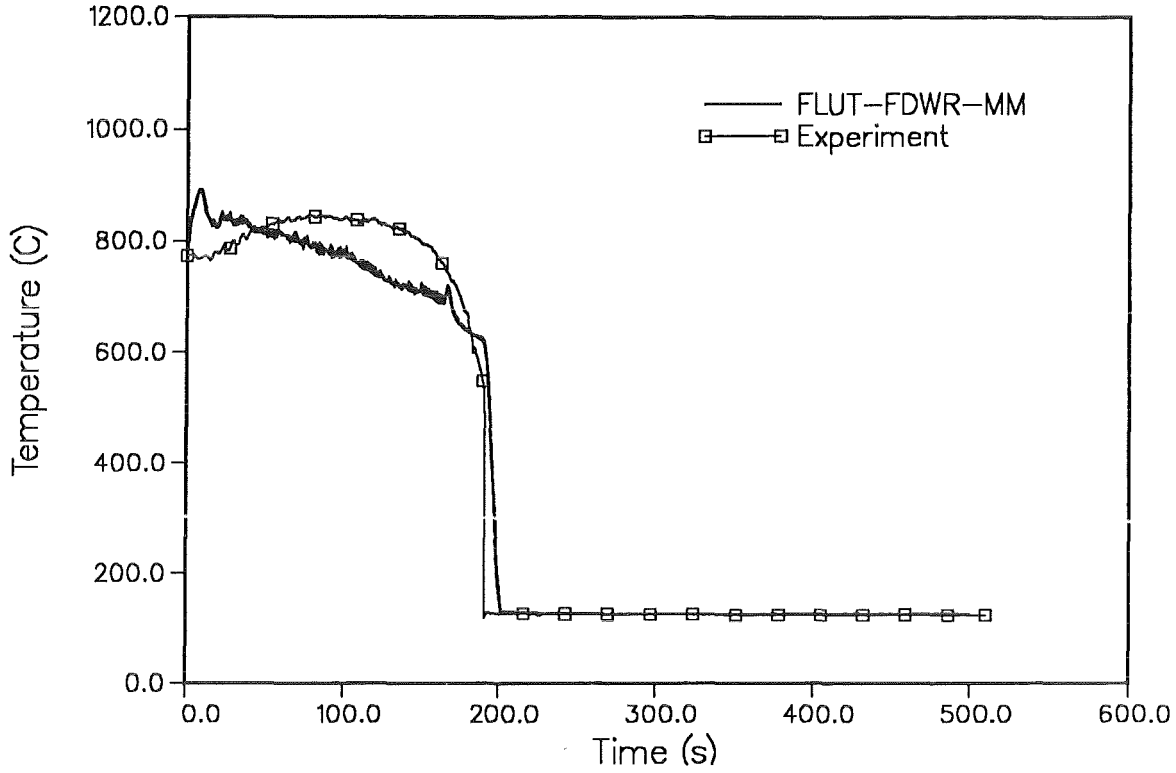

Figure 20. SEFLEX 7 - Cladding temperature at z = 1750 mm.

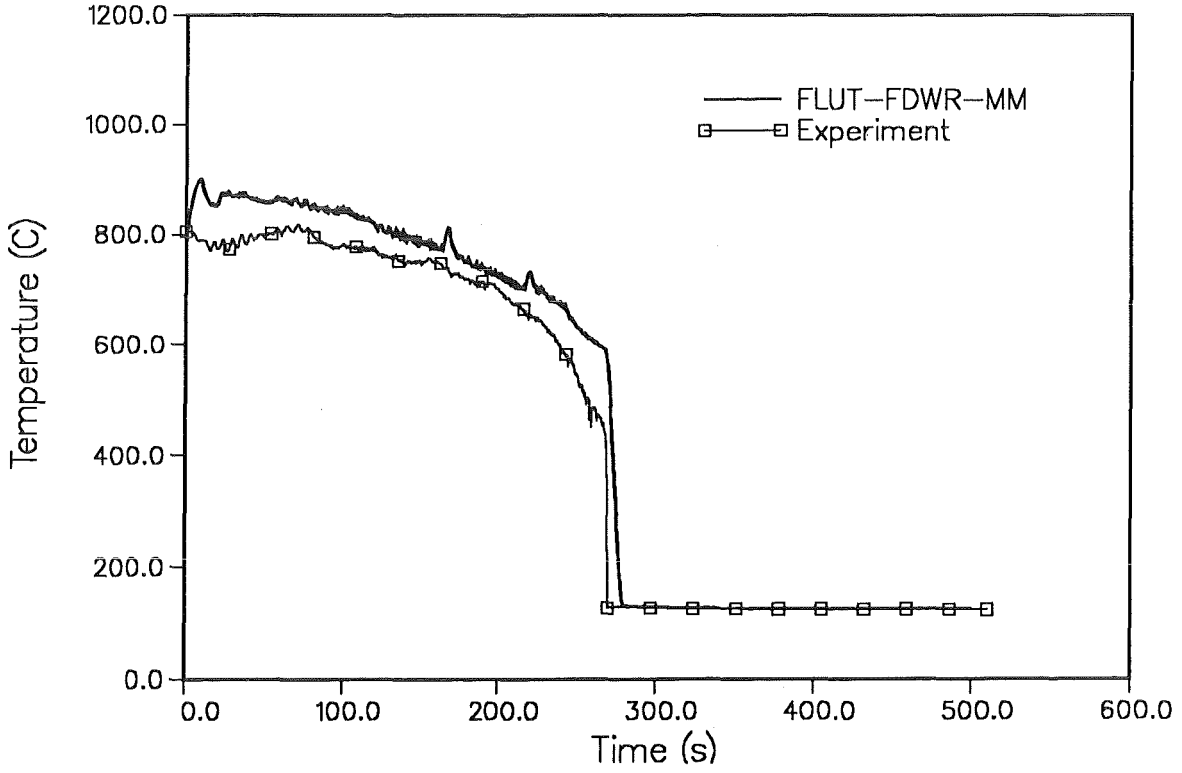

Figure 21. SEFLEX 7 - Cladding temperature at z = 2295 mm.

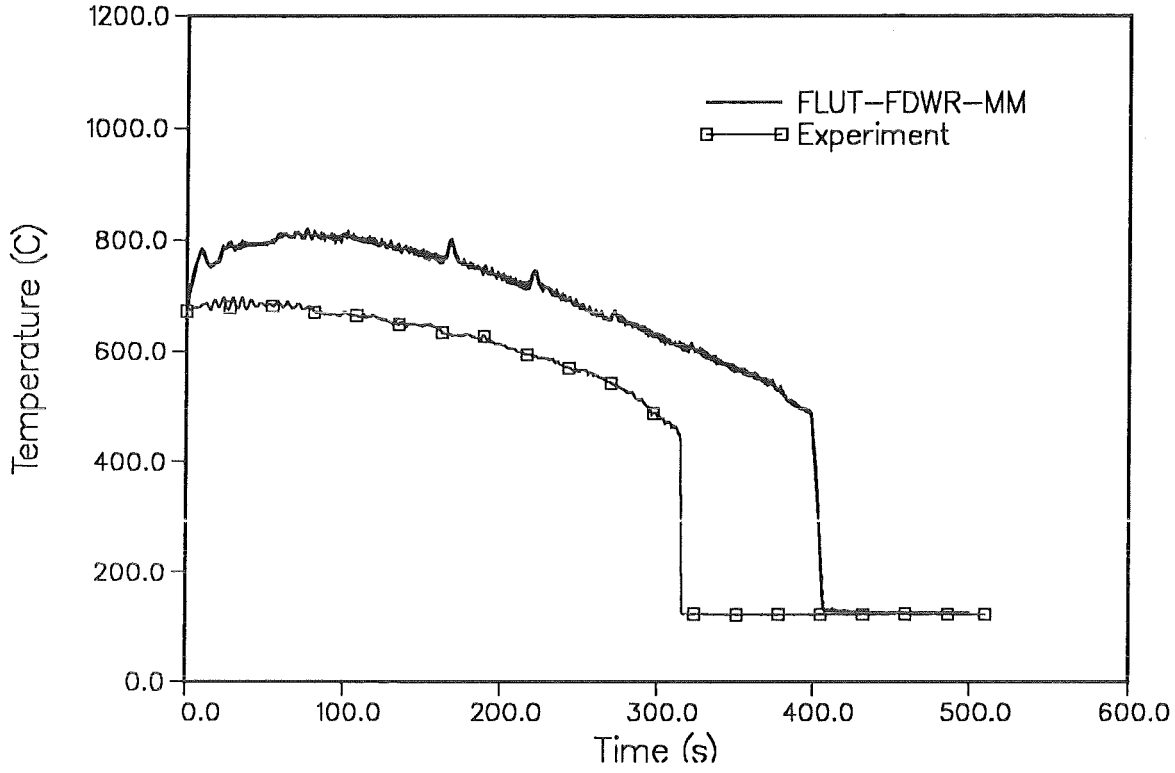

Figure 22. SEFLEX 7 - Cladding temperature at z = 3385 mm.

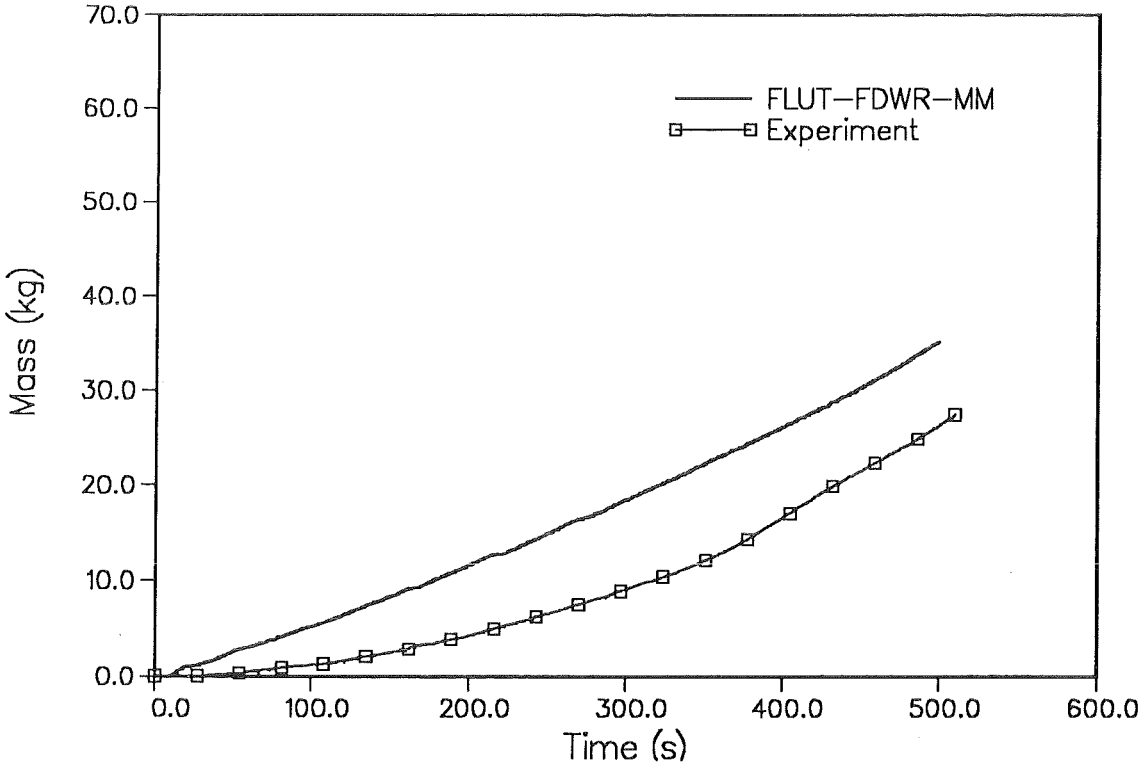

Figure 23. SEFLEX 7 - Water carry over.

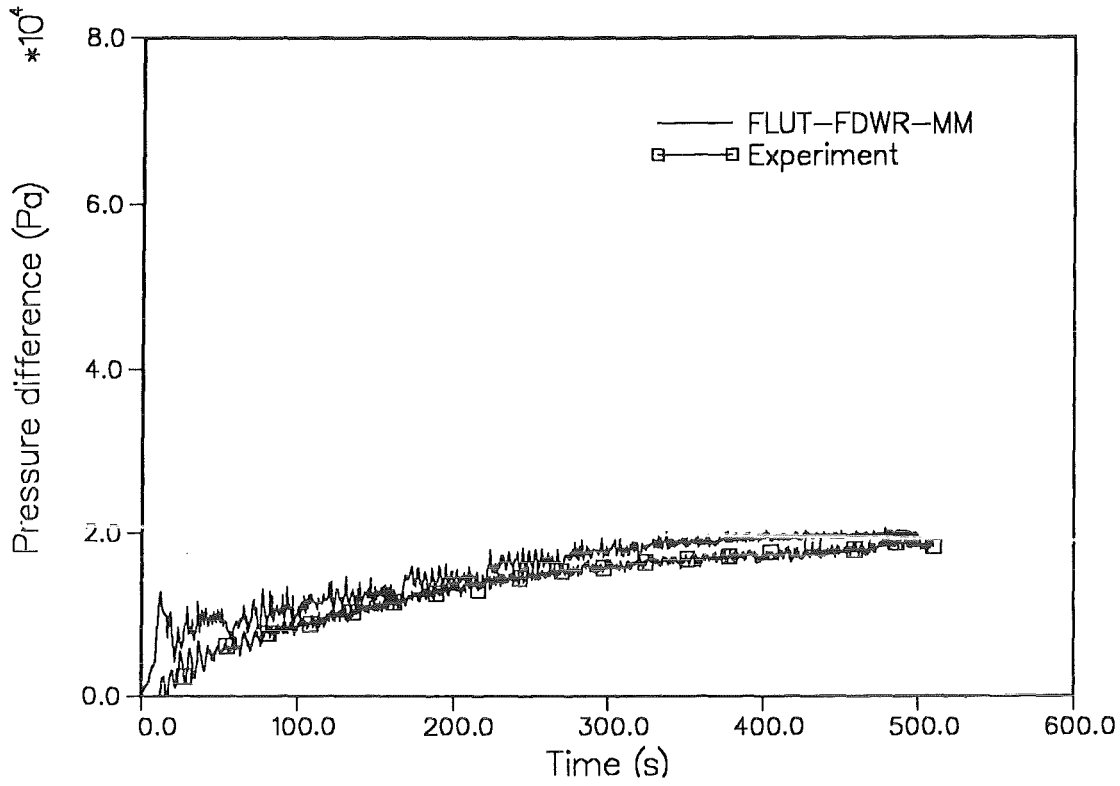

Figure 24. SEFLEX 7 - Pressure difference.

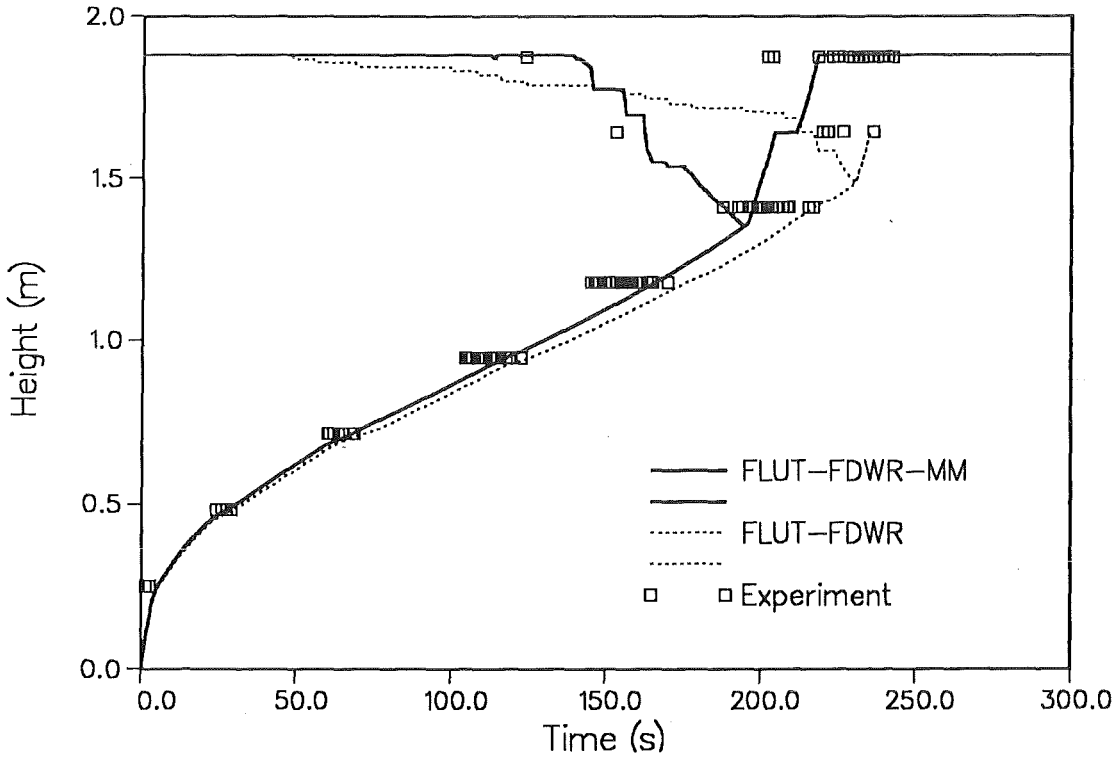

Figure 25. NEPTUN 5036 - Quench-front propagation.

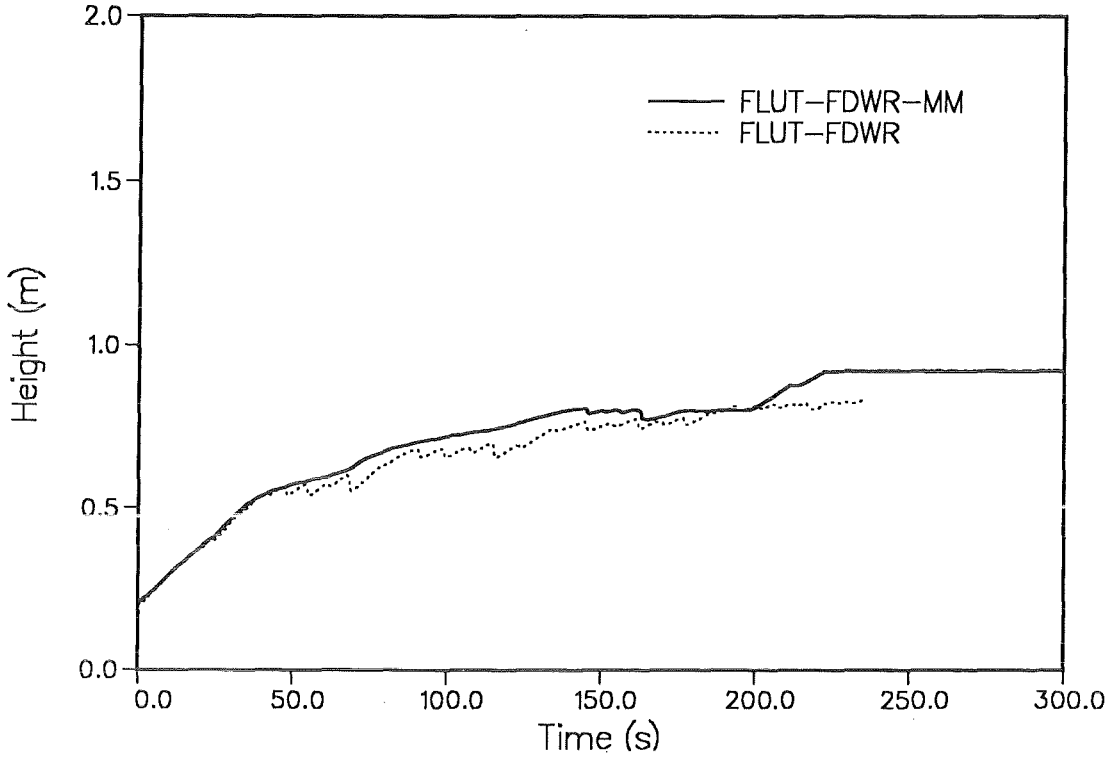

Figure 26. NEPTUN 5035 - Collapsed water level

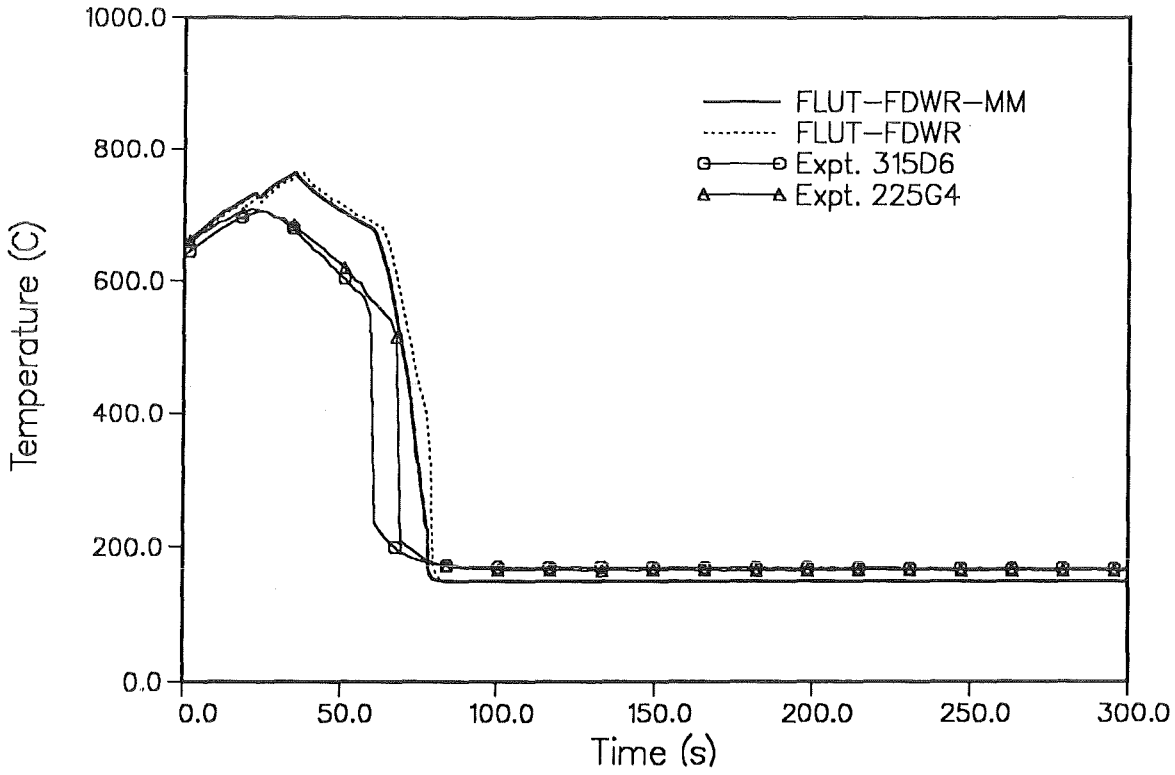

Figure 27. NEPTUN 5036 - Cladding temperature at z=714 mm.

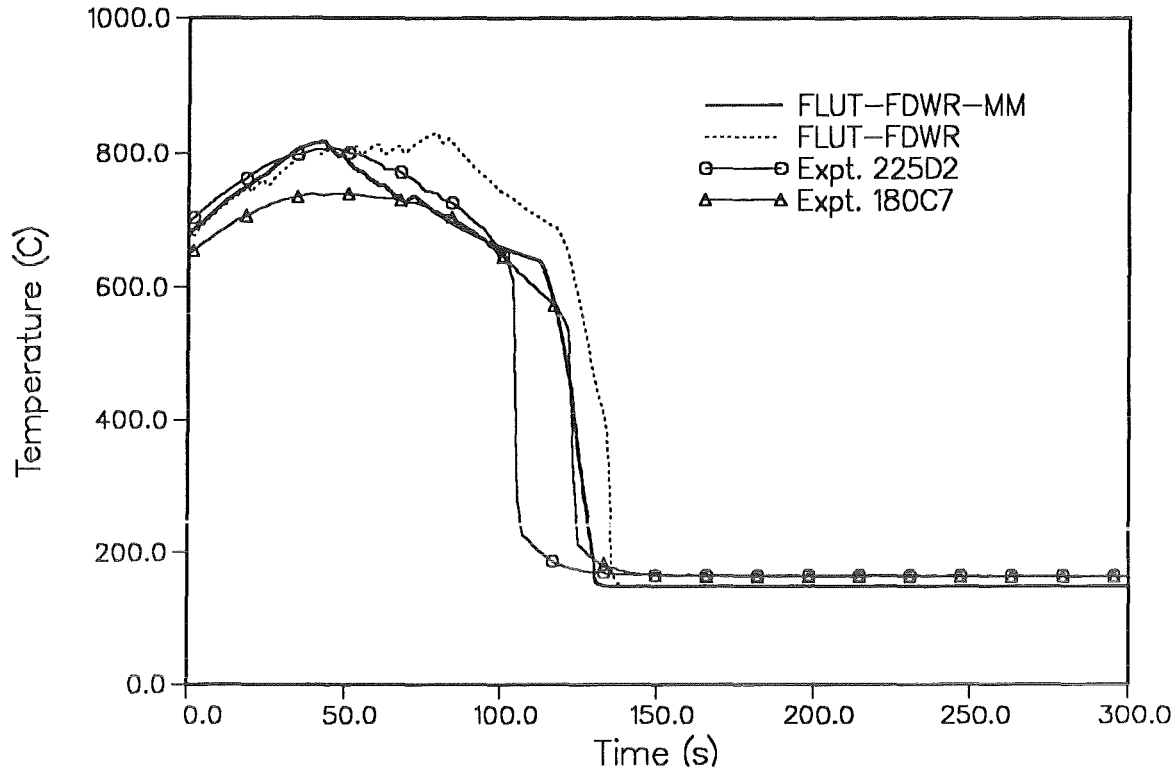

Figure 28. NEPTUN 5036 - Cladding temperature at z = 946 mm.

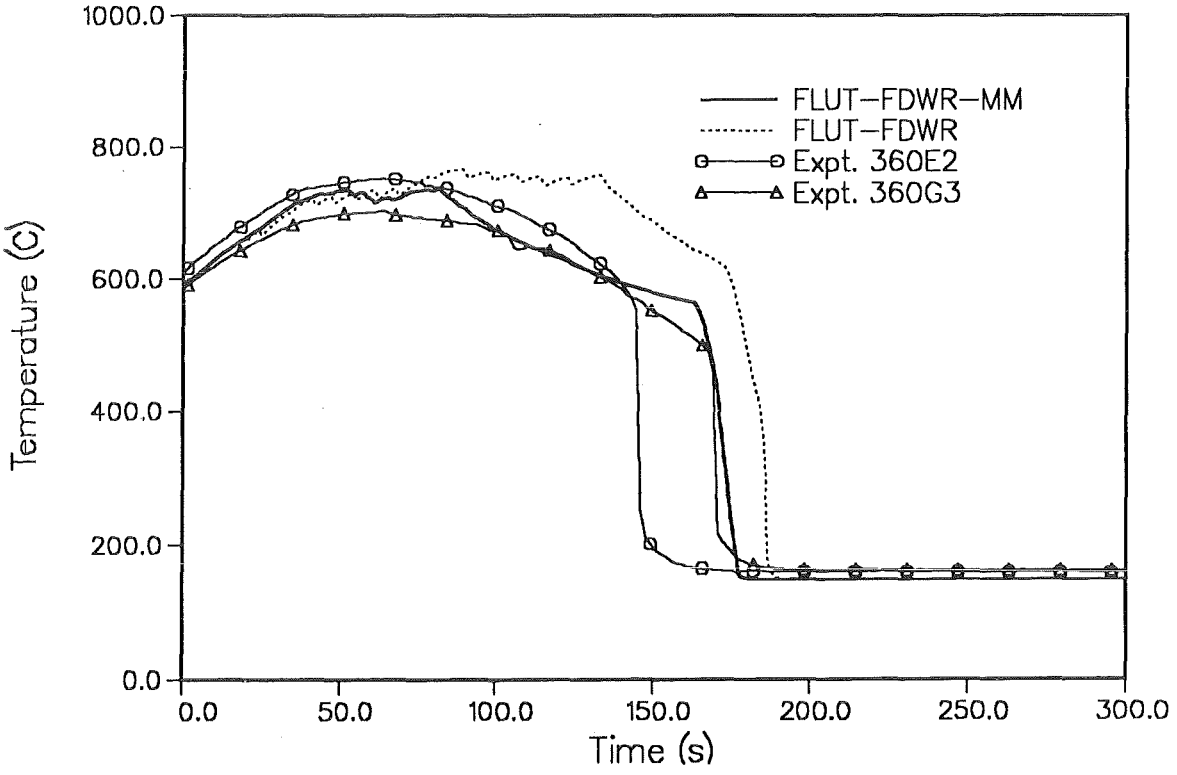

Figure 29. NEPTUN 5036 - Cladding temperature at z = 1178 mm.

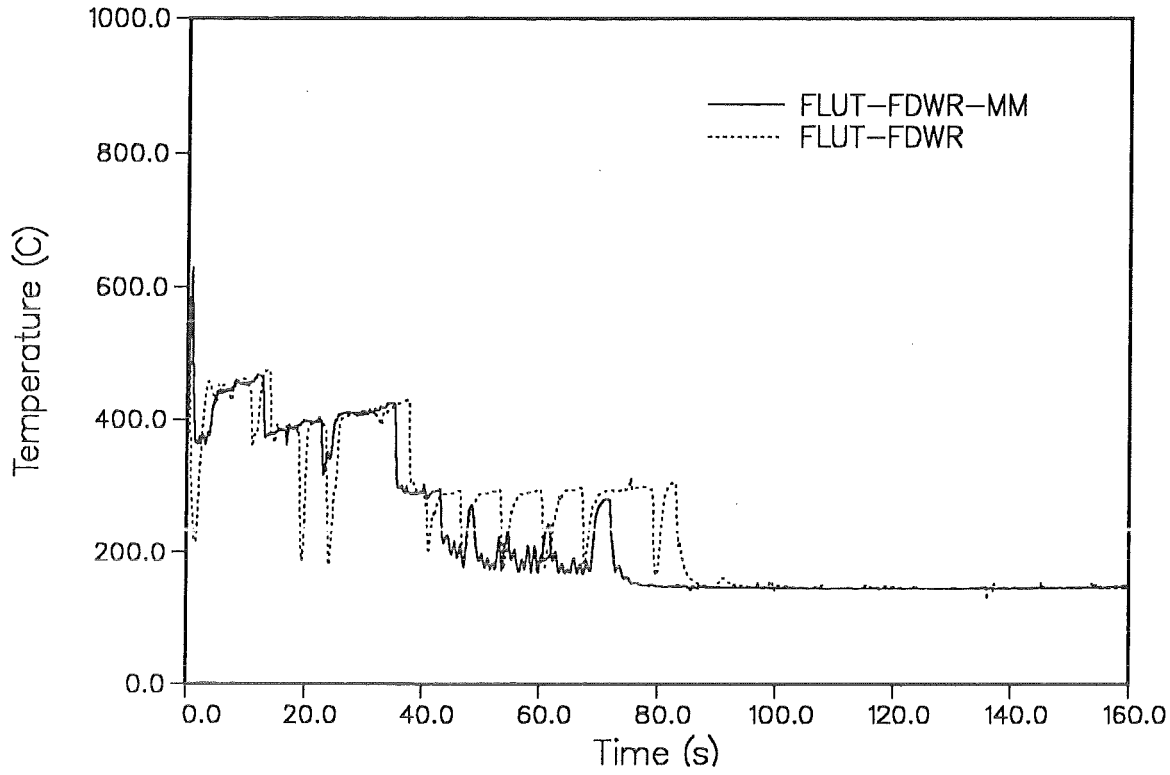

Figure 30. NEPTUN 5036 - Vapour temperature at the 5th fluid cell.

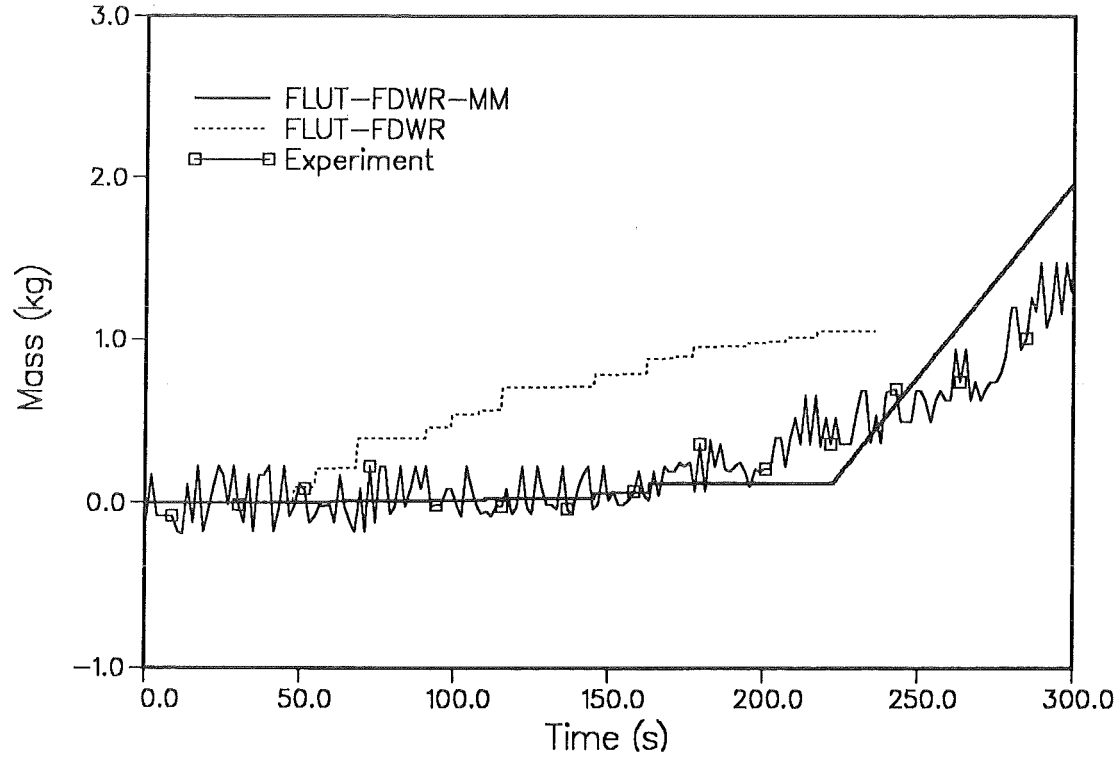

Figure 31. NEPTUN 5036 - Water carry over.

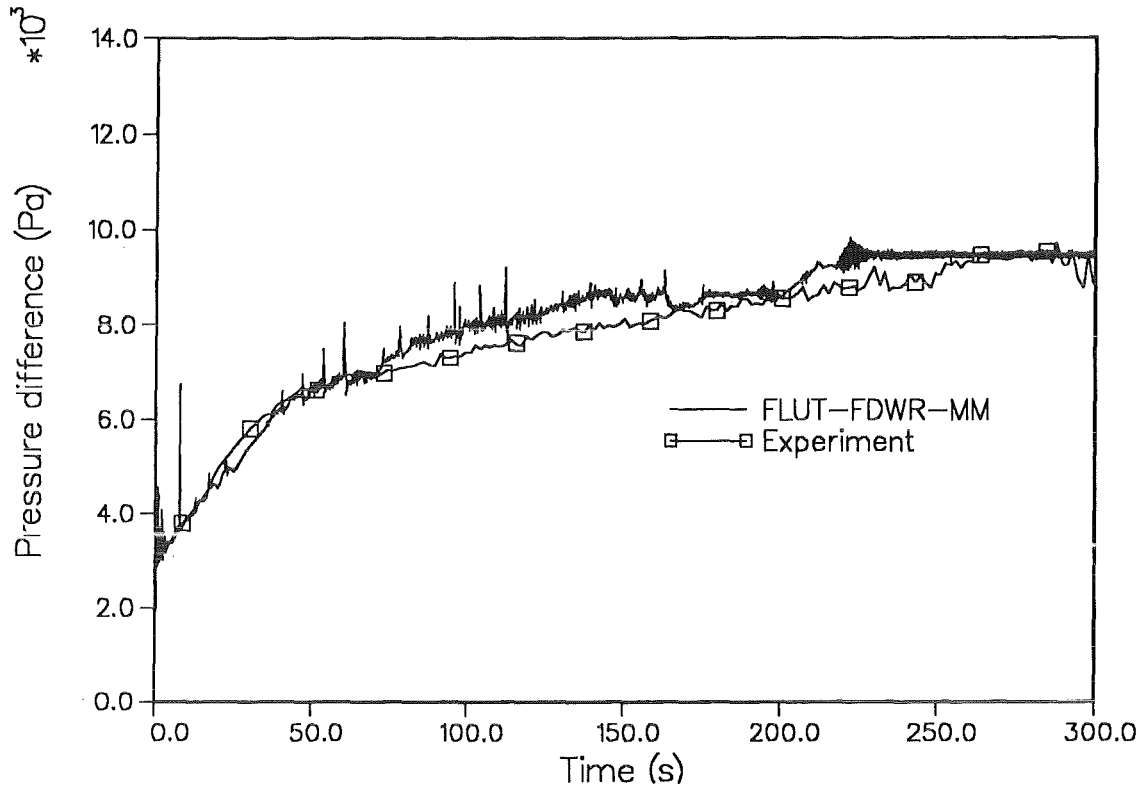

Figure 32. NEPTUN 5036 - Pressure difference (FLUT-FDWR-MM).

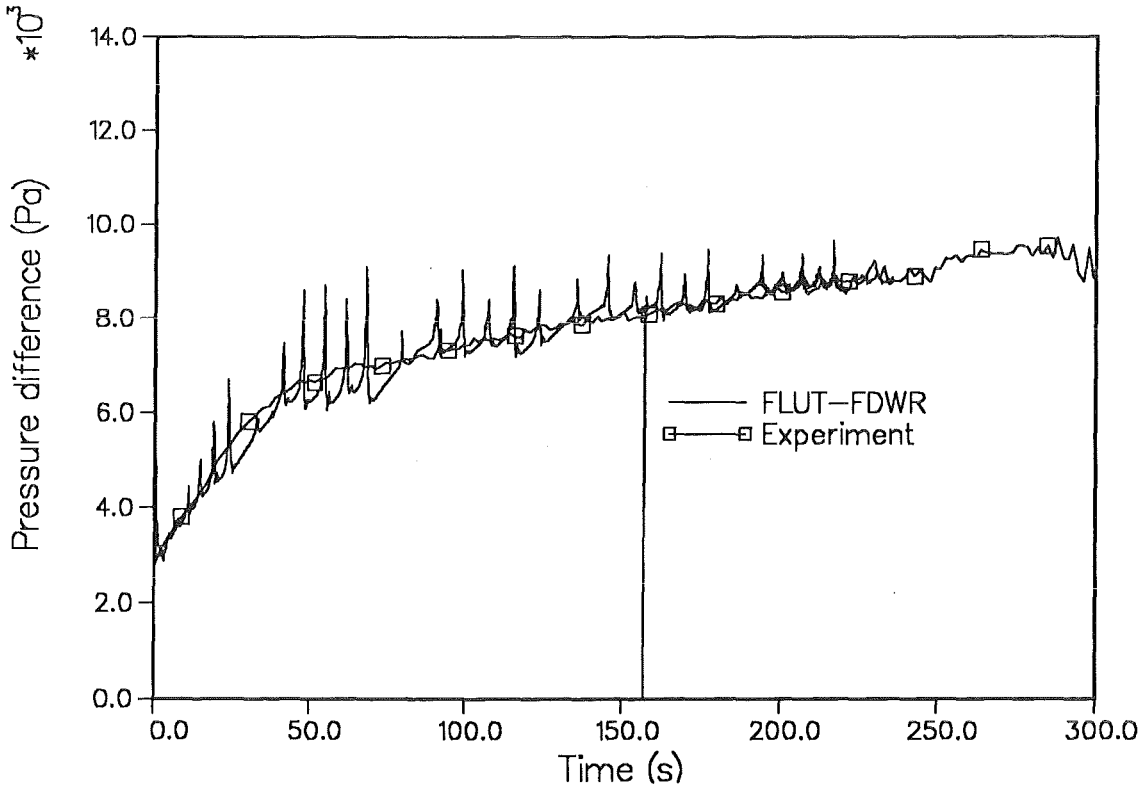

Figure 33. NEPTUN 5036 - Pressure difference (FLUT-FDWR).

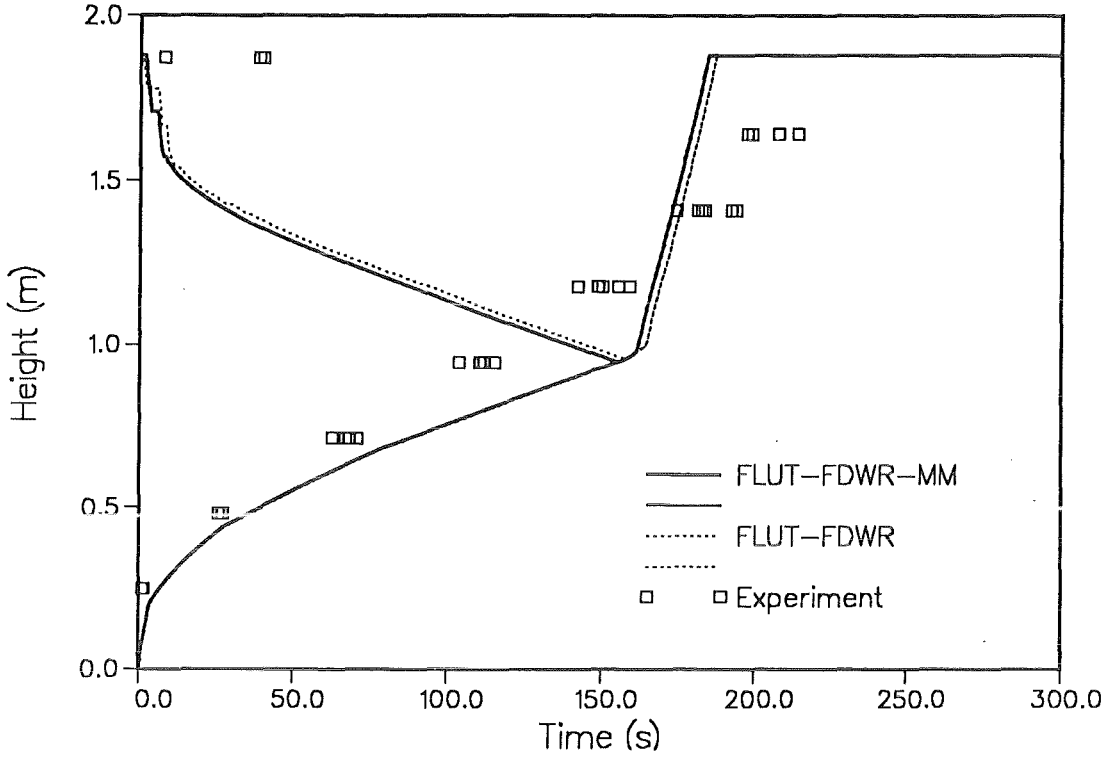

Figure 34. NEPTUN 5171 - Quench-front propagation.

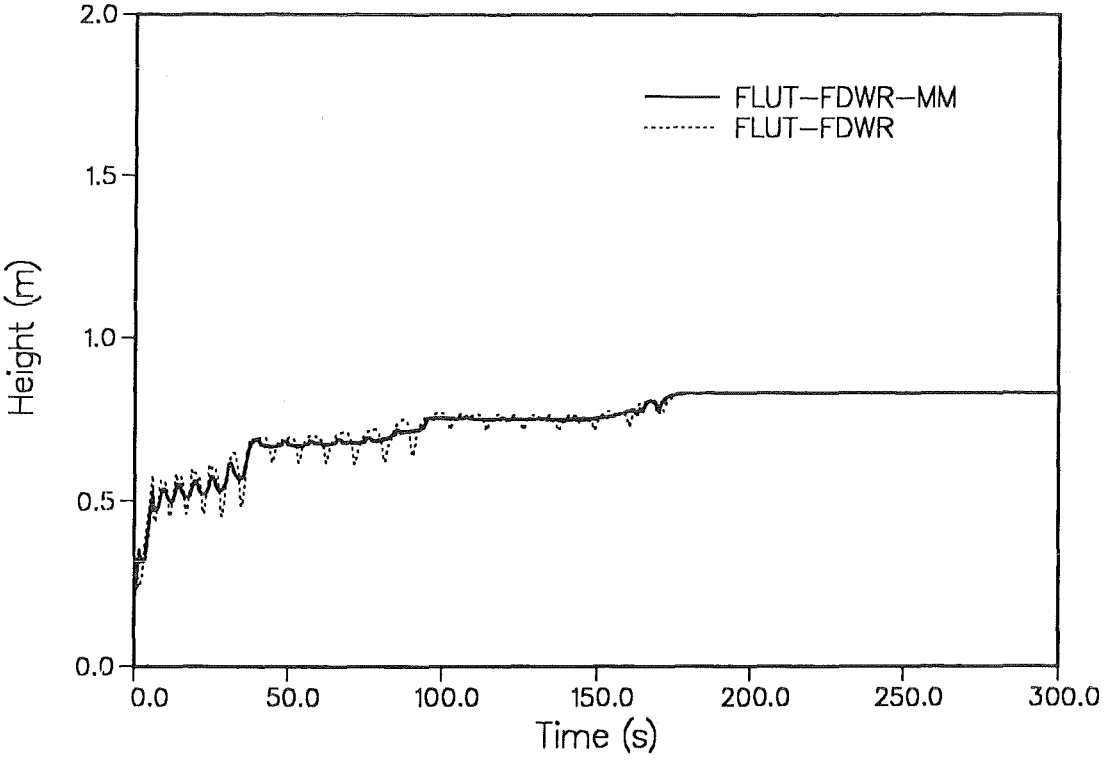

Figure 35. NEPTUN 5171 - Collapsed water level

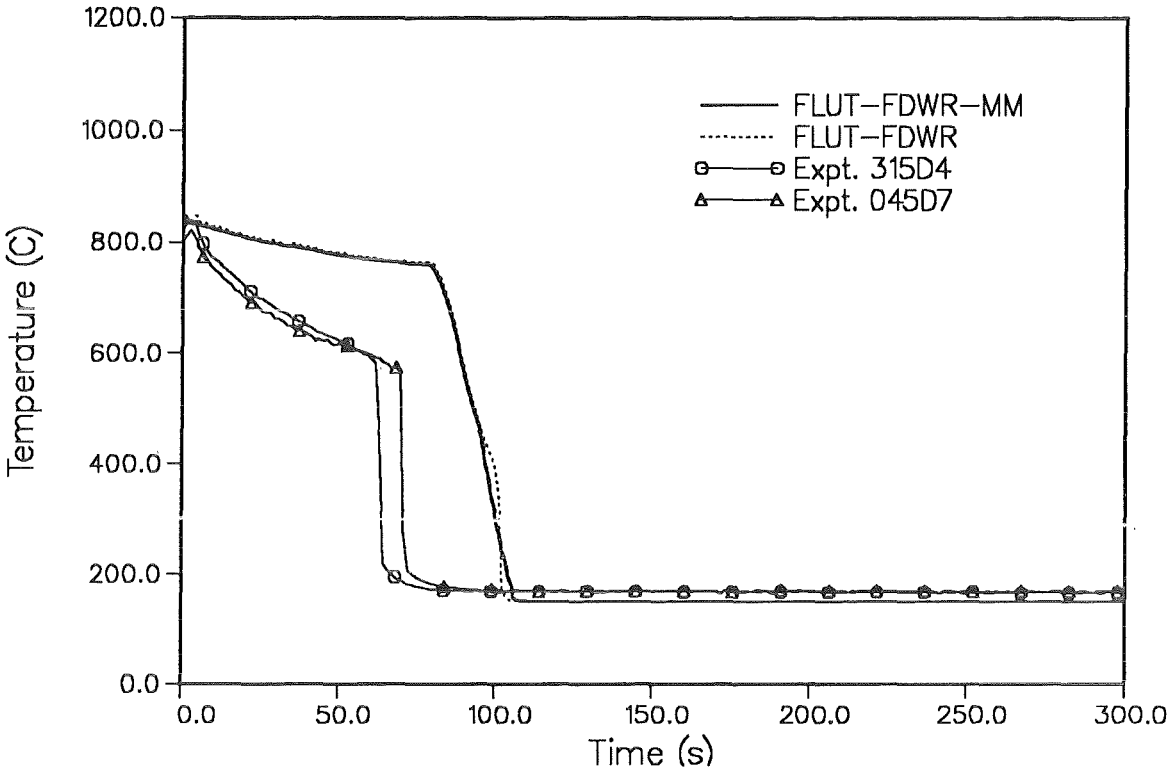

Figure 36. NEPTUN 5171 - Cladding temperature at z = 714 mm.

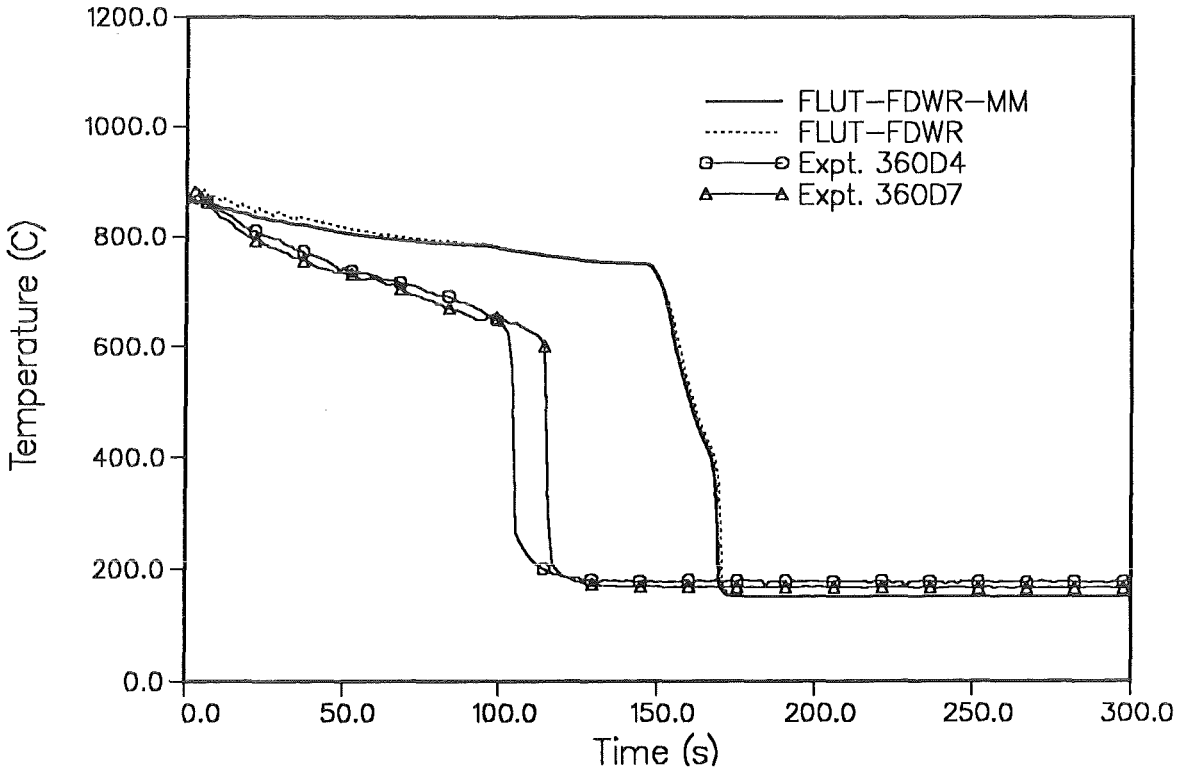

Figure 37. NEPTUN 5171 - Cladding temperature at z = 946 mm.

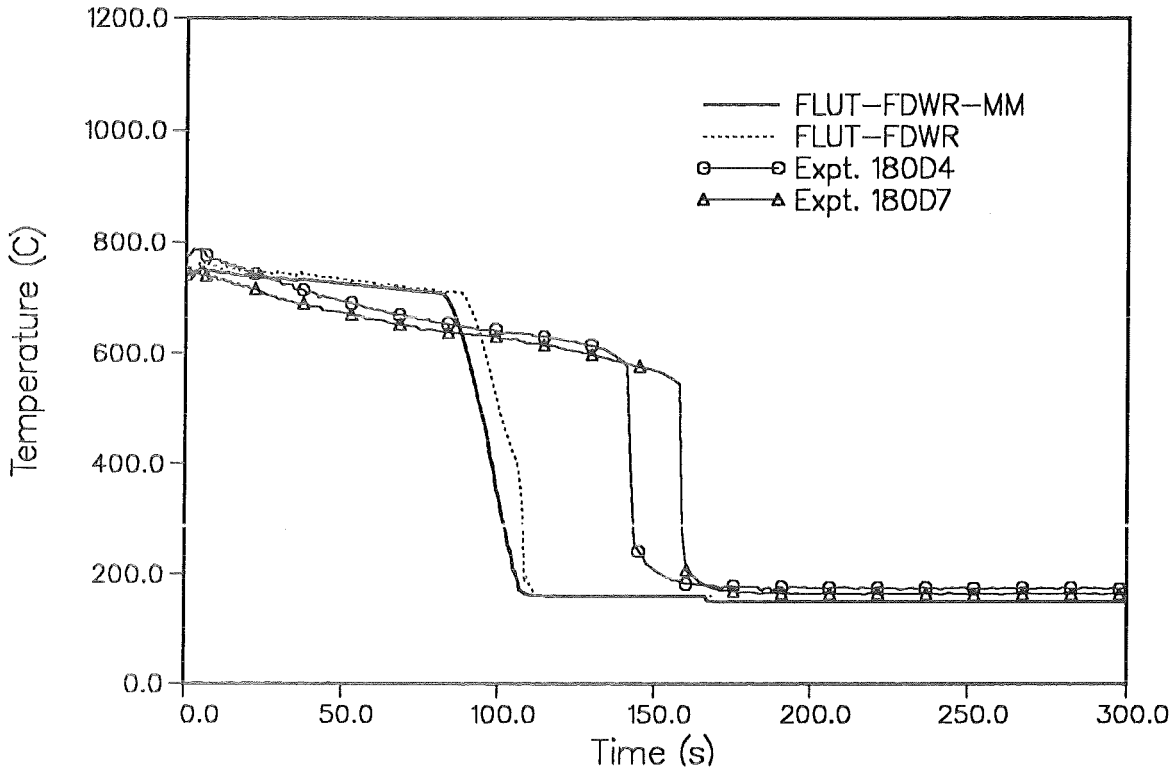

Figure 38. NEPTUN 5171 - Cladding temperature at z=1178 mm.

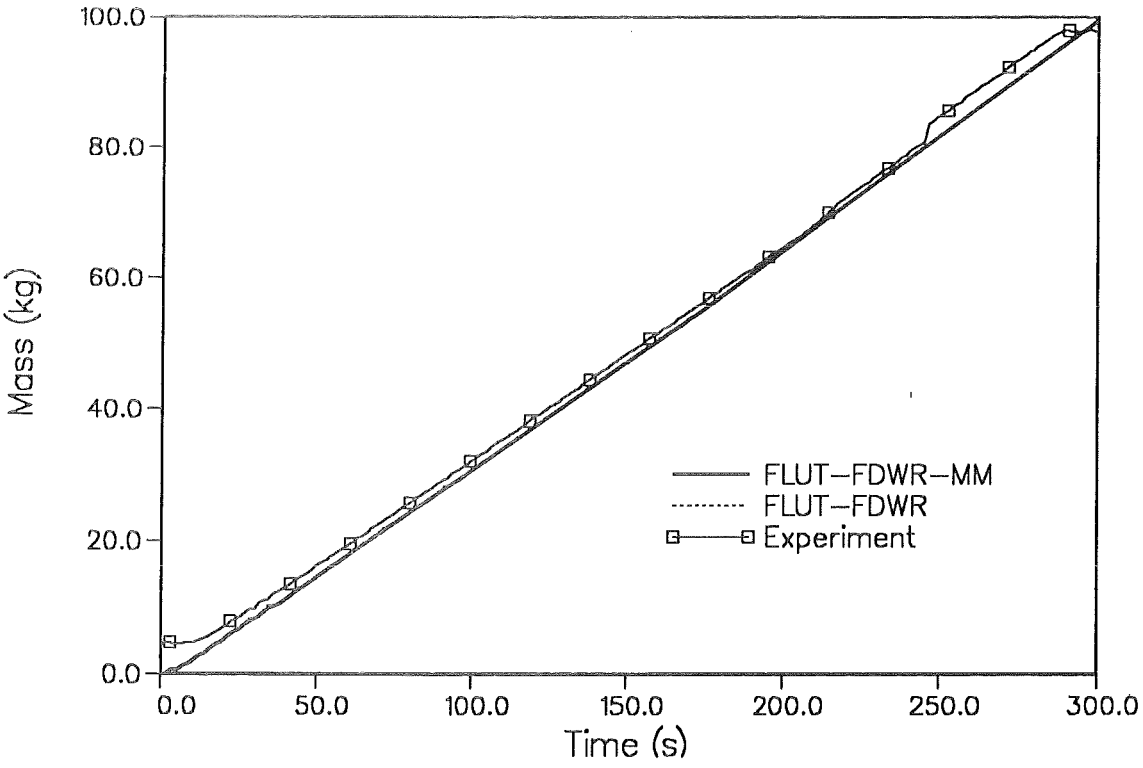

Figure 39. NEPTUN 5171 - Water carry over.

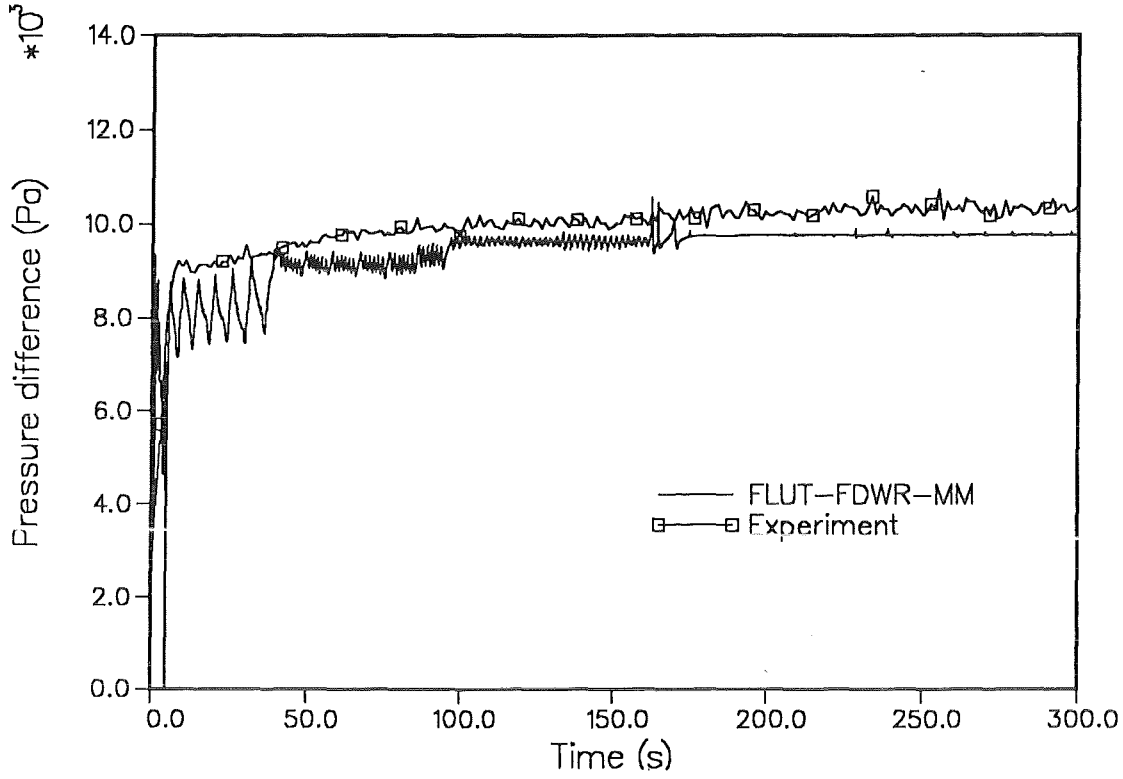

Figure 40. NEPTUN 5171 - Pressure difference (FLUT-FDWR-MM).

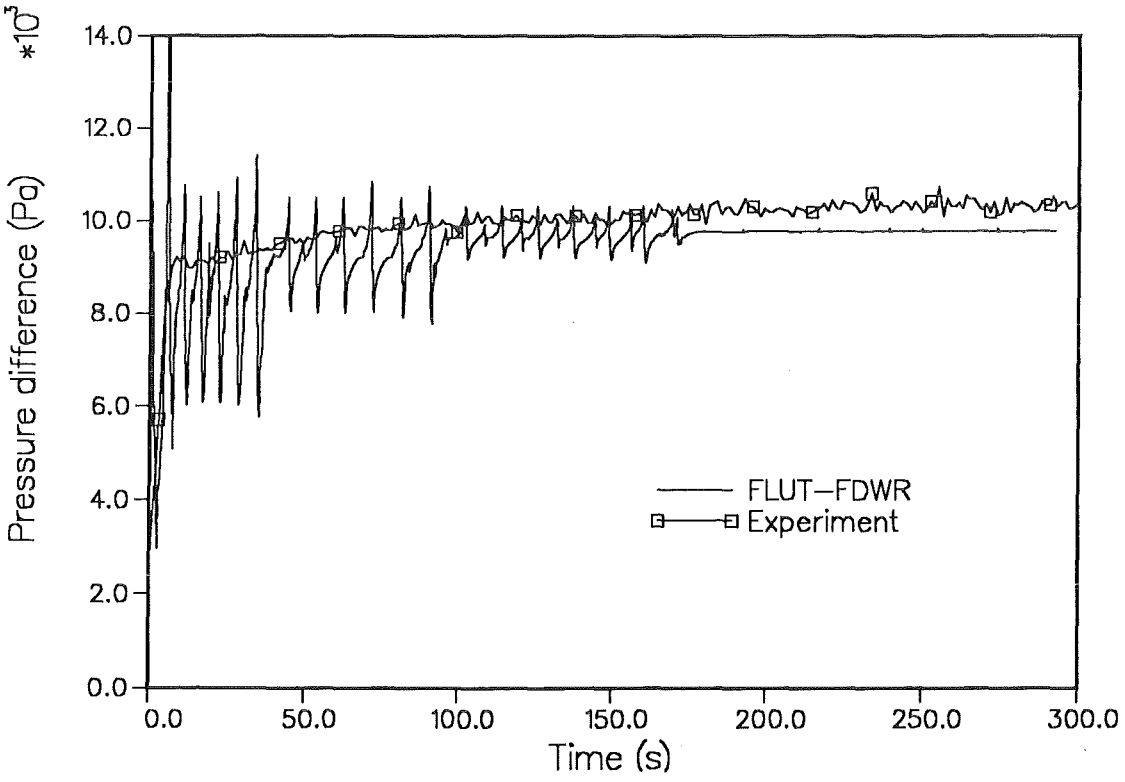

Figure 41. NEPTUN 5171 - Pressure difference (FLUT-FDWR).

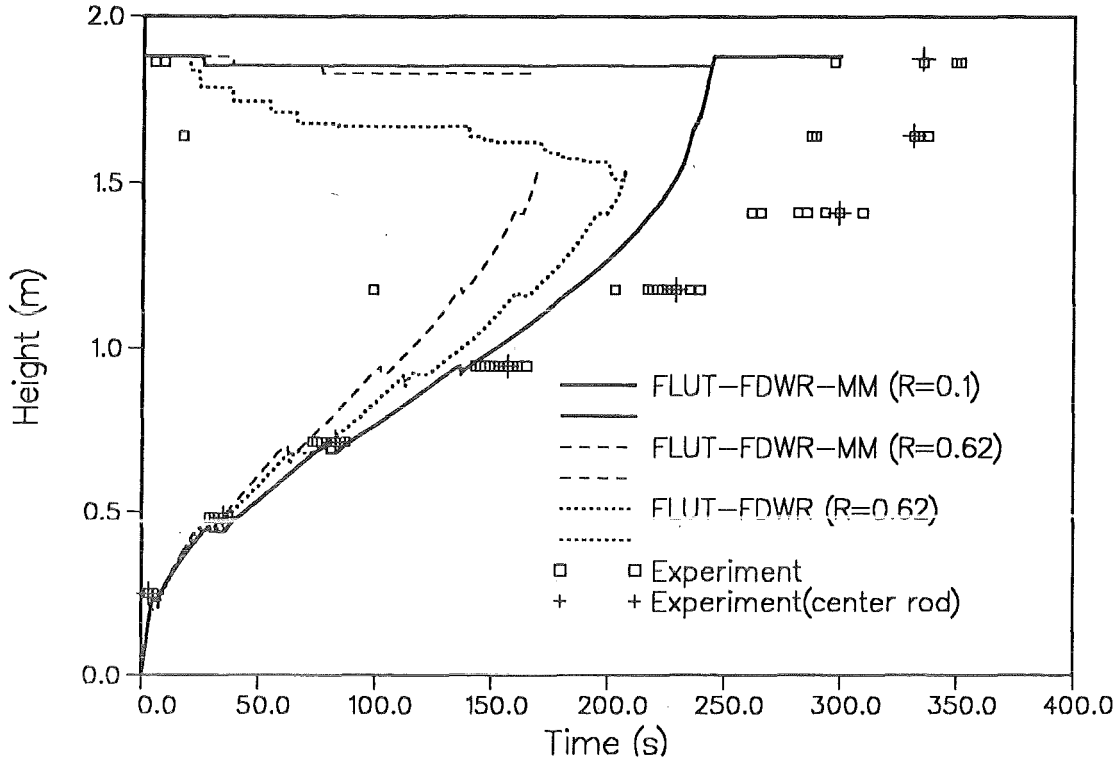

Figure 42. APWR8 (NEPTUN benchmark) - Quench-front propagation.

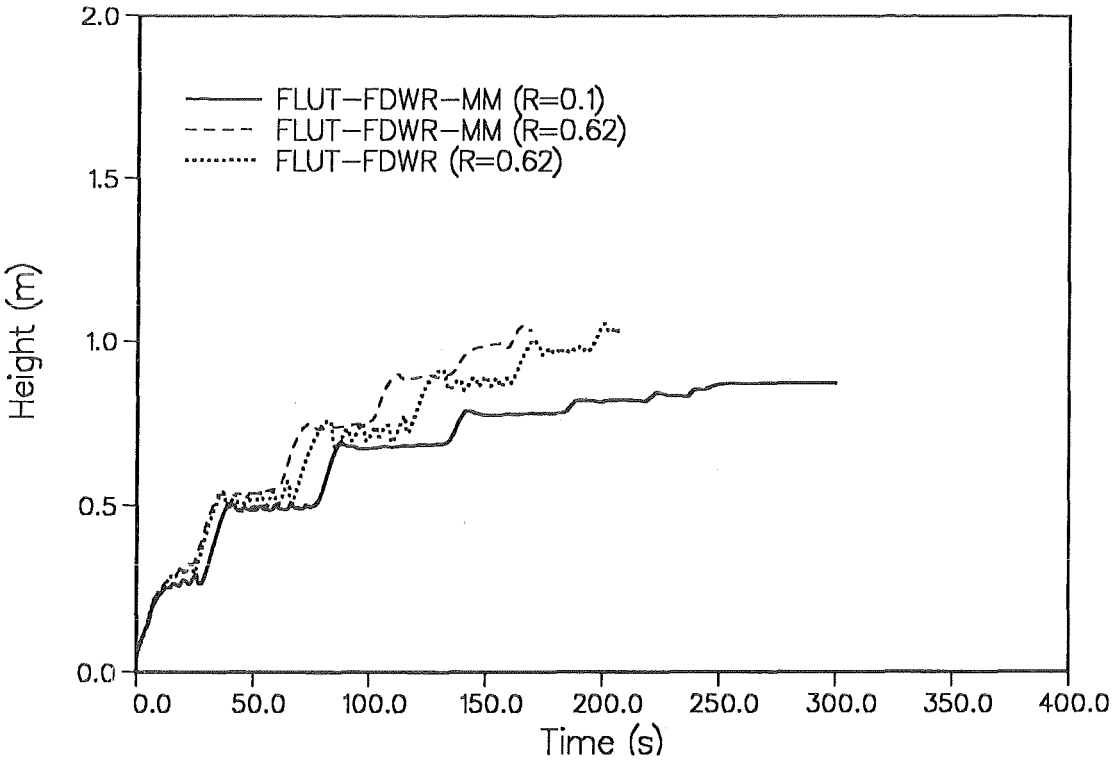

Figure 43. APWR8 (NEPTUN benchmark) - Calculated collapsed water level.

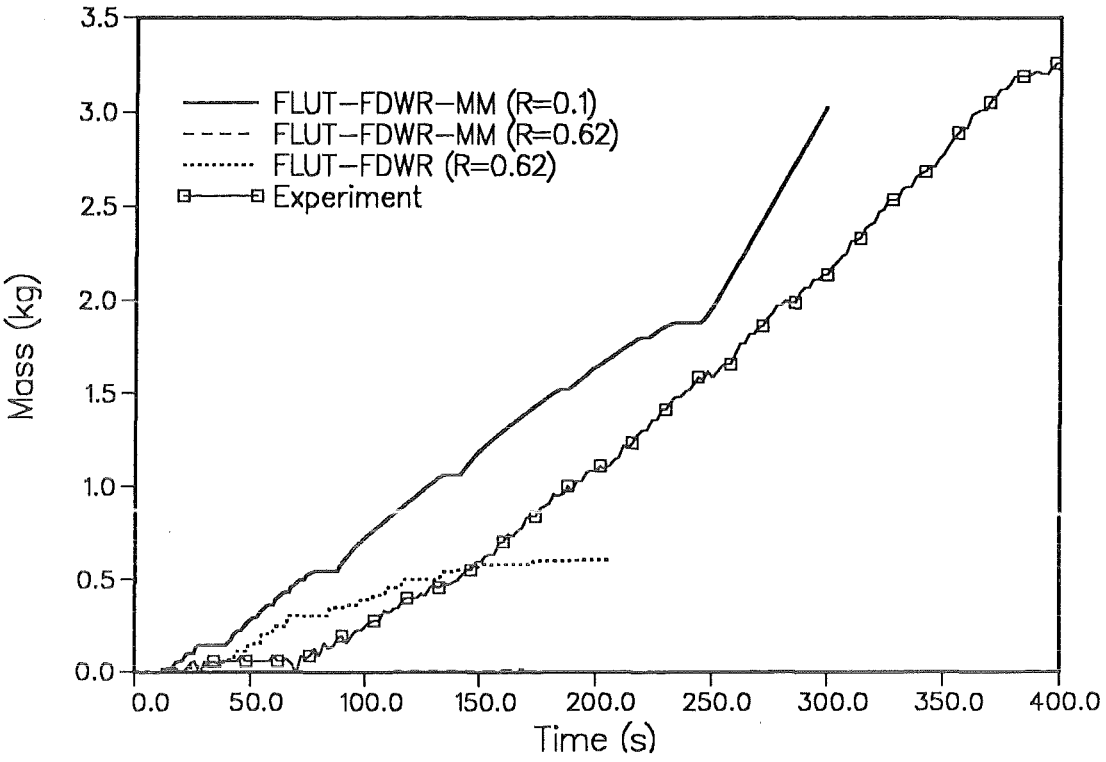

Figure 44. APWR8 (NEPTUN benchmark) - Water carry over.

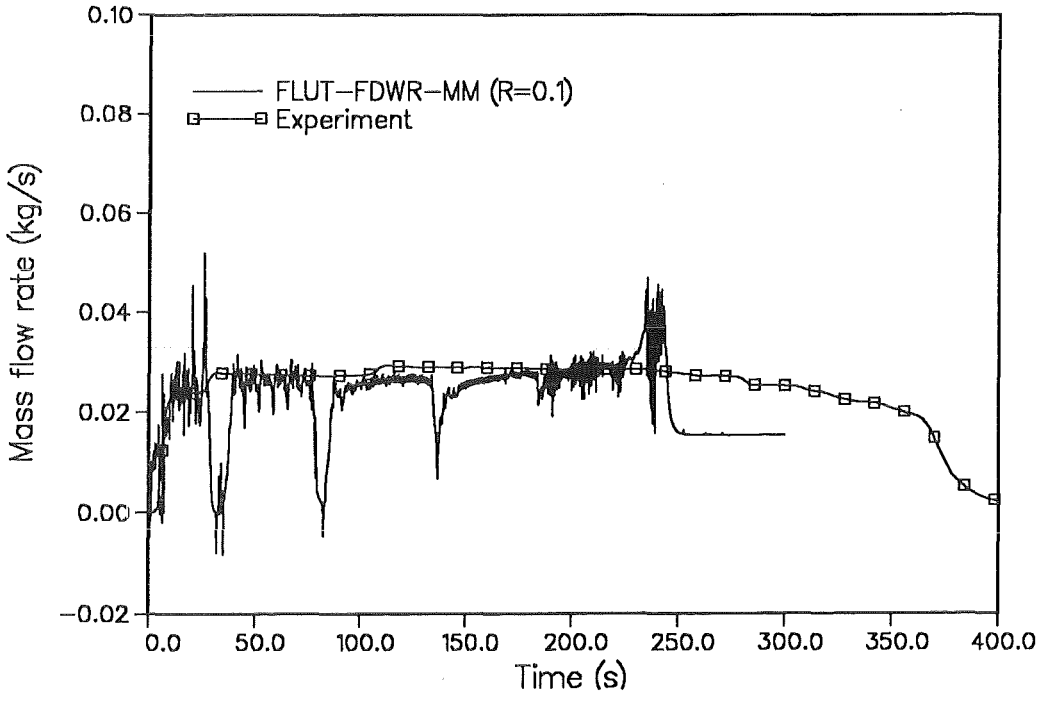

Figure 45. APWR8 (NEPTUN benchmark) - Outlet vapour mass flow rate (FLUT-FDWR-MM).

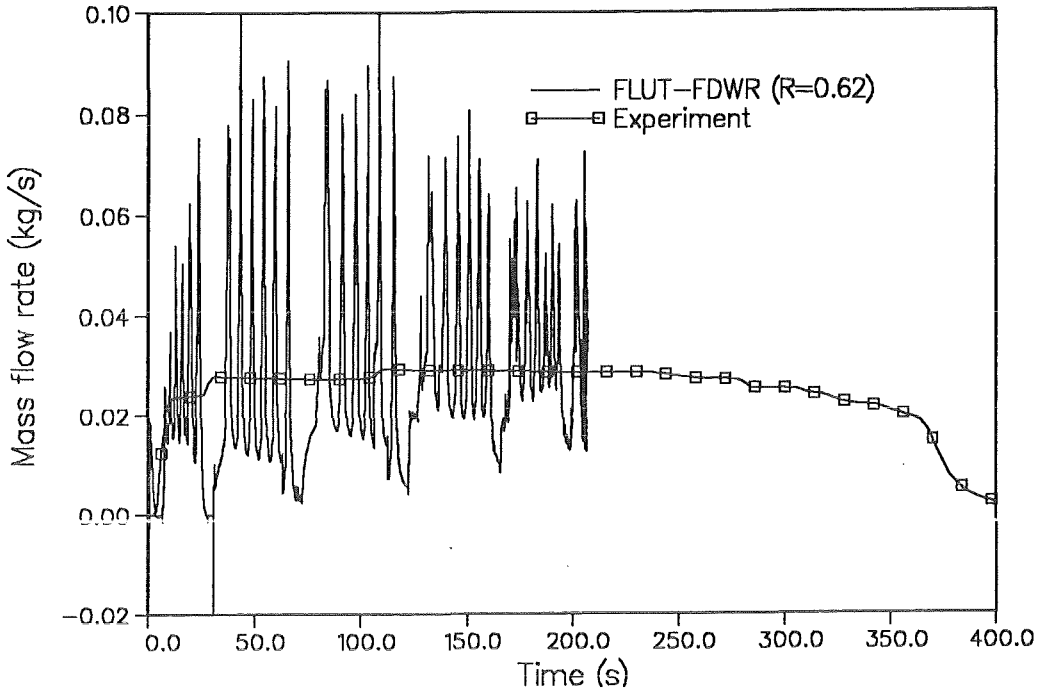

Figure 46. APWR8 (NEPTUN benchmark) - Outlet vapour mass flow rate (FLUT-FDWR).

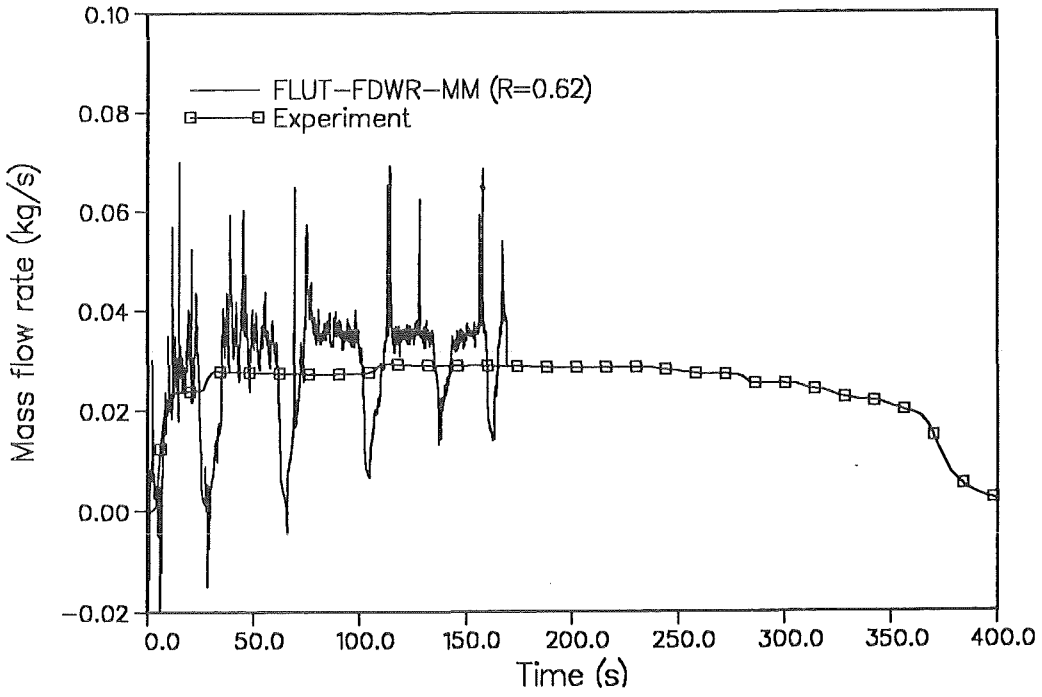

Figure 47. APWR8 (NEPTUN benchmark) - Outlet vapour mass flow rate (FLUT-FDWR-MM(R = 0.62)).

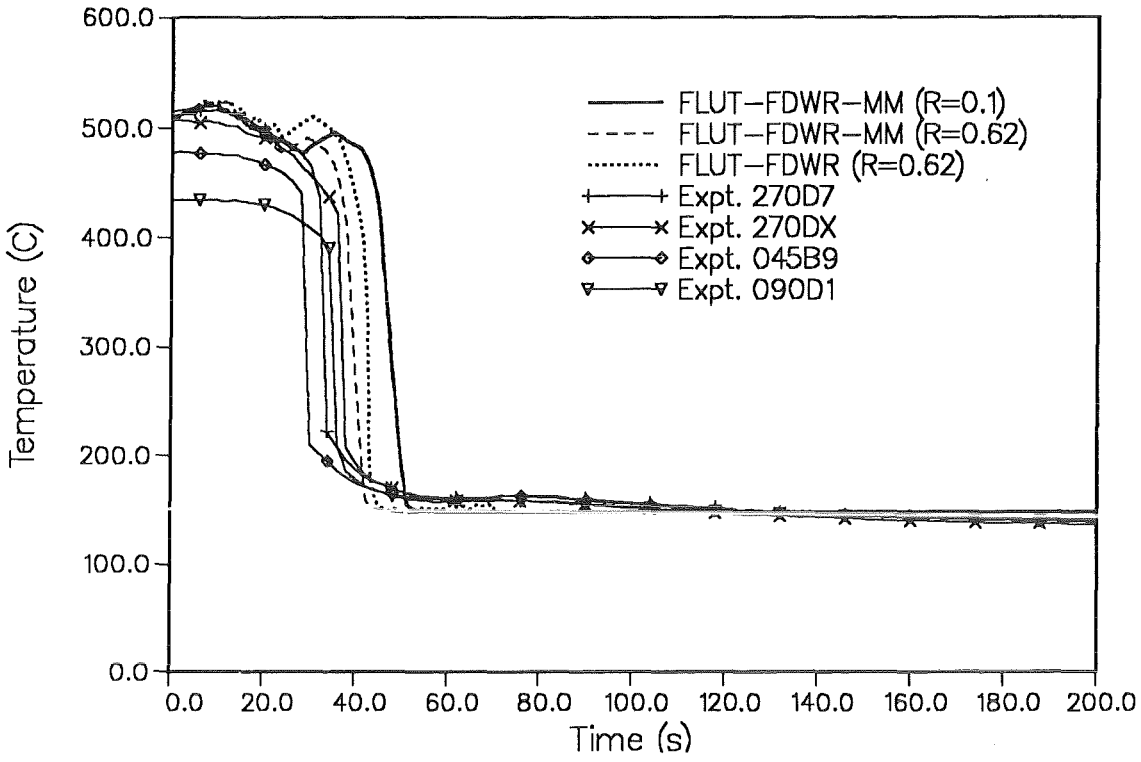

Figure 48. APWR8 (NEPTUN benchmark) - Cladding temperature at z = 482 mm.

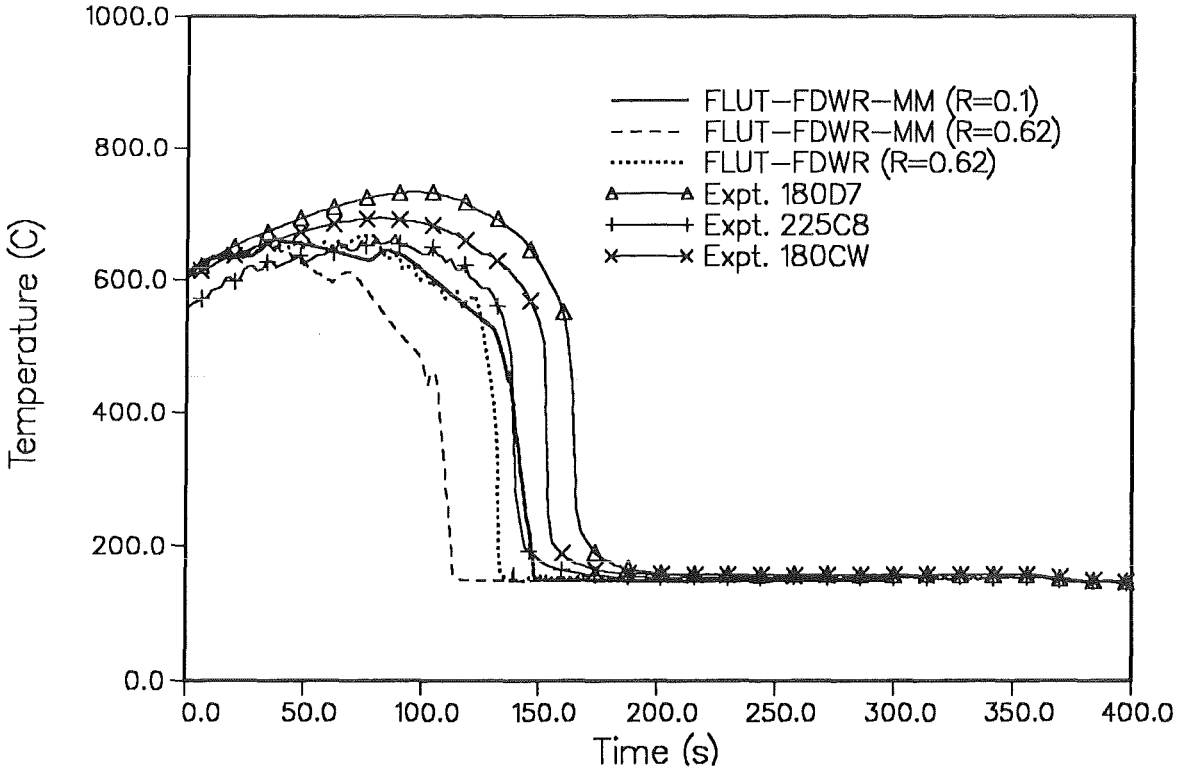

Figure 49. APWR8 (NEPTUN benchmark) - Cladding temperature at z = 946 mm.

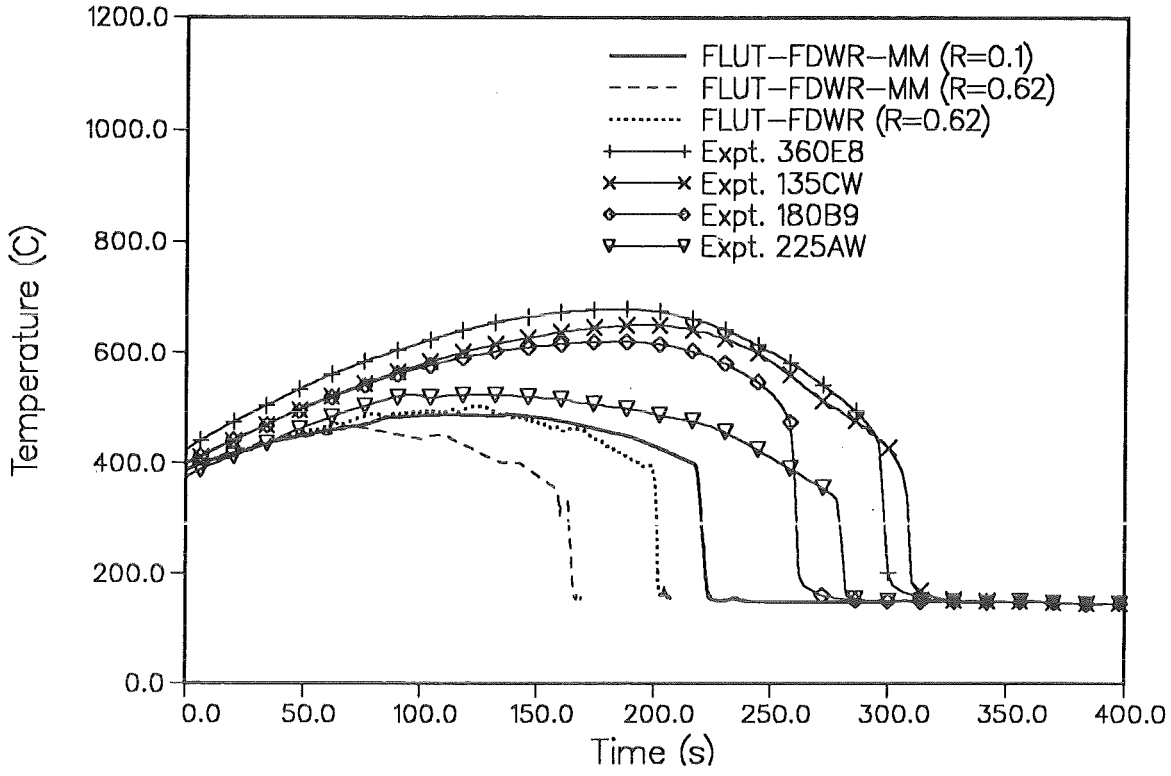

Figure 50. APWR8 (NEPTUN benchmark) - Cladding temperature at z = 1410 mm.

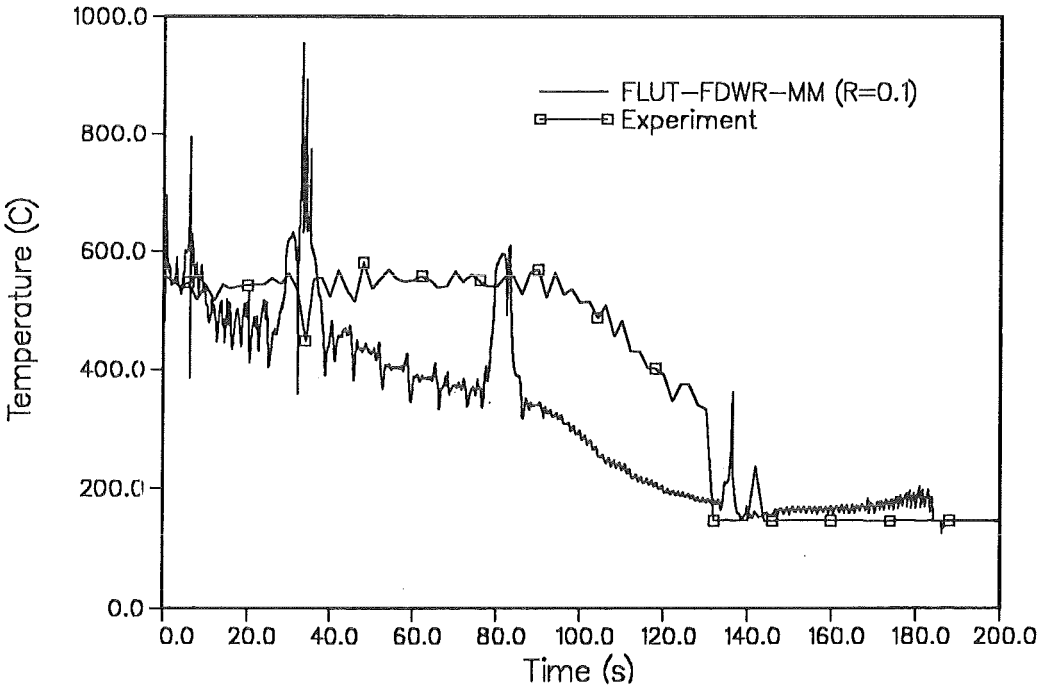

Figure 51. APWR8 (NEPTUN benchmark) - Vapour temperature at z = 946 mm (FLUT-FDWR-MM).

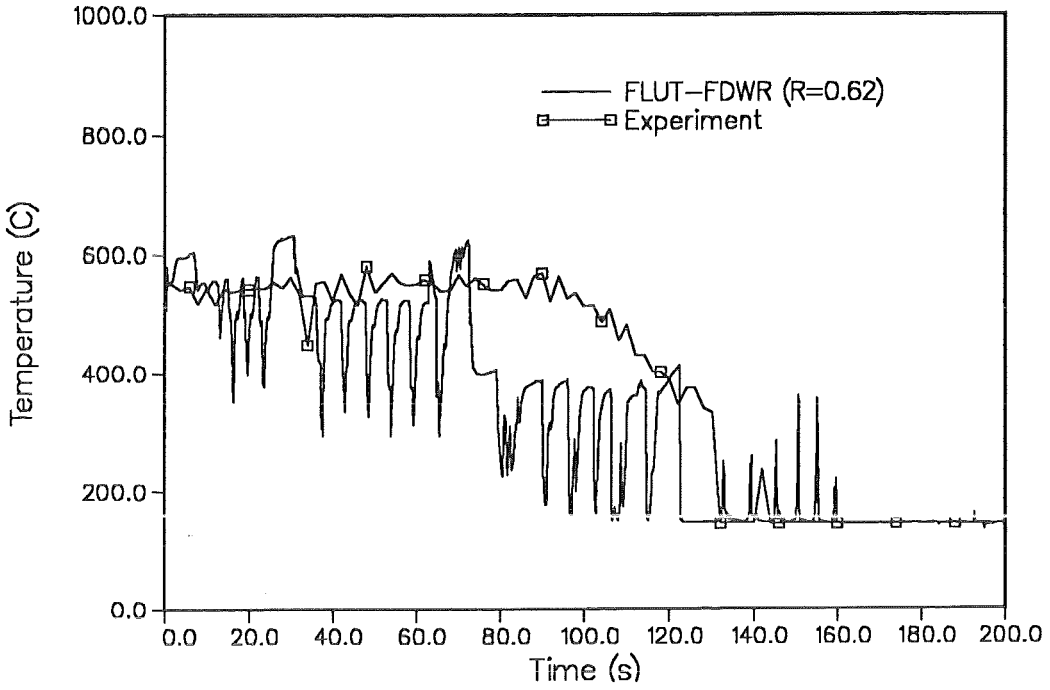

Figure 52. APWR8 (NEPTUN benchmark) - Vapour temperature at z = 946 mm (FLUT-FDWR).

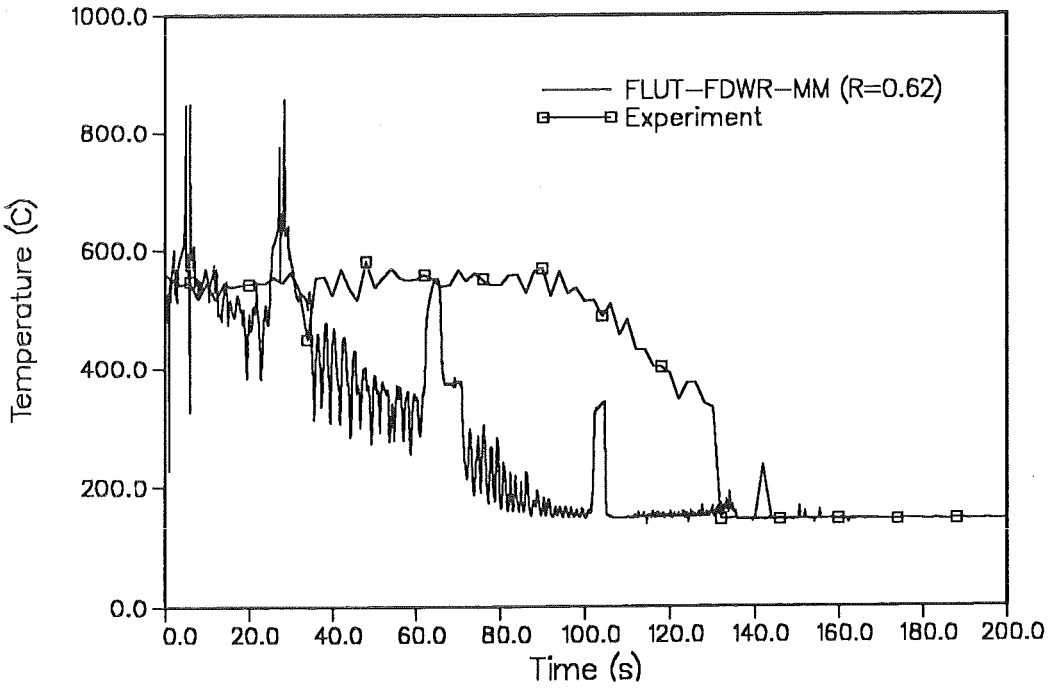

Figure 53. APWR8 (NEPTUN benchmark) - Vapour temperature at z = 946 mm (FLUT-FDWR-MM(R = 0.62)).

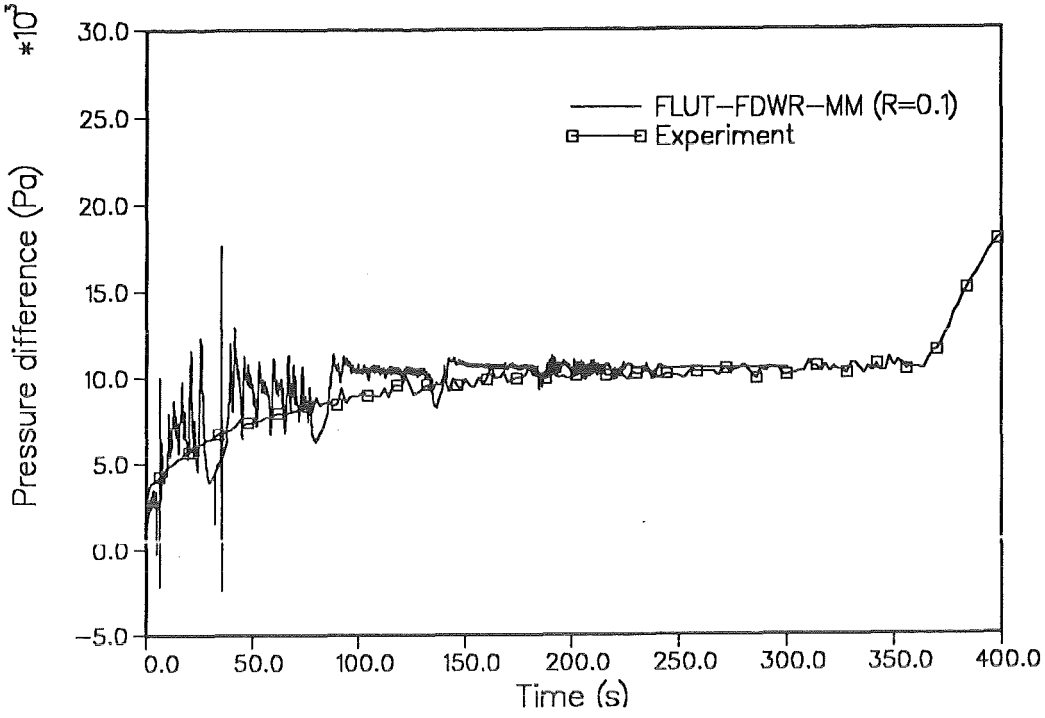

Figure 54. APWR8 (NEPTUN benchmark) - Pressure difference (FLUT-FDWR-MM).

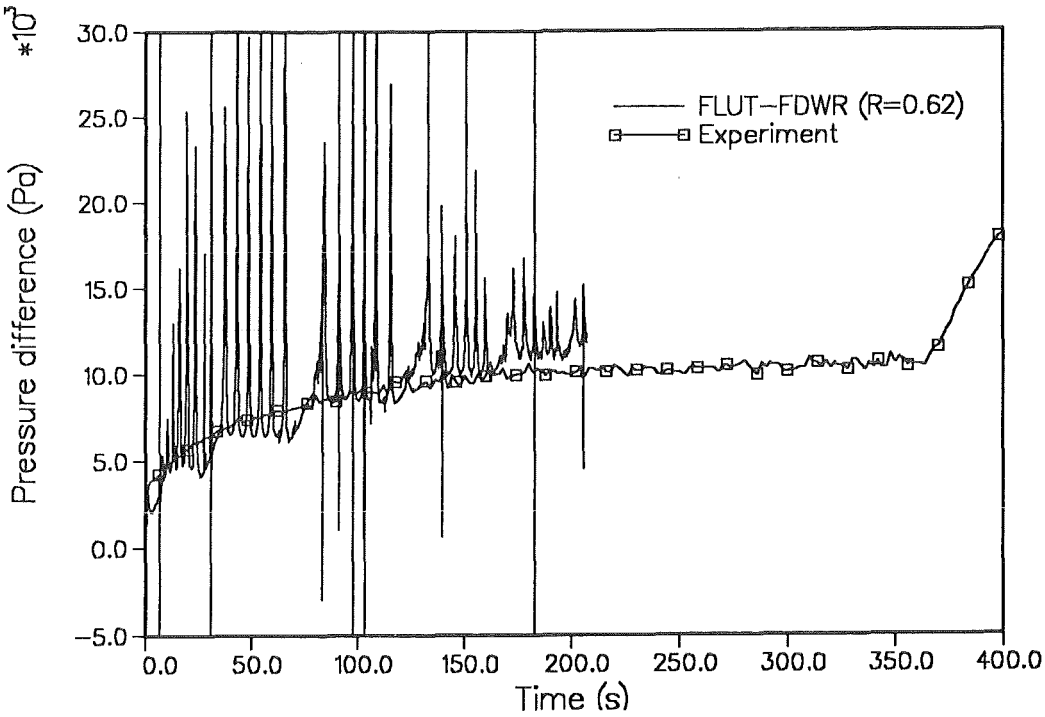

Figure 55. APWR8 (NEPTUN benchmark) - Pressure difference (FLUT-FDWR).

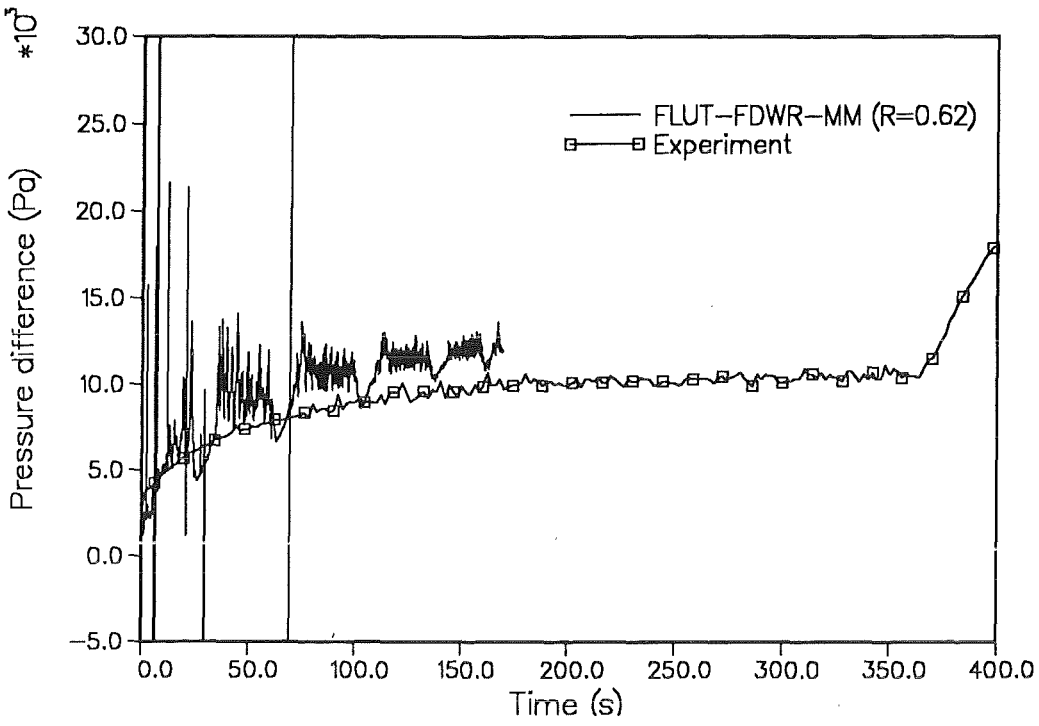

Figure 56. APWR8 (NEPTUN benchmark) - Pressure difference (FLUT-FDWR-MM(R = 0.25)).

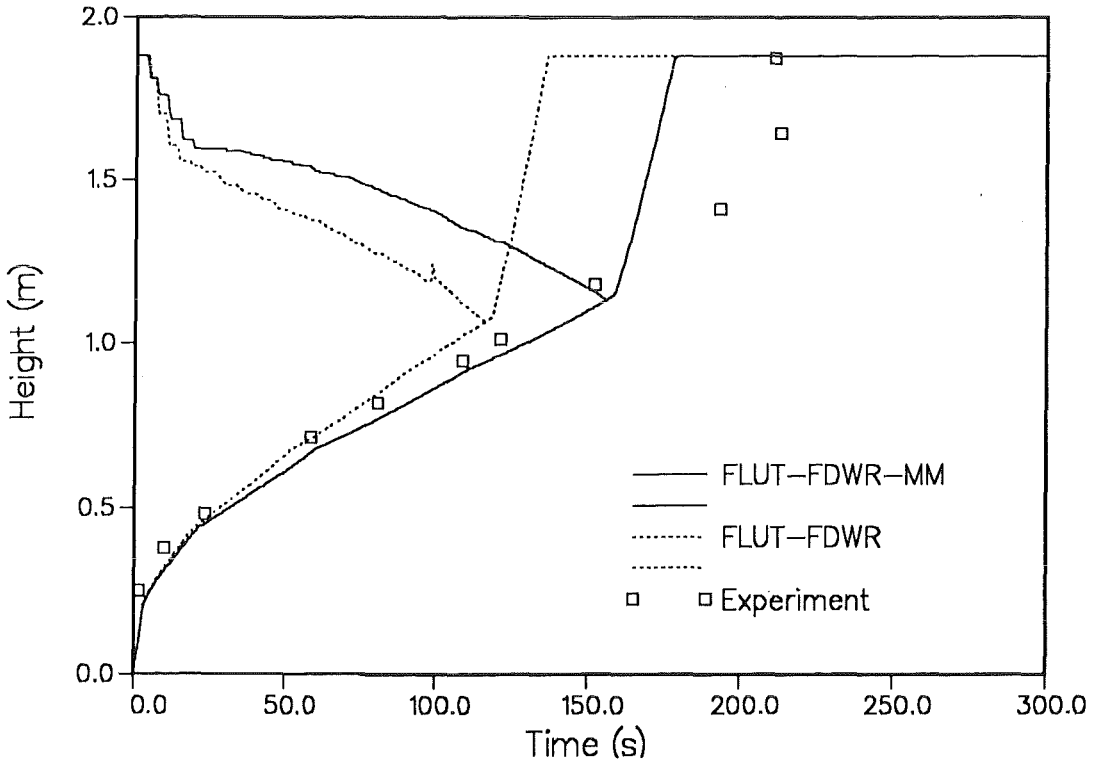

Figure 57. APWR1 - Quench-front propagation

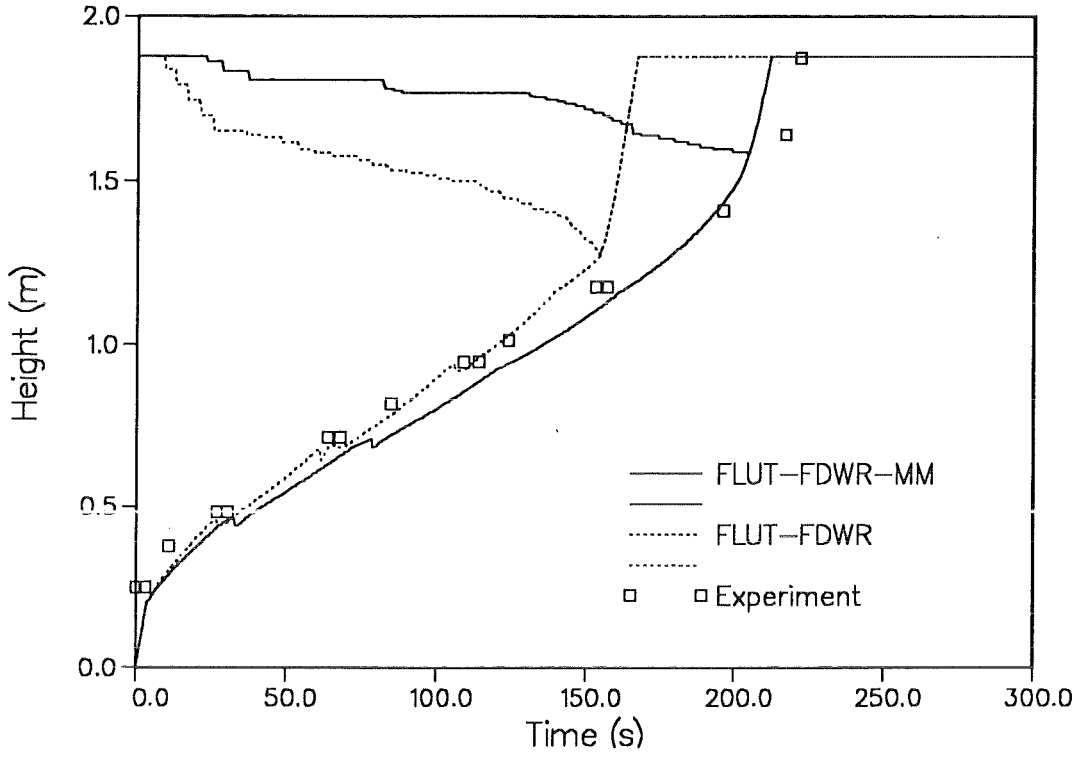

Figure 58. APWR2 - Quench-front propagation

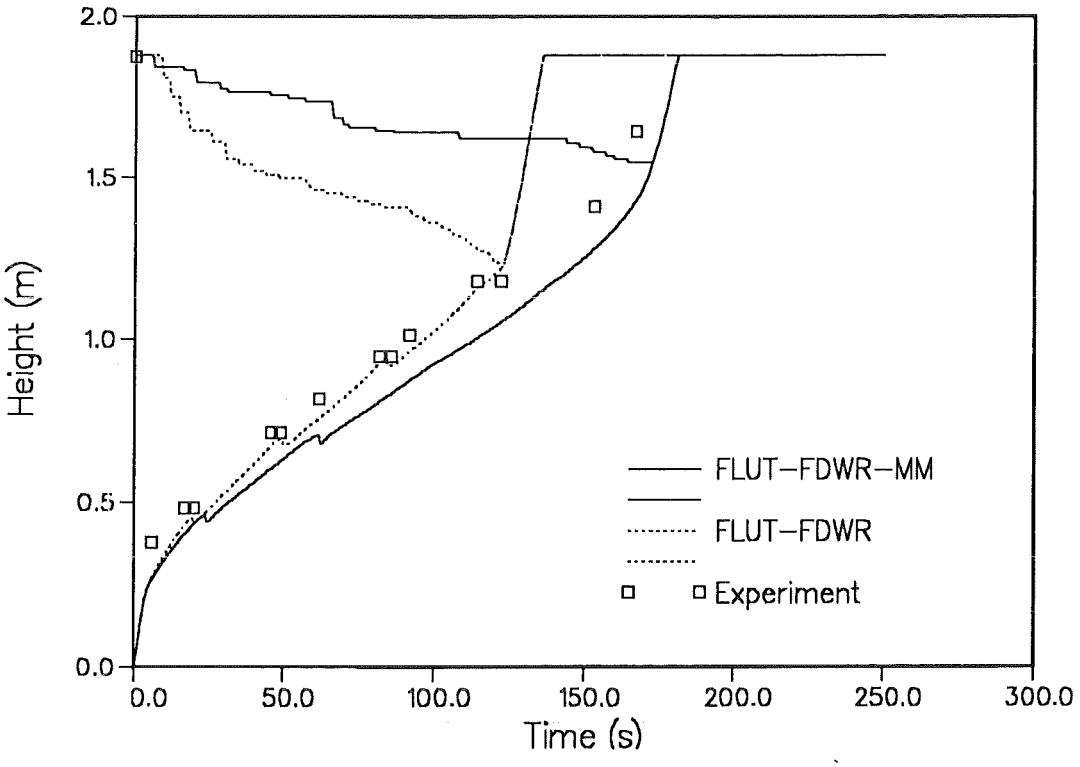

Figure 59. APWR3 - Quench-front propagation

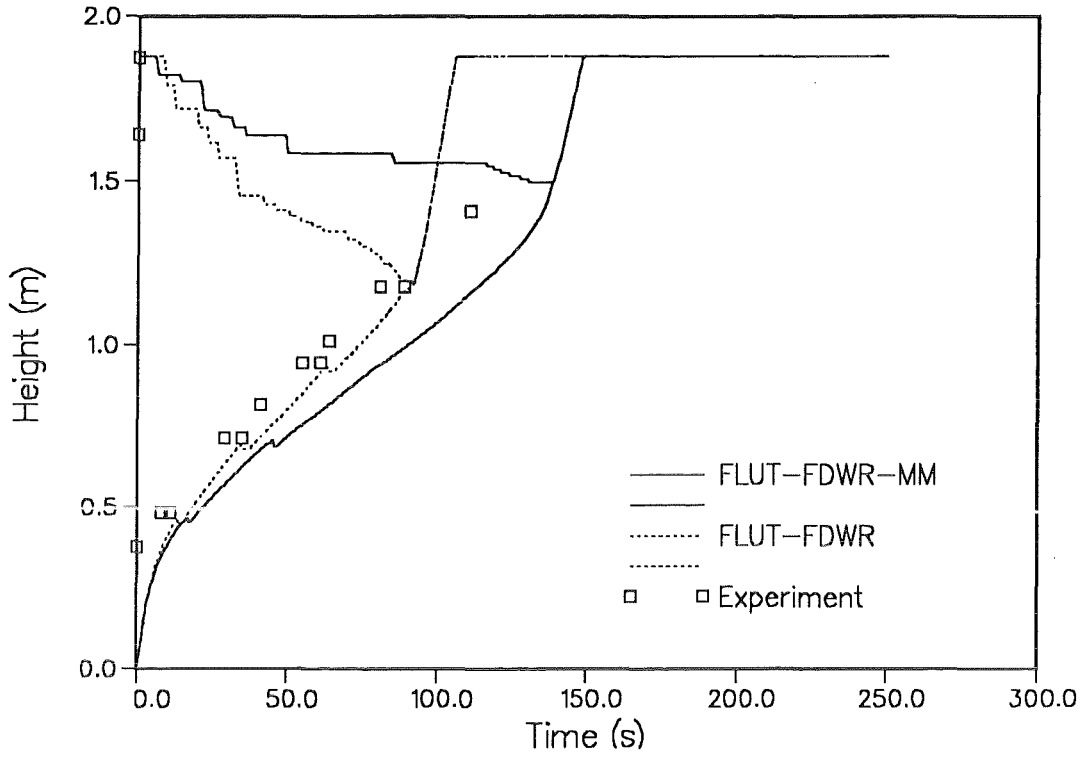

Figure 60. APWR4 - Quench-front propagation

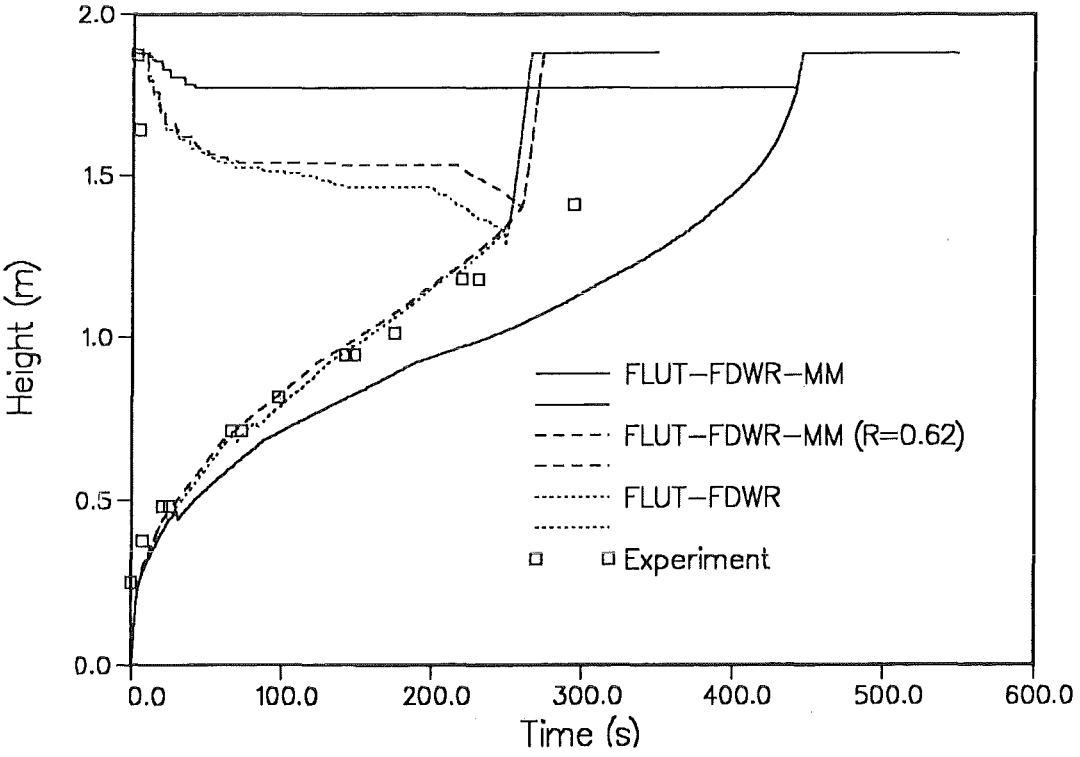

Figure 61. APWR5 - Quench-front propagation

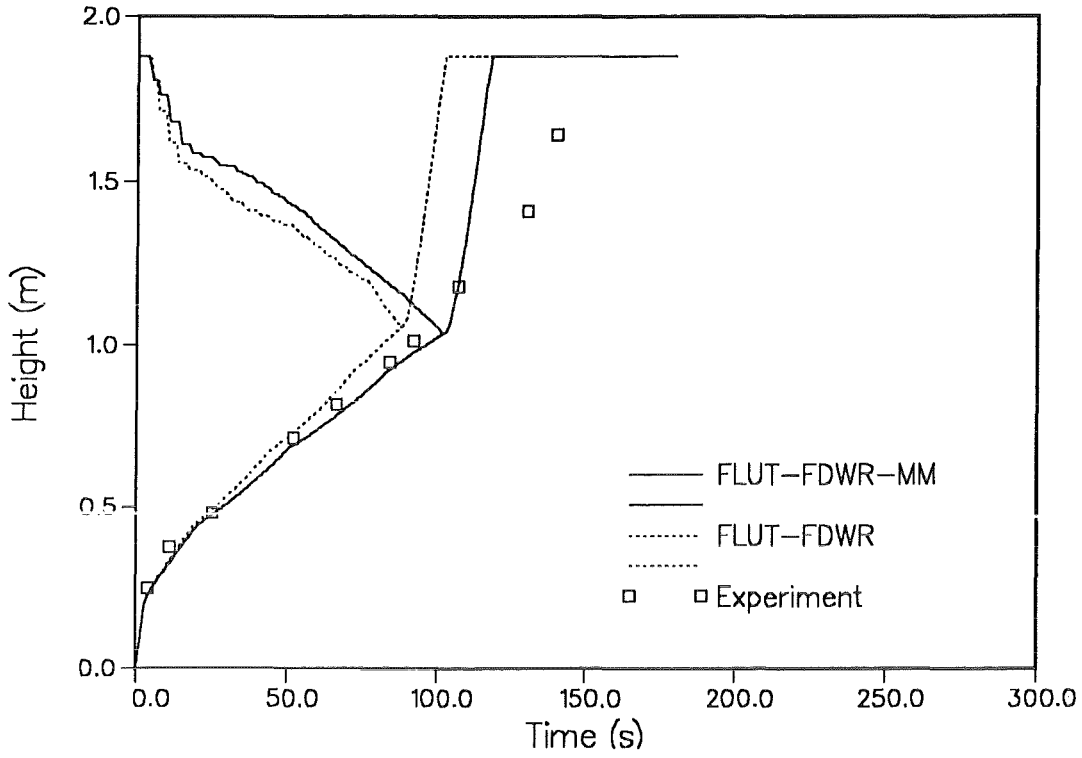

Figure 62. APWR6 - Quench-front propagation

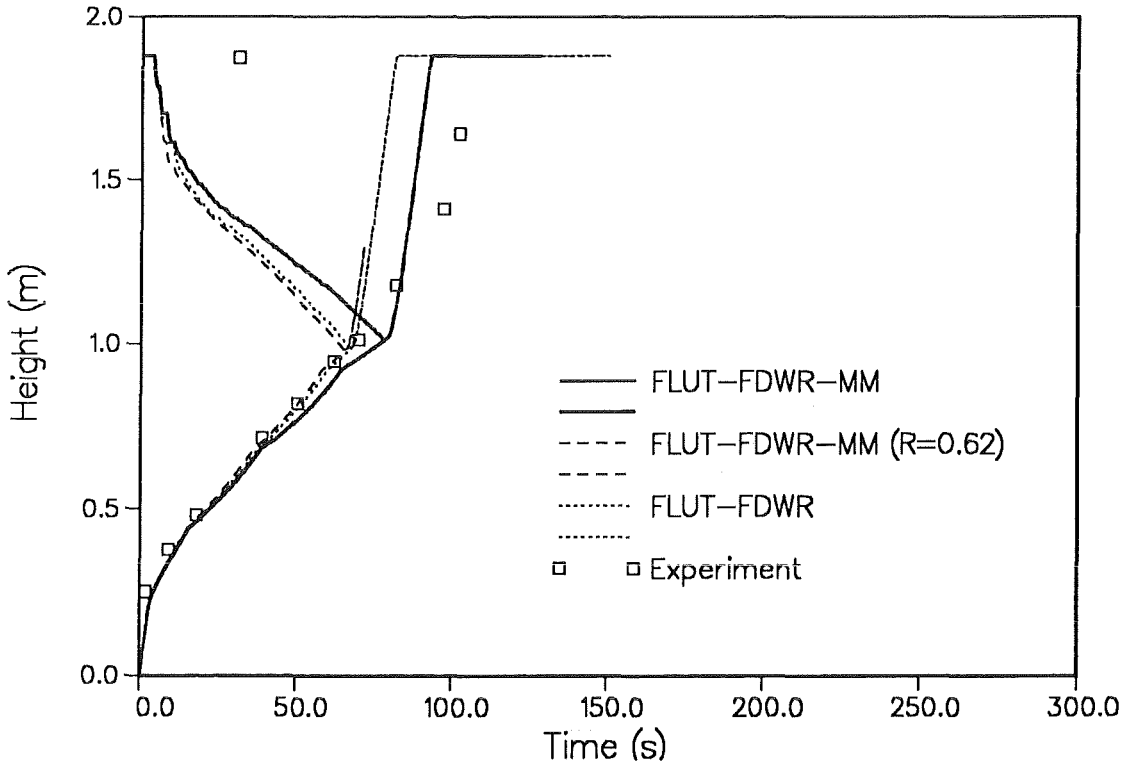

Figure 63. APWR7 - Quench-front propagation

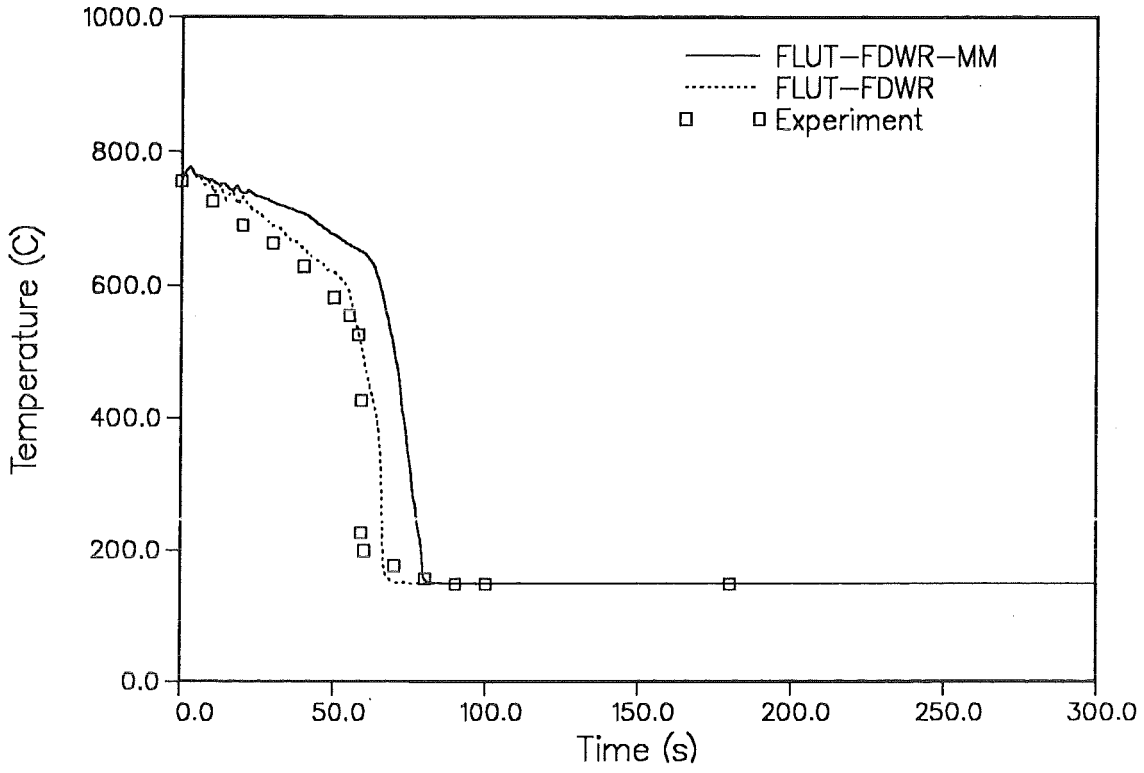

Figure 64. APWR1 - Cladding temperature at z = 714 mm (level 3).

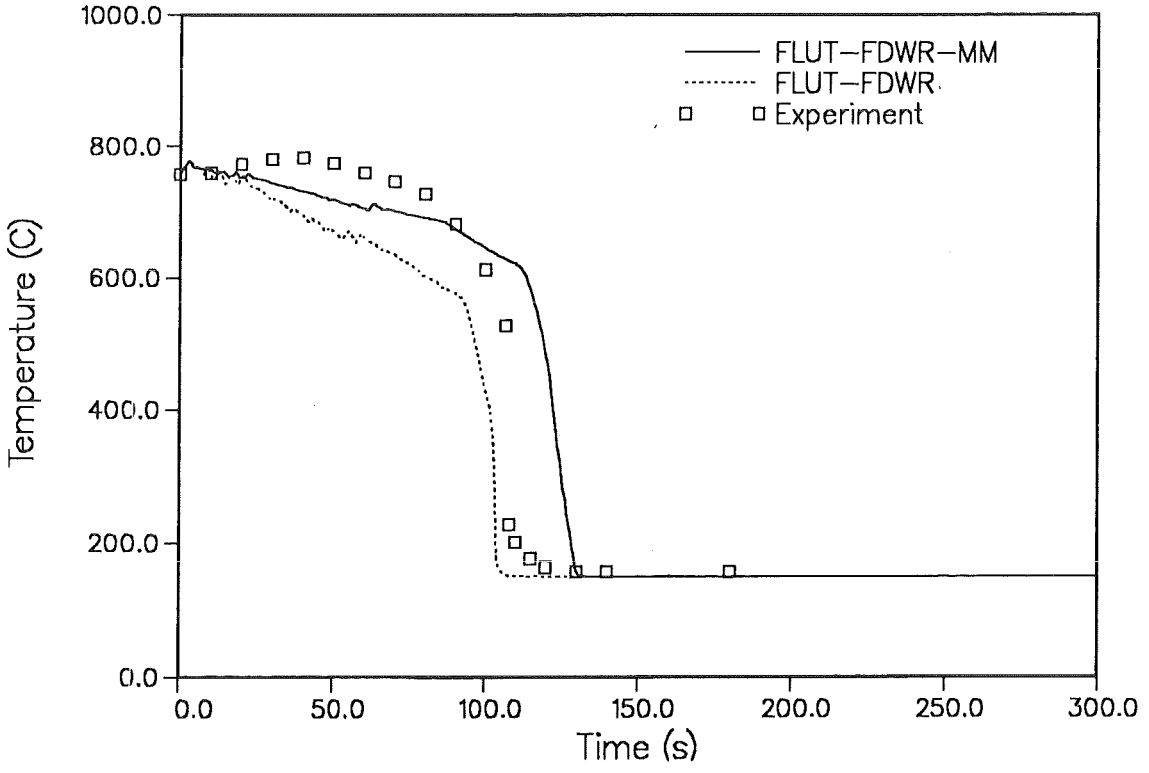

Figure 65. APWR1 - Cladding temperature at z = 946 mm (level 4).

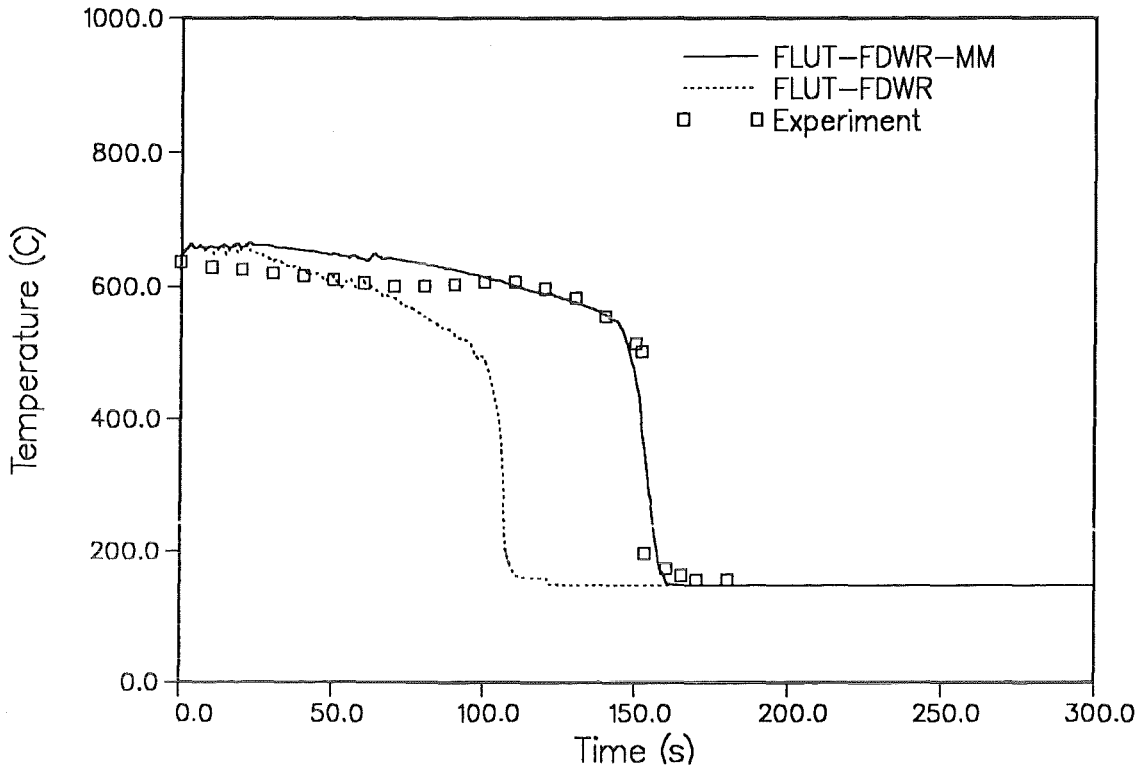

Figure 66. APWR1 - Cladding temperature at z = 1178 mm (level 5).